Universidad de La Habana Instituto de Farmacia y Alimentos

Tesis presentada en opción al grado científico de Doctor en Ciencias Farmacéuticas

Título: Desarrollo de un sistema de recubrimiento pelicular acuoso con quitosana para aplicaciones farmacéuticas

Autor: MSc. Mirna Fernández Cervera

Tutores: Ph.D. Jyrki Heinaamaki
Ph.D. Jouko Yliruusi
Ph.D. Antonio Iraizoz Colarte

Ciudad de La Habana

2004

Resumen

La quitosana es un polisacárido catiónico natural de bajo costo, que por sus buenas propiedades formadoras de películas presenta un elevado interés de utilización en la industria farmacéutica en los procesos de revestimiento de sólidos, objetivo principal del presente estudio. Quitosanas cubanas, obtenidas a partir de exoesqueletos de langostas, fueron caracterizadas y comparadas con quitosanas comerciales quedando demostrada la similitud de sus propiedades físico-químicas, y su dependencia con el proceso de obtención y la fuente de quitina empleada como material de partida Se lograron películas flexibles y resistentes mecánicamente con mezclas acuosas binarias de una quitosana comercial de elevada masa molecular (HMW) y amilosa de almidón de maíz *(Hylon VII)*, plastificadas con polioles, no reportadas con anterioridad. Con el empleo de glicerol como plastificante, las películas formadas resultaron estables físicamente bajo condiciones extremas de temperatura y humedad durante el almacenamiento, no así con eritritol. Se desarrolló un proceso de recubrimiento pelicular de pellets a pequeña escala, con un equipo de lecho fluido miniaturizado con atomización superior, determinándose los rangos más adecuados de trabajo para las diferentes variables que influyeron en el proceso. La optimización de la temperatura del flujo del aire y la velocidad de atomización de la solución de revestimiento satisfacieron los requerimientos de entericidad y rendimiento propuestos. Se desarrolló un nuevo método para la determinación de la adhesividad de las películas en pellets cubiertos, basándose en la velocidad mínima de fluidización. Un novedoso sistema de revestimiento acuoso con quitosana-HMW fue desarrollado requiriendo de agentes antiadhesivos, obteniéndose los mejores resultados con el estearato de magnesio y el monoestearato de glicerilo.

Tabla de Contenidos

Glosario de abreviaturas

CH1: quitosana cubana 1

CH2: quitosana cubana 2

DA: grado de acetilación

DD: grado de desacetilación

DSC: calorimetría diferencial de barrido

EMC: equilibrio de absorción de humedad

FT-NIR: espectroscopia de infrarrojo cercano transformada de Fourier

GMS: monoestearato de glicerilo

HC1: ácido clorhídrico

HMW: alta masa molecular

HPMC: hidroxipropilmetilcelulosa

IR: espectroscopia infrarroja

LMW: baja masa molecular

MINBAS: Ministerio de la Industria Básica

MMW: masa molecular media

NIR: espectroscopia de infrarrojo cercano

PVA: polivinilalcohol

PVP: polivinilpirrolidona

RH: humedad relativa

RMN: resonancia magnética nuclear

$SÍO_2$: dióxido de silicio coloidal

$t_{50}o_0$: tiempo en el cual la mitad de la dosis del fármaco es disuelta

TGA: análisis termogravimétrico

TGI: tracto gastrointestinal

$TÍO_2$: dióxido de titanio

Umf: velocidad minima de fluidización

XRPD: difracción de rayos-X de sólidos

Listado de publicaciones originales

El estudio está basado en las siguientes publicaciones originales, las cuales serán referidas en el texto con números Romanos I-V.

I Fernández Cervera, M., Heinámäki, J., Rásänen, M., Maunu, S.L., Karjalainen, M., Nieto Acosta, O.M., Iraizoz Colarte, A. and Yliruusi, J. (2004). Solid-state characterization of chitosans derived from lobster chitin. Aceptado para publicar en Carbohydr. Polym. (2004).

II Fernández Cervera, M., Heinámäki, J., Krogars, K., Jorgensen A., Karjalainen, M., Iraizoz Colarte, A. and Yliruusi, J. (2004). Solid-state and mechanical properties of aqueous chitosan-amylose starch films plasticized with polyols. AAPS Pharm. Sci. Tech., 5(1) Article 15 (http://www.aapspharmscitech.org) 1-6.

III Fernández Cervera, M., Karjalainen, M., Airaksinen, S., Rantanen, J., Heinámäki, J., Iraizoz Colarte, A. and Yliruusi, J. (2004). Physical stability and moisture sorption of aqueous chitosan-amylose starch films plasticized with polyols. Eur. J. Pharm. Biopharm., 58, 69-76.

IV Fernández Cervera, M., Heinámäki, J., Salgado-Rodriguez, E., Antikainen, O., Iraizoz Colarte, A. and Yliruusi, J. (2004). Effective optimization of enteric film coating of pellets with a miniaturized top-spray coater. Pharm. Ind. (en prensa).

V Fernández Cervera, M., Heinámäki, J., Rásänen, E., Antikainen, O., Nieto Acosta, O.M., Iraizoz Colarte, A. and Yliruusi, J. (2004). Determination of tackiness of chitosan film-coated pellets exploiting minimum fluidization velocity. Int. J. Pharm., 281, 119-127.

1. Introducción

La quitina es el segundo amino polisacárido natural más abundante después de la celulosa Los crustáceos son generalmente la fuente principal de quitina para su procesamiento industrial, siendo las fuentes más explotadas los residuos de cangrejos y camarones (Synowiecki y Al-Khateeb, 2003). La quitosana es el derivado N-desacetilado de la quitina. Su producción a partir de los carapachos de crustáceos, desechos de la industria alimentaria, es económicamente factible (Ravi Kumar, 2000). Sin embargo, una gran cantidad de desechos de alimentos ricos en quitina no es aprovechada, especialmente en los países asiáticos, donde la población tiene dietas ricas en mariscos (Ball, 2002). Por lo tanto, los esfuerzos por transformar estos desechos en productos útiles resultan racionales y ecológicamente importantes. El desarrollo de tecnologías para la utilización de estos polisacáridos pudiera estimular sus producciones.

La historia de la quitosana data desde el siglo pasado. Rouget (1859) la describió como el principal derivado de la quitina. Sin embargo, formalmente fue nombrada “quitosana” en 1894 por Hoope-Seyler. En la década de los años 90 se demostró que la quitosana podía ser un excipiente útil en diferentes formulaciones farmacéuticas (Bernkop-Schnürch, 2000). Por sus favorables propiedades biológicas, como biodegradabilidad, biocompatibilidad y atoxicidad, características de solubilidad, así como por su abundancia en la naturaleza y factibilidad económica de obtención ha recibido la atención de numerosos investigadores (Harish Prashanth y col., 2002). No obstante, su incompleta caracterización y la variabilidad entre las quitosanas comerciales existentes ha desalentado a la industria farmacéutica para adoptarla como excipiente o componente en las formulaciones. La heterogeneidad de las quitosanas se debe principalmente a las fuentes de quitina utilizadas y a los procesamientos relativamente incontrolados, como la desacetilación y la depolimerización, de las quitinas comerciales (Rege y Block, 1999; Rege y col., 2003; Synowiecki y Al-Khateeb, 2003).

Durante los últimos veinte años, la quitosana ha sido evaluada en numerosas aplicaciones farmacéuticas, tales como diluente en la compresión directa, excipiente en la granulación húmeda, agente gelificante y emulsificante y, más recientemente, como agente formador de

películas. La quitosana también ha sido valorada en el desarrollo de sistemas de liberación controlada y de liberación específica de sustancias activas (Felt y col., 1998; Paul y Sharma, 2000; Hejazi y Amiji, 2003). A pesar de las bien conocidas características de la quitosana como gel y formador de películas, muy poca atención ha sido brindada a las potencialidades de este material polimérico para el revestimiento pelicular (Ritthidej y col., 2000; Koizumi y col., 2001).

El desarrollo de nuevos materiales poliméricos en la industria farmacéutica ha conllevado a un cambio desde los sistemas de revestimiento orgánico hacia los sistemas acuosos, debido a los problemas asociados con el costo, seguridad y contaminación ambiental de los solventes orgánicos. Además, significativas innovaciones se han realizado en la tecnología de los procesos y en el diseño de los equipos aumentando el interés en los procesos de recubrimiento acuoso. Hoy en día, se comprende como nunca antes la necesidad de conocer los requerimientos farmacéuticos de los polímeros con vistas a lograr procesos de revestimiento cada vez más controlados y reproducibles, constituyendo la quitosana un ejemplo de ello. Sus reconocidas propiedades formadoras de películas, la convierten en candidato ideal para el diseño de nuevos sistemas de revestimientos acuosos requiriendo por tanto, el estudio de su capacidad como material de recubrimiento.

Es por ello que en el presente trabajo se considera la siguiente hipótesis.

Hipótesis:

La quitosana de alto peso molecular posee favorables propiedades físico-químicas y tecnológicas para ser empleada en el diseño de sistemas de revestimientos acuosos para la industria farmacéutica.

Para comprobar esta hipótesis se proponen los siguientes objetivos.

Objetivo general:

Estudiar las propiedades como formador de películas de una quitosana comercial de alto peso molecular (HMW) y desarrollar, a partir de dicho polímero, un novedoso sistema de recubrimiento pelicular acuoso a pequeña escala.

Objetivos específicos:

- Caracterizar y comparar las propiedades físico-químicas de dos quitosanas cubanas, preparadas por diferentes procesos, con quitosanas comerciales.

- Elaborar y evaluar películas compuestas por quitosana-HMW y amilosa de almidón de maíz *(Hylon VII)* plastificadas con polioles según su morfología, propiedades del estado sólido y resistencia mecánica.

- Determinar la estabilidad física y el comportamiento de absorción de humedad de las películas compuestas por quitosana-HMW y amilosa de almidón de maíz *(Hylon VII)* y estudiar el efecto del plastifícante sobre las cualidades de las películas.

- Diseñar y optimizar el proceso de recubrimiento pelicular de pellets mediante un sistema miniaturizado con atomizador superior con películas acuosas de quitosana- HMW y un reconocido copolímero del ácido metacrílico (Eudragit® S), como modelo.

- Desarrollar una metodología para la selección y optimización de los agentes antiadhesivos a emplear en el proceso de revestimiento acuoso de pellets con quitosana-HMW.

Al cumplimentar los objetivos trazados en el presente trabajo, se habrán desarrollado los siguientes **aspectos novedosos:**

- La caracterización de las quitosanas cubanas con el empleo de las técnicas de ^{13}C RMN, difracción de rayos-X de sólidos con temperatura variable, así como la determinación de las propiedades físicas, incluyendo la utilización de la microscopía electrónica de barrido, demostrando la similitud de sus propiedades físico-químicas con quitosanas comerciales.

- La obtención de películas flexibles y resistentes mecánicamente compuestas por quitosana-HMW y amilosa de almidón de maíz *(Hylon VII)* plastifícadas con polioles.

- El desarrollo de un nuevo método para la determinación de la adhesividad de las películas en pellets cubiertos, empleando la velocidad mínima de fluidización, demostrándose su utilidad para la cuantifícación de la adherencia de las películas.

- La obtención de un sistema de recubrimiento pelicular acuoso con quitosana-HMW empleando agentes antiadhesivos.

2. Revisión Bibliográfica

2.1 Manufactura de la quitosana

La quitosana es obtenida de la parcial desacetilación de la quitina, el segundo más abundante polímero natural, que se encuentra en los crustáceos, insectos, plantas inferiores y que es disponible fácilmente a partir del procesamiento de los desechos de los mariscos. A través de la desacetilación los grupos acetilos son removidos, y el producto resultante es un polisacárido compuesto por copolímeros de glucosamina y N-acetil glucosamina. Por lo tanto, la quitosana es un poli (2-amino 2-deoxi D-glucopiranosa) en el cual las unidades repetidas están enlazadas por enlaces 3(1-4) (Kurita, 1986; Roberts, 1992) (Figura 1).

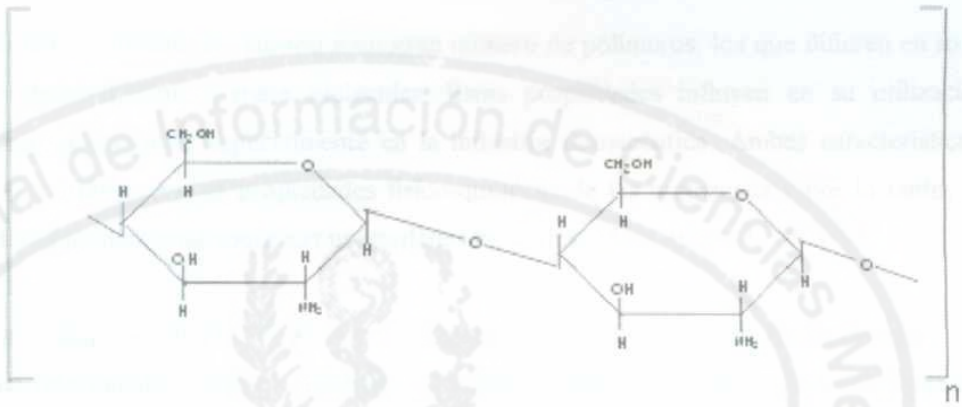

Figura 1. Estructura química de la quitosana.

El procesamiento de la quitina puede realizarce a través de métodos químicos, la N- desacetilación alcalina, o por vía enzimàtica. La quitina es parcialmente desacetilada empleando diferentes condiciones en los procesos industriales obteniendo una gran variedad de polímeros (Brugnerotto y col., 2001). Para la obtención de quitosana, los carapachos pulverizados son tratados con álcali o ácido para remover las proteínas y minerales como el carbonato de calcio y el fosfato de calcio. En el segundo paso, el producto intermediario estable para la desacetilación es tratado con solución fuerte de hidróxido de sodio a elevadas

temperaturas (Ilango y col., 1998). Cuando el grado de desacetilación (DD) es del 75% o mayor, el producto es denominado quitosana (Roberts, 1992). Este se hace más soluble en agua debido a la protonación de los grupos NH_2 en la unidad de la glucosamina. En muchos casos, el proceso de produción de la quitosana a partir de la N-desacetilación de la quitina no es completo.

Los cambios en el grado de desacetilación y masa molecular de la quitosana, causados por las condiciones en los procesos, influyen en propiedades tan importantes como la solubilidad y la viscosidad de sus soluciones (Synowiecki y Al-Khateeb, 2003). Todo esto nos demuestra la necesidad de la estandarización de la quitina y la quitosana.

2.2 Propiedades físico-químicas de la quitosana

El término quitosana es referido a un gran número de polímeros, los que difieren en su grado de N-desacetilación y masa molecular. Estas propiedades influyen en su utilización en muchas aplicaciones, especialmente en la industria farmacéutica. Ambas características son muy importantes en las propiedades físico-químicas de las quitosanas y por lo tanto, tienen un efecto fundamental sobre sus propiedades biológicas (Sannan y col., 1976).

La quitosana es soluble en ácidos diluidos como el ácido acético, ácido fórmico y otros ácidos relacionados, pero es insoluble en medio alcalino y pH neutro. En medio ácido, los grupos aminos del polímero son protonados originando un polisacárido soluble, cargado positivamente con una elevada densidad. Su solubilidad es altamente influenciada por la adición de sales a las soluciones. Posee una rígida estructura cristalina debido a los enlaces de hidrógeno inter e intramoleculares y a la presencia de grupos aminos e hidroxilos, originando la alta viscosidad de sus soluciones. Los requerimientos farmacéuticos de la quitosana son resumidos en la Tabla I.

Tabla I. Resumen de las propiedades físico-químicas de la quitosana (tomado de Knapczyk y col., 1989; Sanford, 1990).

Propiedades físicas	
Tamaño de partícula	< 30 µm
Densidad	1.35 - 1.40 g/cc
pH	6.5
Solubilidad	Insoluble en agua, parcialmente soluble en ácidos
Propiedades químicas	
	Poliamina catiónica
	Alta masa molecular, polieléctrolito lineal
	Viscosidad, alta a baja
	Forma quelatos con ciertos metales de transición
	Vulnerable a modificaciones químicas
	Grupos reactivos amino/hidroxilo

2.3 Aplicaciones farmacéuticas de la quitosana

Durante más de tres décadas una amplia variedad de aplicaciones farmacéuticas y médicas han sido reportadas para la quitina y la quitosana. La escasa solubilidad de la quitina constituye la razón limitante principal para su uso.

Todas las posibles aplicaciones de la quitosana son debidas a su biodegradabilidad, biocompatibilidad y no toxicidad (Singla y Chawla, 2001). La quitosana ha recibido un amplio uso en formulaciones farmacéuticas convencionales. Ha sido empleada como agente aglutinante en la granulación húmeda (Upadrashtra y col., 1992; Ilango y col., 1997; Santos y col., 2002), desintegrante (Nigalaye y col., 1990; Ritthidej y col., 1994), promotor de la disolución de fármacos pobremente solubles (Amadóttir y col., 1996; Portero y col., 1998; Thanou y col., 2001) y como excipiente retardador de la liberación de fármacos en tabletas y gránulos (Kristl y col., 1993; Tapia y col., 1993; Kristmundsdóttir y col., 1995; Sabnis y col.,

1997b). Su empleo en sistemas novedosos de liberación controlada, administración de genes y péptidos, así como los de liberación específica en el colon han sido descritos en algunos artículos de revisión (Dodane y Vilivalam, 1998; Singla y Chawla, 2001; Hejazi y Amiji,
2003).

2.4 Propiedades formadoras de películas de la quitosana

Las quitosanas de elevada masa molecular tienen buenas propiedades formadoras de películas como resultado de los puentes de hidrógeno intra e intermoleculares (Muzzarelli y Peter, 1997). Estudios recientes sobre revestimientos farmacéuticos y de alimentos con películas de quitosana han examinado la permeabilidad al vapor de agua y la absorción de humedad de esas películas (Remuñán-López y Bodmeier, 1996b; Rueda y col., 1999; Wiles y col., 2000; Nunthanid y col., 2001; Gocho y col., 2001). Han sido evaluadas también la influencia de la masa molecular así como del grado de desacetilación sobre el comportamiento de absorción de humedad, propiedades de hinchamiento y la velocidad de transmisión de vapor de agua (Wiles y col., 2000; Gocho y col., 2001). En muchos estudios han sido descritos el entrecruzamiento de las películas con compuestos hidrofílicos como la celulosa, alginato, polivinilalcohol (PVA) o polivinilpirrolidona (PVP) (Tabla II). Por otra parte, películas de quitosana conteniendo cloruro y formato han mostrado su valor como embalaje biodegradable o como soporte de películas con agentes antimicrobianos (Begin y Van, 1999).

Estudios relacionados han reportado el efecto de las propiedades físico-químicas de las películas de quitosana observándose su influencia sobre la resistencia mecánica, contenido de las películas, transmisión de vapor de agua, la masa molecular del polímero e interacción fármaco-polímero (Lim y Wan, 1995; Remuñán-López y Bodmeier, 1996b; Chen y Hwa, 1996; Nogales y col., 1997; Wiles y col., 2000; Nunthanid y col., 2001; Puttipipalklachom y col., 2001; Ritthidej yPhaechamud, 2003).

Las características de las películas de quitosana varían de un reporte a otro. Las diferencias en las fuentes de quitina empleadas para producir quitosana, las propiedades de las

quitosanas, tipos de solventes, plastificantes y los métodos de preparación de las películas constituyen las principales razones. Debido a esto, la comparación de los resultados obtenidos por diferentes investigadores se hace difícil. Adicionalmente, se ha brindado poca atención a los efectos de las condiciones de almacenamiento sobre la estabilidad de las películas de quitosana.

Polímeros hidrofilicos sintéticos y biocompatibles han resultado ser candidatos ideales en el mejoramiento de la fragilidad natural y permeabilidad de las películas o membranas de quitosana. Entre ellos, pueden citarse las mezclas de quitosana con polietilenglicol y óxido de polietileno (Alekseev y col., 2000; Alekseev y col., 2001; Zhang y col., 2002b; Parag y Rangaramanujam, 2003).

La quitosana ha sido investigada como material de recubrimiento en diferentes tecnologías de microencapsulación, por ejemplo la gelación ionotrópica (Bodmeier y col., 1989; Lim y col., 1997), procesos por evaporación del solvente (Hassan y col., 1992) y el método de extrusión (Polk y col., 1994). Mi y col. (1997b) obtuvieron microesferas de quitosana a través de los métodos de acetilación interfacial y de atomización congelante. Microesferas similares con insulina encapsulada, entrecruzadas interfacialmente con el palmitato de ascorbilo, íúeron preparadas por Aiedeh y col. (1997). Recientemente, las microesferas de quitosana entrecruzadas con el polianión de tripolifosfato de sodio y con los copolímeros del óxido de polietileno-óxido de polipropileno fueron sugeridas como transportadores de proteínas y en vacunas para administración oral (Illum, 1998). Además, la quitosana ha sido utilizada en la producción de microesferas y microcápsulas para sistemas orales de liberación controlada (Tabla II).

Este polisacárido ha sido extensivamente estudiado en la industria farmacéutica por su potencialidad en el desarrollo de sistemas de liberación controlada debido a su carácter de polímero catiónico y a las propiedades de los geles y películas que forma (Tabla II). Su capacidad para formar geles que controlan la liberación en pH ácido, sus propiedades mucoadhesivas, además de su biocompatibilidad y biodegradabilidad justifican su valor en estos sistemas.

Tabla II. Aplicaciones farmacéuticas de las películas de quitosana

Aplicación	Referencias
Películas entrecruzadas • Celulosa • Alginato • PVP/PVA • Aldehido • Pectina • Gelatina	Hosokawa y col., 1990; Hasegawa y col., 1992 Remuñán-López y Bodmeier, 1997; Liu y col., 1997 Kim y col., 1992; Nakatsuka y Andrady, 1992; Arvanitoyannis y col., 1997; Sukurai y col., 2000; Srinivasa y col., 2003 Tacharodi y Panduranga, 1993a,b Meshali y Gabr, 1993; Hoagland y col., 1999; Macleod y col., 1999a; Hiorth y col., 2003 Arvanitoyannis y col., 1998
Microesferas y Microcápsulas	Bodmeier y col., 1989; Hassan y col., 1992; Polk y col., 1994; Yao y col., 1995; Hari y col., 1996; Okhamafe y col., 1996; Remuñán-López y Bodmeier, 1996a; Lim y col., 1997
Liberación controlada	Kawashima y col., 1985; Hou y col., 1985; Meshali y Gabr, 1993; Mi y col., 1997a; Macleod y col., 1999a; Senel y col., 2000; Ritthidej y col., 2000; Gupta y Ravi Kumar, 2000; Koizumi y col., 2001; Shu y col., 2001; Hejazi y Amiji, 2003
Liberación específica en el colon	Tozaki y col., 1997; Munjeric y col., 1997; Fernández- Hervás y Fell, 1998; Lorenzo-Lamasa y col., 1998; Macleod y col., 1999b; Zhang y col., 2002a; Shimono y col., 2002; Orienti y col., 2002; Shimono y col., 2003; Zambito y Di Colo, 2003; Chourasia y Jain, 2003; Hiorth y col., 2003

Un gran número de polisacáridos como la amilosa, goma agar, pectina, inulina, ciclodextrinas, dextranas y sulfato de condroitina han sido investigados en sistemas de liberación de fármacos en el colon. La quitosana también ha mostrado su valor en los sistemas de liberación colònica ya que es degradada por la microflora colònica permitiendo la liberación de los principios activos (Chourasia y Jain, 2003). Las mezclas de quitosana con algunos de estos polímeros han mostrado su eficiencia en estos sistemas (Tabla II). Debido a sus múltiples aplicaciones, la quitosana emergerá como nombre familiar y como una importante sustancia biomédica para el siglo XXI (Paul y Sharma, 2000).

Otro polisacárido natural, la amilosa de almidón (Figura 2), también ha sido estudiada por numerosos investigadores en películas de almidón en forma de solución o gel (Bader y Góritz, 1994; Lourdin y col., 1995; Rindlav y col., 1998; Palviainen y col., 2001; Krogars y col., 2003). Wolff y col. (1951) prepararon películas de amilosa plastificadas o no con glicerol. Lourdin y col. (1995) y Rindlav y col. (1998) estudiaron la influencia de la relación amilosa-amilopectina en las propiedades mecánicas de las películas. Recientemente se ha demostrado que los almidones entrecruzados poseen propiedades únicas como excipientes en los sistemas de liberación controlada de fármacos por vía oral (Lenaerts y col., 1991; Lenaerts y col., 1998).

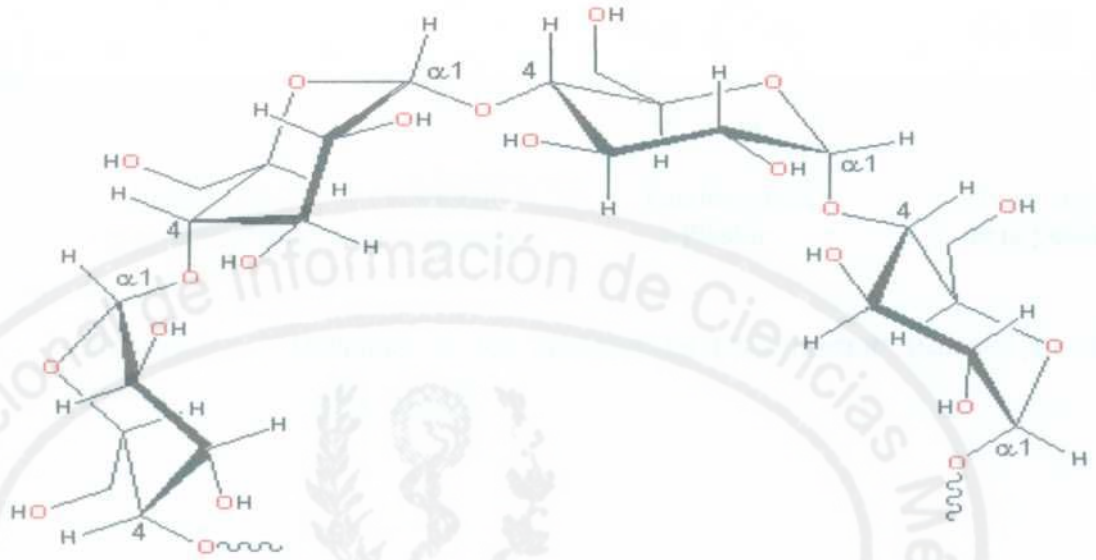

Figura 2. Estructura química de la amilosa de almidón de maíz *(HylonVH).*

Según nuestro conocimiento, ningún estudio ha sido llevado a cabo sobre el efecto de la combinación de los polisacáridos quitosana y amilosa de almidón de maíz en las propiedades de las películas y la liberación de fármacos. Consecuentemente, la preparación de estas películas combinadas pudiera mejorar las propiedades de la quitosana por lo que resulta interesante su estudio y evaluación.

2.5 Revestimiento de formas dosificadas sólidas

El revestimiento es una etapa importante en los procesos de elaboración de formas farmacéuticas sólidas que puede mejorar las características organolépticas, incrementar la estabilidad y modificar las propiedades de liberación del producto final. Los revestimientos acuosos u orgánicos son aplicados para la protección de fármacos lábiles al agua o a la luz UV, para el enmascaramiento de olores y sabores desagradables así como para el control de la liberación o del sitio de absorción. Cada uno de estos usos requiere un medio balanceado para lograr la formación de una película adecuada sobre el sustrato (Figura 3).

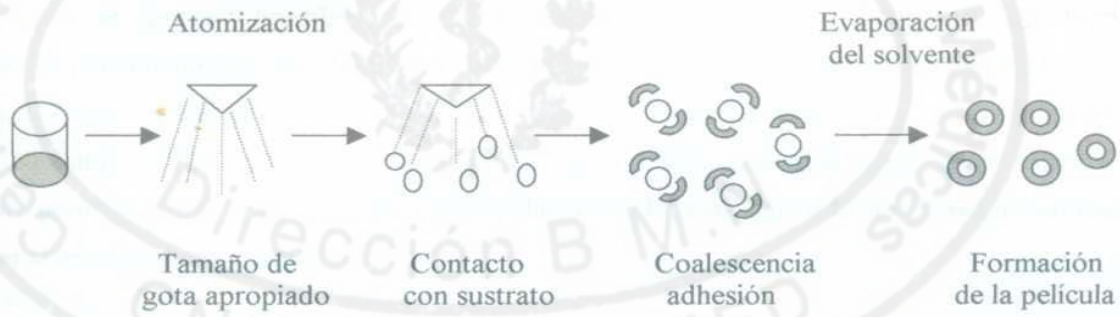

Figura 3. Dinámica de los procesos de revestimiento (tomado de Mehta, 1997).

2.6 Materiales para el revestimiento pelicular

Además del polímero, las formulaciones de revestimiento pelicular incluyen generalmente solventes, agentes plastificantes, antiadhesivos y pigmentos (Lippold y col., 1989; Bodmeier y Paeratakul, 1994).

Tiempos atrás, los solventes orgánicos fueron los más usados, sin embargo debido a los requerimientos regulatorios, la inflamabilidad y los controles sobre los residuos de los solventes en los productos recubiertos su empleo ha sido limitado. Actualmente, la tecnología de las cubiertas con películas ha cambiado hacia los sistemas acuosos. La función de un solvente es disolver o dispersar los polímeros y los aditivos para transportarlos hacia la superficie del núcleo sólido. Los principales disolventes empleados son agua, alcoholes y cetonas.

La incorporación de un plastificante mejora las propiedades mecánicas y formadoras de películas de los polímeros (Banker, 1966; Porter, 1980). Esto reduce el riesgo de que la película se agriete y posiblemente mejore la adhesión de la película al sustrato. La selección de un plastificante es una decisión muy importante con vistas a desarrollar y perfeccionar la estabilidad y las propiedades de liberación del fármaco desde la forma farmacéutica (O'Donnell y McGinity, 1997). Los plastificantes solubles en agua como el propilenglicol, los polietilenglicoles de bajo peso molecular y la glicerina han sido ampliamente utilizados en el revestimiento acuoso.

Los pigmentos comúnmente empleados en los sistemas farmacéuticos incluyen lacas de aluminio de colorantes solubles en agua, opacantes y varios materiales inorgánicos como el óxido de hierro (Felton y McGinity, 1999). Estos son adicionados para mejorar la presentación y para facilitar la identificación del producto dosificado. Las sustancias antiadhesivas se usan para prevenir la agregación de los sustratos sólidos.

Los polímeros que se utilizan en el recubrimiento pelicular de formas sólidas están basados en los polímeros celulósicos o acrílicos. Los polímeros acrílicos son comercializados con el

nombre de Eudragit*. El principal derivado celulósico empleado para retardar la liberación es la etilcelulosa. Muchos de estos polímeros han sido formulados en dispersiones acuosas coloidales (por ejemplo látex o pseudolátex) con vistas a superar los problemas asociados con el uso de las soluciones orgánicas poliméricas (Bodmeier, 1997).

Polímeros protectores y enmascaradores, hidroxipropilmetilcelulosa (HPMC) de bajo peso molecular y Eudragit E, son empleados como materiales no entéricos. Otros sustitutos celulósicos aceptables son la hidroxipropilcelulosa y la metilcelulosa, la cual ha sido reportada como retardadora de la disolución de los fármacos. Otros polímeros como el Eudragit RS y RL, producen películas para acción controlada (pH-independiente) similares a las formulaciones de etilcelulosa. Las cubiertas entéricas acuosas son posibles con Eudragit. Las mezclas con Eudragit de diferentes grados pueden ser capaces de controlar la liberación en pH desde aproximadamente 5.5 a 7.0 y también la permeabilidad de la película a pH constante (Rhodes y Porter, 1998).

Un número creciente de nuevos candidatos a fármacos son compuestos lábiles-ácidos o requieren de un sitio específico de absorción en la zona distal de tracto gastrointestinal (TGI). Las formas farmacéuticas entéricas son diseñadas para resistir las condiciones ácidas del estomágo y para que desintegren rápidamente a mayores valores de pH como los del fluido intestinal o el colon. Las películas poliméricas para cubiertas entéricas son aplicadas usualmente sobre esferas pequeñas (pellets, gránulos o microcápsulas) de preparaciones de dosis múltiples seguras, independientemente de la etapa de la digestión durante su tránsito por el TGI. Los polímeros amónicos basados en el ácido metacrílico y los ésteres del ácido metacrílico (Eudragit L y S) son ampliamente usados como polímeros entéricos. El copolímero del ácido metacrílico Eudragit S, de mayor sensibilidad al pH (relación de grupos carboxilos y unidades ésteres 1:2) también es aplicado en sistemas de liberación específica en el colon (Peeters y Kinget, 1993; Takaya y col., 1998; Nykanen y col., 2001). Otros polímeros entéricos incluyen los derivados ésteres de celulosa como el acetoftalato de celulosa y el acetato trimelitato de celulosa.

La adherencia de las películas durante el proceso de recubrimiento es una limitante que origina la aglomeración extensiva de los sustratos y consecuentemente, incrementa el número de defectos en la cubierta perjudicando el rendimiento y calidad de los lotes cubiertos. Puesto que la quitosana ha sido reportada por su potencial como aglutinante y mucoadhesivo (Upadrashta y col., 1992; Patel y col., 1999), pudiera esperarse que el comportamiento adherente de este polímero sea evidente durante el recubrimiento con película. También es conocido que las cargas positivas de la quitosana pudieran originar íuertes interacciones electrostáticas con las superficies cargadas negativamente (He y col., 1998). Durante el recubrimiento con otros polímeros celulósicos o acrílicos, ha sido reportada una indeseable e irreversible aglomeración debido a la adhesividad de los lotes, debido, principalmente a la influencia del tipo de polímero así como también del tipo y concentración del plastificante (Wesseling y col., 1999). Por lo tanto, efectivos agentes antiadhesivos fueron necesarios para mejorar la cubierta de película (Petereit y col., 1995; Wesseling y col., 1999).

2.7 Equipos y procesos para el recubrimiento pelicular

El recubrimiento pelicular usualmente es llevado a cabo empleando las técnicas de suspensión en aire (lecho fluido) o de bombos con paredes perforadas. El equipamiento y la creación de condiciones óptimas de procesamiento son fundamentales para obtener un buen proceso de recubrimiento de película, así como disponer de una solución de cubierta apropiada (Seitz y col., 1986; Mehta, 1997). Las innovaciones en la tecnología del equipamiento de recubrimiento, especialmente la introducción del equipo Wurster, han sido esenciales para estimular el interés por la tecnología del recubrimiento pelicular en la investigación, diseño y desarrollo de formas dosificadas.

Las condiciones óptimas de recubrimiento varían de un producto a otro. La magnitud del estrés interno que inevitablemente se genera durante el proceso de revestimiento, es dependiente de la interrelación entre numerosos parámetros que involucran tanto al material polimèrico de cubierta como al sustrato (Okutgen y col., 1995).

La calidad de un producto recubierto está influenciado grandemente por las variables del proceso empleadas en la operación de revestimiento, por lo que se hace necesario estudiar sus efectos (Figura 4). El significado de estas variables y los factores de escalado son dependientes del tipo de equipamiento y proceso.

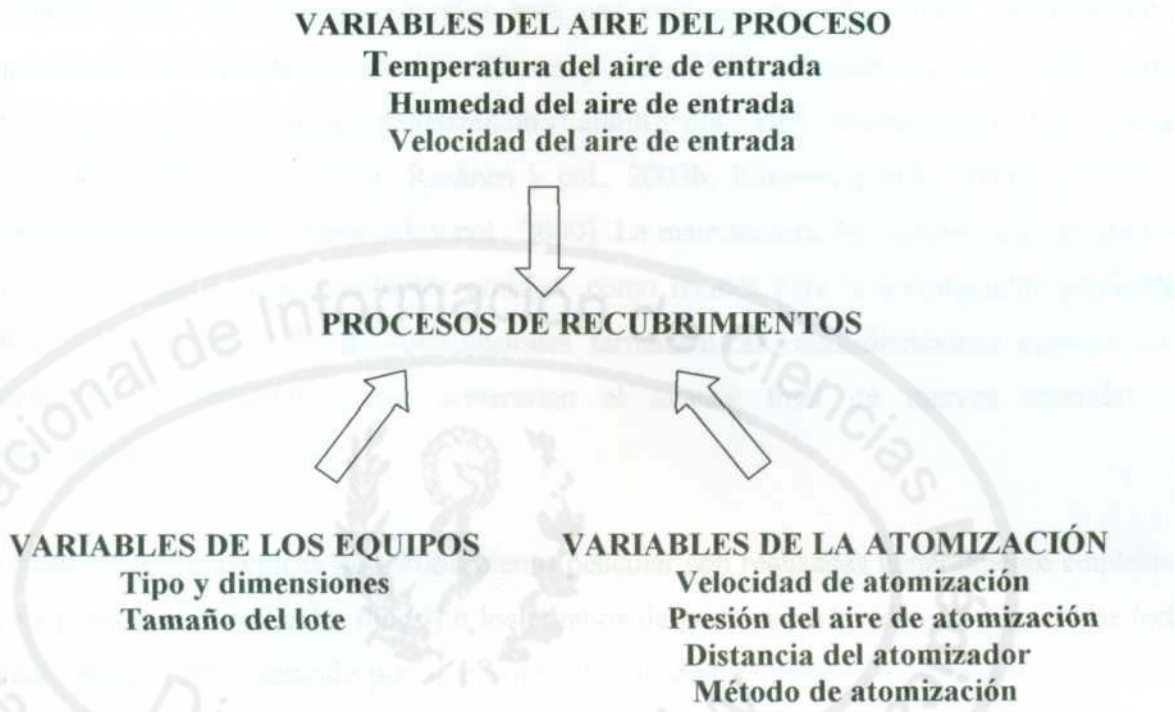

Figura 4. Variables críticas en los procesos de recubrimiento.

Debido al interés creciente en la tecnología de recubrimiento acuoso, significativos progresos han sido alcanzados en el diseño de equipos. El mejoramiento en las capacidades de secado ha permitido el incremento del uso de las formulaciones de recubrimiento acuoso. Por lo tanto, las condiciones operativas requieren ser establecidas para definir las necesidades de procesamiento final con vistas a lograr procesos cada vez más controlados y reproducibles.

2.8 Procesos de recubrimiento pelicular a pequeña escala

El número creciente de nuevos y costosos candidatos a fármacos, ha motivado el interés por desarrollar y diseñar pequeños equipos de manufactura muy útiles en las primeras etapas de formulación de un producto terapéutico. En años recientes, algunos equipos novedosos a pequeña escala han sido introducidos para una variedad de aplicaciones que incluyen las operaciones de mezcla/granulación (Nunes y col., 1990; Marechal y col., 1997; Rowe, 2000), granulación húmeda y pelletización (Landin y col., 1996; Rowe, 2000; Bock y Kraas, 2001; Murtomaa y col., 2002; Rásánen y col., 2003b; Rásánen y col., 2004), así como la compresión de tabletas (Hancock y col., 2000). La manufactura de sistemas miniaturizados o de pequeña escala ofrece múltiples ventajas, como técnica para la investigación profunda y efectiva en el desarrollo de formulaciones farmacéuticas, consideraciones económicas y cuestiones de seguridad, que acelerarían el avance final de nuevos candidatos a medicamentos.

A gran escala las técnicas de recubrimiento pelicular son realizadas generalmente empleando la suspensión en aire (lecho fluido) o los bombos de paredes perforadas. El proceso de lecho fluido, equipo bien conocido por su elevada eficiencia en el secado, ha sido empleado para el recubrimiento rápido de tabletas, gránulos o cápsulas. El recubrimiento pelicular de materiales fluidizados puede ser aplicado con atomizadores situados en la parte superior, inferior (Wurster) o tangencialmente.

Hasta hoy, se le ha brindado muy poca atención al desarrollo de sistemas miniaturizados o de pequeña escala para el recubrimiento pelicular y muy pocos trabajos están disponibles en la literatura (Thoma y col., 1986; Alkan y col., 1988). Esto se debe, obviamente, al gran desafio que supone la comprensión de los fenómenos termodinámicos y las relaciones existentes en el revestimiento a pequeña escala y las dificultades para controlar los procesos multivariados en bombos perforados o en lecho fluido a muy pequeña escala.

La Federación Europea de las Ciencias Farmacéuticas ha establecido un proyecto denominado “New safe medicines faster” con vistas a acelerar los procesos, generalmente

lentos y costosos, de desarrollo de nuevos fármacos. Entre sus principales líneas de trabajo se encuentra la creación de sistemas miniaturizados automatizados, ganando el interés de muchos investigadores en la industria farmacéutica (Bjerrun, 2002). Algunos prototipos de estos equipos están siendo producidos y comercializados por la firma Caleva Process Solutions (Rowe, 2000). Un reciente e interesante acercamiento en esta área es el equipo miniaturizado para el recubrimiento de película (Caleva) con atomizador superior que genera el lecho fluido de pequeñas esferas mediante vibración mecánica y flujo de aire empleado en este trabajo.

2.9 Estudio de películas aisladas

Durante el desarrollo de un sistema de recubrimiento pelicular, la evaluación de las películas ha sido establecida como una herramienta valiosa para caracterizar y evaluar las propiedades fundamentales del recubrimiento (Li y Peck, 1989).

Las formulaciones de películas deben ser evaluadas preliminarmente a través de los métodos de atomización o el moldeo por vaciamiento. Una película farmacéutica adecuada es dura, resistente y sin quebraduras, caracterizada por una elevada resistencia a la fractura, moderada elongación a la fractura y un elevado módulo de Young (Lever y Rhys, 1968; Aulton, 1982).

Los datos de esfuerzo-deformación pueden ser utilizados para definir las propiedades mecánicas de las películas y compararlos en función de algunos factores de formulación como la combinación de polímeros, plastificantes, sistemas de solventes y otras propiedades (Banker, 1966). El ensayo de resistencia a la fractura es uno de los mejores medios para optimizar el nivel de los aditivos en las formulaciones (Seitz y col., 1986).

La humedad tiene un efecto sinèrgico sobre la mayoría de los plastificantes al disminuir la temperatura de transición vitrea del polímero y hacerlos más flexibles (O'Donnell y McGinity, 1997). La variación del contenido de humedad sobre las películas influye en la permeabilidad del polímero. Por lo tanto, los estudios de estabilidad son necesarios para obtener evidencias sobre la protección que brindarán las películas.

La estabilidad física y química de los productos recubiertos puede ser afectada con el tiempo y las condiciones de almacenamiento. Durante el envejecimiento, factores ambientales como la temperatura, humedad y la exposición a la luz pueden originar inestabilidades físicas en las películas, cambios de color o velocidades de liberación de los fármacos no predecibles desde las formas dosificadas recubiertas (Figura 5).

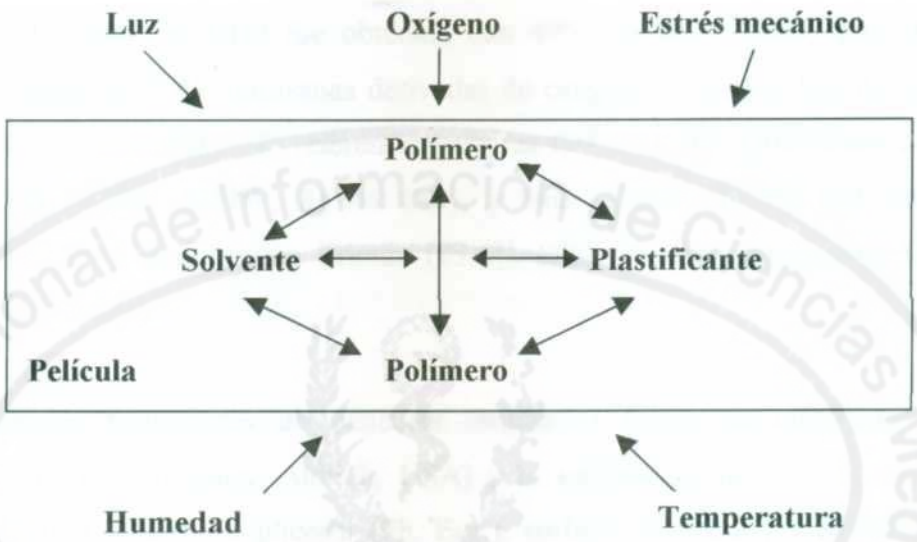

Figura 5. Influencia de los parámetros físicos y químicos sobre la estabilidad de las películas (modificado de O'Donnell y McGinity, 1997).

3. Materiales y Métodos

3.1 Materiales

Las quitosana 1 (CH1) y quitosana 2 (CH2), fueron obtenidas en la empresa "Mario Muñoz" del grupo QUIMEFA del MINBAS, por N-desacetilación de la quitina de langosta. La quitina fue suspendida en una solución alcalina, 45% NaOH, a 130°C por 30 min para obtener CH1, mientras CH2 fue obtenida con 49% NaOH a 130°C por 30 min. Cuatro muestras comerciales de quitosanas derivadas de cangrejo o carapachos de camarón fueron utilizadas como materiales de referencia para las CH1 y CH2. Quitosanas de alta (HMW, 79.0% DD), media (MMW, 81.4% DD), y baja (LMW, 85.0% DD) masa molecular (Aldrich, USA) y la quitosana Primex (85.6% DD) (Primex Ingredients ASA, Noruega) fueron empleadas (I).

Los materiales formadores de películas estudiados fueron la quitosana de alta masa molecular (HMW-quitosana, Aldrich, USA) y la amilosa de almidón de maíz *{Hylon VII*, National Starch, USA). El glicerol (Ph. Eur.), sorbitol (Ph. Eur.) y el i-eritritol (Sigma®, Suiza), 20% m/m del peso del polímero, fueron utilizados como plastificantes y el ácido acético (Riedel-de Haén, Alemania) y el agua purificada como solventes (II, III).

Para el recubrimiento entérico, la solución básica de recubrimiento contenía un 7.5% (m/m) del polímero entérico (Eudragit® S 100, Rohm Pharma GmbH, Alemania), el dibutilftalato (Fluka, Suiza) como plastificante (10% m/m del peso del polímero), etanol absoluto (Primalco, Finlandia) y agua purificada en relación de 9:1 como sistema de solvente (IV). La composición de los núcleos de los pellets utilizados en los experimentos de recubrimiento fue la siguiente: teofilina anhidra (Ph. Eur.) 5%, lactosa monohidratada (Pharmatose 80M, DMV International, Países Bajos) 35%, celulosa microcristalina (Emcocel 90M, E. Mendell, USA) 60% y agua purificada como líquido de granulación (IV, V).

En los experimentos de recubrimiento acuoso, las soluciones de cubierta contenían HMW- quitosana, hidroxipropilmetilcelulosa (HPMC, Methocel E5, Dow Chemical, USA), ácido

acético (Riedel-de Haèn, Alemania), y glicerol (Ph. Eur.) en agua purificada. Como agentes antiadhesivos fueron utilizados el estearato de magnesio (Ph. Eur), dióxido de titanio (TiO_2, Ph. Eur), dióxido de silicio coloidal, aerosil (SiO_2, Ph. Eur.) y monoestearato de glicerilo (GMS, Genay, Francia). En la preparación de los núcleos de las tabletas para la determinación del ángulo de contacto se emplearon los siguientes excipientes: celulosa microscristalina (Emcocel 90M, E. Mendell, Nastola, Finlandia), lactosa monohidratada (Pharmatose 80M, DMV International, Veghel, Países Bajos) y estearato de magnesio (Ph Eur.) (V).

El esquema de trabajo seguido en el presente estudio se ilustra en la Figura 6. Las publicaciones originales son referidas en el organigrama con números romanos I-V.

3.2 Caracterización físico-química de la quitosana

3.2.1 Determinación de la masa molecular (1)

La masa molecular promedio (MW) de las quitosanas fue calculada a partir de la relación clásica de Mark-Houwink,

$$[\eta] = K_m(MW)^a$$

donde [r|] = viscosidad intrínseca, K_m = 1.81 x IO'^{3} *y a* = 0.93 (Ravi Kumar, 2000). La viscosidad relativa fue determinada por triplicado empleando un viscosimetro Ubbelohde a temperatura constante de 25.0 ± 0.1°C.

3.2.2 Viscosidad (I)

Las mediciones de viscosidad de las soluciones al 1% de CHI y CH2 en 1% ácido acético, respectivamente, fueron realizadas en un viscosimetro digital Brookfield (Model DV-II +, Stoughton, USA) con un husillo LV número 1 a la temperatura de 25.0 ± 0.1°C.

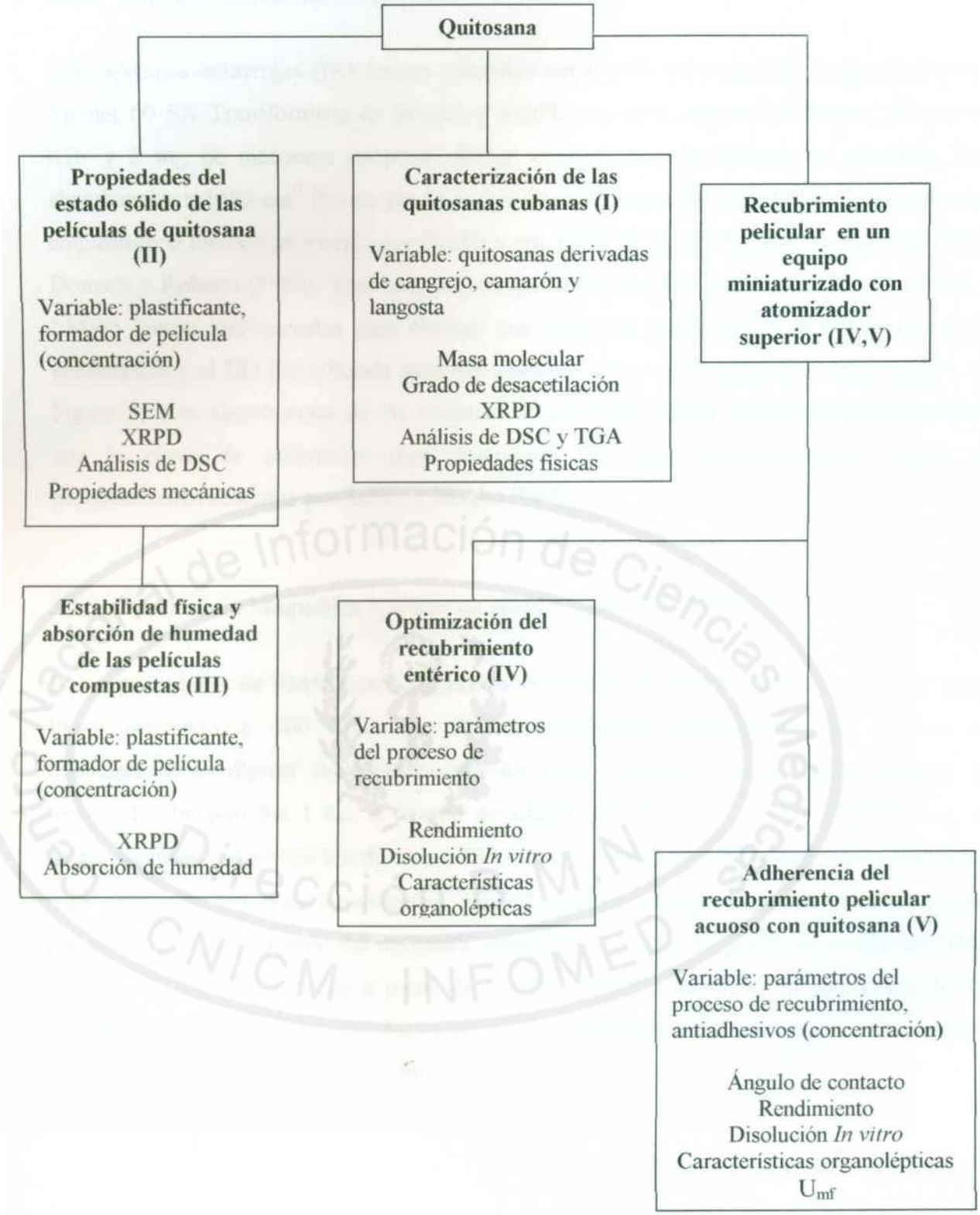

Figura 6. Organigrama del estudio.

3.2.3 Espectroscopia Infrarroja (I)

Los espectros infrarrojos (IR) fueron obtenidos empleando un espectrofotómetro Infrarrojo Nicolet 60 SX Transformada de Fourier y pastillas de KBr. Aproximadamente 150 mg de KBr y 2 mg de quitosana en polvo fueron empleados para elaborar las muestras. Las absorbancias a 1655 cm^{-1} (banda amida I) y 3450 cm^{-1} (banda hidroxilo) fueron determinadas empleando el método propuesto por Baxter y col. (1992) y las modificaciones reportadas por Domszy y Roberts (1985). Tres muestras de quitosana con DD conocidos (HMW, MMW y LMW) fueron seleccionadas para obtener una curva de calibración y la relación entre la absorbancia y el DD fue utilizada para determinar el DD de las quitosanas desconocidas (I, Figura 2). Las absorbancias de las muestras de quitosana fueron analizadas conjuntamente con la curva de calibración para determinar sus DD correspondientes, según los procedimientos descritos por Sabnis y Block (1997a).

3.2.3 Resonancia Magnética Nuclear en estado sólido (^{13}C RMN) (1)

Los experimentos de RMN fueron realizados empleando el espectrofotómetro Varían Unity Inova operando a 300 MHz por ^{1}H de frecuencia, combinando las técnicas de desacoplamiento dipolar del protón, spin de ángulo mágico y polarización cruzada. El tiempo de contacto fue 1 ms, el tiempo de adquisición 51.2 ms y el de relajación 4 s. El ancho del pulso del protón fue de 6 µs y 18 kHz. Un número de 2000 scans fueron realizados para cada espectro. Los corrimientos químicos fúeron externamente comparados con la resonancia del grupo metilo del hexametilbenceno a 17.3 ppm. El grado de acetilación (DA) de la quitosana fue calculado a partir de las intensidades relativas de la resonancia de los carbonos (I_{c1}. I_{c2}, I_{c3}. I_{c4}, I_{c5} ,I_{c6}) y el carbono del metilo I_{cH3}) obtenido con el espectro ^{13}C RMN (Ottoy y col., 1996).

3.2.5 Difracción de rayos-X (XRPD)

Los difractogramas de los polvos (antes y después de molinados) fueron obtenidos empleando un difractómetro de rayos-X de temperatura variable (D8 Advance Bruker AXS GmbH, Karlsruhe, Alemania) (VT-XRPD) (I). Los experimentos fueron realizados con el modo de reflexión simétrico de radiación CuK$_a$ (1.54 Á). El rango angular fue desde 5° a 40° con incrementos de 0.2°, y el tiempo de medición fue de 10 s/incremento (I, II). Las cristalinidades de las muestras fueron estimadas fijando las intensidades del componente cristalino y amorfo para la curva de intensidad experimental. Las cristalinidades fueron calculadas como la razón de las integrales de las intensidades del componente cristalino y la muestra estudiada (I, II, III).

3.2.6 Calorimetría diferencial de barrido (DSC)

Los termogramas DSC de los polvos de quitosana fueron determinados empleando un calorímetro diferencial de barrido (DSC 821^e, Mettler Toledo AG, Schwerzenbach, Suiza), utilizando una corriente de nitrógeno con un flujo de 80 ml/min. Los barridos fueron obtenidos con un primer calentamiento hasta 190°C, enfriando hasta 25°C y un segundo calentamiento hasta 400°C. Cada corrida fue realizada por triplicado (I).

3.2.7 Análisis Termogravimétrico (TGA) (1)

Los termogramas TGA de los polvos de quitosana fueron obtenidos empleando un analizador termogravimétrico (TGA/SDTA 85 l^e, Mettler Toledo AG, Schwerzenbach, Suiza), utilizando una corriente de nitrógeno de 50 ml/min. Las mediciones fueron obtenidas desde 25-250°C y la pérdida de peso fue calculada a partir de tres determinaciones.

3.2.8 Propiedades físicas de los polvos (I)

Las densidades real, de asentamiento y de vertido de los polvos fueron determinadas según el método de la Farmacopea Europea (2002). La densidad real de los materiales fue estimada empleando un picnòmetro (Micrometrics, Model 1305, Norcroos, GA) y el helio como gas inerte, y las restantes con el analizador de densidades vibracional estandarizado (Erweka SVM1, Erweka GmbH, Heusenstamm, Alemania). Los resultados son el promedio de tres determinaciones. El índice de Carr y el de Hausner fueron calculados a partir de las densidades de asentamiento, de vertido y real (Wells y Aulton, 1998). Los valores experimentales fueron procesados según el análisis de varianza (ANOVA). Cuando fueron obtenidas diferencias estadísticamente significativas ($p < 0.05$), fue realizado el test de Tukey HSD.

3.3 Preparación y evaluación de las películas de quitosana

3.3.1 Preparación de las películas (II, III)

Soluciones poliméricas sin plastificar y plastificadas (1% m/m) fueron preparadas por disolución de la quitosana en una solución de ácido acético diluido (1%) a la temperatura de 21± 2°C. Los plastificantes (contenido de plastificante basado en el peso del polímero = 20% m/m) empleados fueron glicerol, sorbitol y eritritol (II).

Las soluciones poliméricas acuosas contenían un 2% (m/m) del formador de película (mezcla de quitosana-HMW y *Hylon VII),* glicerol o eritritol como plastificantes (20% m/m del peso del polímero), ácido acético (1%) y agua purificada. Las composiciones de las soluciones de quitosana- *Hylon VII* estudiadas fúeron: 100:0%, 80:20%, 60:40%, y 50:50% con glicerol; 100:0%, 80:20% y 60:40% con eritritol. Las soluciones de *Hylon Vil* fúeron mezcladas con las soluciones de quitosana aproximadamente a 50 - 60°C (II, III).

Para la preparación de las películas se añadieron 8.0 g de la solución polimèrica en moldes de politetra-fluoroetileno (Teflon*). Las películas fúeron secadas durante 4 h a 60°C y

estabilizadas en una desecadora al menos 24 h a 21± 2°C y 60% HR antes del análisis (II, **III)**

3.3.2 Difracción de rayos-X (XRPD)

Los espectros XRPD de los polvos y las películas fueron obtenidos empleando el difractómetro de rayos-X (D8 Advance Bruker AXS GmbH, Karlsruhe, Alemania) con radiación CuKa (1.54 Á) (II, III). Las muestras fueron escaneadas desde 5 - 40° (2θ) con un incremento de 0.02° y un tiempo de medición de 10 s/incremento. La determinación de la cristalinidad se realizó según lo descrito en la sección 3 .2.5 (II).

3.3.3 Calorimetría diferencial de barrido (DSC)

Los termogramas de los polvos y las películas de quitosana fúeron determinados empleando un calorímetro diferencial de barrido (model 910 DSC, TA Instruments, USA). Las muestras de 2 - 5 mg fueron debidamente pesadas en depósitos de aluminio sin sellar. Las mediciones fueron obtenidas a una velocidad de calentamiento de 10°C/min desde 60 - 400°C (II).

3.3.4 Determinación de la resistencia mecánica (II)

El equipo analizador de materiales Lloyd LRX (Lloyd Instruments Ltd., Inglaterra) fue utilizado para determinar las propiedades mecánicas de las películas. Las determinaciones fueron realizadas empleando un esfuerzo de carga de 2000 N y una velocidad de carga cruzada de 5 mm/min. Cinco determinaciones paralelas fueron realizadas para cada muestra, reportándose la resistencia a la fractura final y el porciento de elongación.

3.4 Estudio de estabilidad de las películas de quitosana (III)

Las películas de las mezclas binarias de quitosana-HMW y *Hylon VII* (80:20%) y (60:40%) plastificadas con glicerol o eritritol fueron almacenadas a 25°C / 60% HR y 40°C / 75% HR durante 3 meses (III).

3.4.1 Difracción de rayos-X (XRPD)

Los materiales puros fueron analizados en el rango angular desde 2^{o} a 40° (20) con incrementos de 0.1° y un tiempo de medición de 5 s/incremento (III). Los espectros XRPD para las películas (15 días, 1, 2, y 3 meses) fueron determinados en una amplitud angular desde 5^{o} a 40° en 20 con incrementos de 0.02° y un tiempo de medición de 10 s/incremento. La determinación de la cristalinidad se realizó según lo descrito en las secciones 3.2.5 y 3.3.2, respectivamente (III).

3.4.2 Isotermas de absorción de humedad (III)

Las isotermas de absorción de humedad fúeron determinadas mediante la colocación de los polvos y las películas binarias de quitosana-HMW y *Hylon Vil* en ambientes de humedad controlada a temperatura constante. Los polvos y películas secos fúeron colocados en las siguientes humedades relativas: 0%, 11%, 23%, 33%, 43%, 52%, 59%, 75%, 85% y 95%. Las muestras completamente secas y pesadas en los frascos fueron mantenidas en las desecadoras por 9 días a 21 ± 2°C. La ganancia de peso de los polvos y las películas fúe determinada a los 2, 5 y 9 días. Las mediciones fueron realizadas por triplicado determinándose el equilibrio de absorción de humedad (EMC).

3.4.3 Espectroscopia de Infrarrojo Cercano (NIR) (III)

Los espectros del infrarrojo cercano (NIR) fueron determinados con un espectrofotómetro de Transformación de Fourier (FT)-NIR (Bomem MD-160 DX, Hartmann & Braun, Quebec, Canadá) Los espectros fueron registrados en un rango de 10,000-4000 cm^{-1} con una resolución de 16 cm-1 y un promedio superior a las 32 corridas. Las transformaciones de la segunda derivada de la absorbancia, log (1/R), fueron realizadas según el ajuste propuesto por Savitzky-Golay (Savitzky y Golay, 1964) empleando el software Matlab (v. 5.3, MathWorks Inc., Natick, MA, USA).

3.5 Recubrimiento pelicular de los pellets

3.5.1 Preparación de los núcleos de pellets (IV, V)

Los pellets fueron producidos empleando el equipo de extrusión-esferonización NICA (NICA System AB, Suecia). La fracción de tamaño comprendida entre 1.00-1.25 mm fue utilizada en los experimentos de recubrimiento subsiguientes (IV, Tabla 1) (V, Tabla 3).

3.5.2 Recubrimiento pelicular de los pellets en un equipo miniaturizado con atomizador superior (IV, V)

Los revestimientos fueron aplicados en un equipo de revestimiento miniaturizado de suspensión en aire con atomizador superior (Caleva Mini Coater, Caleva Process Solutions, Dorset, Reino Unido) (Figura 7) (IV, V).

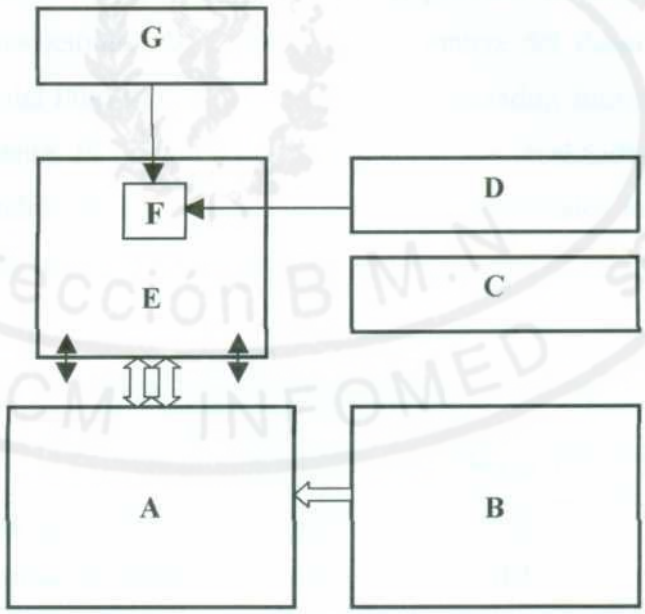

Figura 7. Diagrama del equipo de recubrimiento miniaturizado Caleva con atomizador superior. Clave: (A) unidad de calentamiento, (B) suministrador del flujo de aire, (C) microprocesador de la bomba de la jeringuilla, (D) jeringuilla, (E) cono de vibración mecánica, (F) atomizador y (G) suministrador de aire comprimido a baja presión.

En el presente estudio, cada lote recubierto fue de 20.0 g de pellets. El incremento teórico fue del 20% (m/m) del peso total de los pellets (IV).

En la fase preliminar del estudio, cinco parámetros independientes fueron evaluados mediante un diseño factorial fraccionado. Las variables estudiadas fueron la temperatura del flujo de aire, X_1 (30, 40 y 50°C), presión del aire de atomización, X_2 (0.2, 0.3 y 0.4 bar), velocidad de atomización de la solución de revestimiento, X_3 (25, 40 y 55 ml/h), velocidad del fújo de aire, X_4 (4.0, 5.0 y 6.0 m/s), y la posición (altura) del atomizador, X_5 (120, 140 y 160 mm). La modelación se realizó empleando el sistema Modde for Windows (Versión 3.0, Umetrics, Umeá, Suecia). El número total de experimentos (realizados en forma aleatoria) fúe de 19 (IV).

Basados en los resultados de la fase preliminar, un diseño experimental compuesto central (CCD) fue realizado con el objetivo de optimizar el proceso de revestimiento pelicular a pequeña escala. Las condiciones experimentales y la matriz del diseño se muestran en la Tabla III. La velocidad del flujo de aire y la altura del atomizador, fúeron ajustados a 6.0 m/s y 120 mm, respectivamente. El número total de experimentos (realizados aleatoriamente) fue de 17. Para la optimización final del proceso, cinco lotes adicionales fúeron elaborados a la menor velocidad de atomización de la solución de revestimiento (25 ml/min) (IV).

Tabla III. Niveles del diseño experimental compuesto central (CCD).

Factor	Nivel -1	Nivel 0	Nivel 1
Temperatura del flujo de aire (°C)	50	60	70
Presión del aire de atomización (bar)	0.4	0.5	0.6
Velocidad de atomización (ml/h)*	25	55	75

* Los niveles más bajos ensayados fueron -1 (25 ml/h) y-0.6 (35 ml/h).

3.5.3 Evaluación de los pellets recubiertos (IV, V)

Las respuestas evaluadas a los pellets con cubierta entérica fueron la resistencia gástrica *in vitro*, el rendimiento y la calidad del lote (apariencia de la película de cobertura). Los

ensayos de disolución fueron realizados con el aparato I USP (método de cesta) a 50 rpm. El medio ensayado fue de 900 ml de HC1 0.1 N a 37.0 ± 0.3°C (IV). Las muestras fueron analizadas por espectrofotometría UV (Perkin-Elmer, Analytical Instruments, Norwalk, CT, USA) a una longitud de onda de 273 nm para la teofilina. El rendimiento de los pellets no aglomerados fue obtenido mediante la tamización cuidadosa de los lotes cubiertos a través de un tamiz de 1.8 mm y pesando la masa de pellets que atravesaba el tamiz. La apariencia física de los pellets cubiertos fue determinada por expertos mediante inspección visual (asignando un rango de puntuación desde 1 a 10) (IV, V).

3.6 Determinación de la adhesividad de los pellets cubiertos con quitosana (V)

3.6.1 Determinación del ángulo de contacto

Para la determinación del ángulo de contacto, soluciones acuosas no plastifícadas y plastificadas de quitosana-HMW al 0.5, 1.0 y 1.5% fueron preparadas disolviendo la quitosana en una solución de ácido acético diluido con glicerol. La solución acuosa de HPMC al 10% m/m plastifícada con glicerol fue utilizada como solución de referencia. Dos tipos de tabletas (Tabla IV), fueron comprimidas en una máquina tabletera Korsch EK-0 de simple impacto (Erweka Apparatebau, Alemania) manteniendo constante la altura.

Tabla IV. Composición de los núcleos de tabletas empleados en la determinación de los ángulos de contacto.

Formulación	Composición (%)	
	Tableta I	Tableta II
Lactosa monohidratada	99.0	49.5
Celulosa microcristalina	-	49.5
Estearato de magnesio	1.0	1.0

Los ángulos de contacto entre las soluciones y los núcleos de tabletas fueron determinados a través del método de la gota impregnada (Optical Contact Angle Meter CAM 200, KSV Instruments Ltd.) según un diseño experimental dos factorial (V, Tabla 2).

3.6.2 Procedimiento de revestimiento pelicular (V)

La composición básica de las soluciones de revestimiento fue de 1% de quitosana-HMW en ácido acético diluido (1%) plastificadas con glicerol (20% m/m del peso del polímero). Cada lote recubierto estuvo compuesto por 8.0 g de pellets.

Un diseño factorial 3^2 fue empleado para el análisis de las variables de posición (altura del atomizador, X_1 (120, 140 y 160 mm) y la temperatura del flujo de aire, X_2 (50, 60 y 70°C). Las velocidades de atomización, flujo de aire y la presión de atomización del aire, fueron ajustadas a 15 ml/h, 6.0 m/s y 0.5 bar, respectivamente. El incremento teórico fue del 3 % (m/m) del peso total de los pellets. Ocho lotes adicionales fúeron realizados para investigar el efecto de cuatro agentes antiadhesivos, estearato de magnesio, dióxido de titanio, dióxido de silicio coloidal y el GMS (en los valores de 0.1 y 0.3%), sobre la adhesividad de los pellets durante el proceso de revestimiento.

El rendimiento y calidad (apariencia de la película de cubierta) fueron utilizados como indicadores de la adhesividad de las películas. El rendimiento fúe obtenido según lo descrito en la sección 3.5.3. La disolución *in vitro* de los pellets fúe realizada en el aparato I USP (método de cesta). El medio de disolución fúe de 900 mi de buffer fosfato pH = 6.8 y 7.4 a 37.0 ± 0.1°C. Las muestras fúeron analizadas según lo descrito en la sección 3.5.3.

3.6.3 Determinación de la adhesividad de las películas en los pellets cubiertos

Un equipo de lecho fluido de pequeño formato (Ariacon Oy, Helsinki, Finlandia) fue empleado para estudiar la tendencia de adherencia y las propiedades de flujo de los pellets cubiertos. Este sistema de lecho fluidizado y su instalación ha sido descrito en detalle con anterioridad (Rásánen y col., 2003a). La velocidad mínima de fluidización experimental, (//mf) fue determinada a partir del incremento y la disminución de las velocidades. El tamaño de las muestras de pellets fue de 5 mi equivalente a 2-4 g. Los pellets fueron fluidizados por el incremento paulatino del flujo de aire hasta 400 ml/s manteniendose durante 1 min a velocidad constante (400 ml/s). Posteriormente, la velocidad de fluidización del aire fue disminuida gradualmente hasta cero. Los pellets sin revestir fueron utilizados como muestra de referencia representando un producto fácilmente fluidizable (antiadhesivo). Las determinaciones fueron realizadas en condiciones idénticas. La muestra de referencia fue analizada por triplicado y las otras solo una vez (V).

4. Resultados y discusión

4.1 Caracterización de las quitosanas derivadas de quitina de langosta (I)

La masa molecular de CH1 (309 000 g/mol) fue ligeramente mayor que CH2 (290 000 g/mol). Como se esperaba, el incremento en la masa molecular se corresponde con el aumento en la viscosidad intrínseca ($[\eta]_{CH1}$ = 231 ml/g y $[\eta]_{CH2}$ = 218 ml/g), atribuido a la concentración de álcali utilizada en el proceso. Con el incremento en la fortaleza del álcali el contenido de los grupos acetilo disminuye mientras que el contenido de nitrógeno aumenta, en forma de grupos aminos alifáticos primarios, originando la disminución de la viscosidad La menor viscosidad para CH2 (9.60 mPas) evidencia una masa molecular menor para la CH2 comparada con la CHI (10.2 mPas).

Los espectros infrarrojo de todos los polvos de quitosana exhibieron picos anchos correspondientes al stretching OH, lo que muestra los enlaces de hidrógeno intermoleculares de las moléculas de quitosana (Figura 8). Como resultado del proceso de N-desacetilación alcalina, se produjo el debilitamiento de la banda a 1655 cm^{-1}, correspondiente al stretching de la amida I.

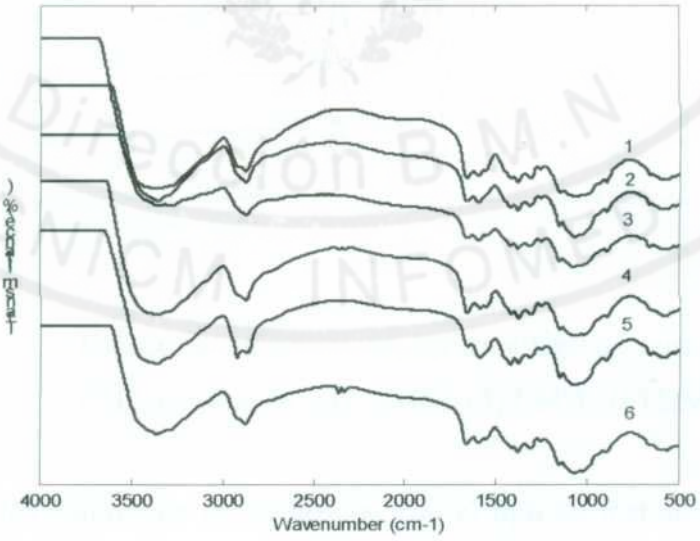

Figura 8. Espectros de transmisión infrarroja de las muestras de quitosana.
(1) CHI, (2) CH2, (3) Primex, (4) MMW, (5) LMW, (6) HMW.

Aplicando este procedimiento los valores de desacetilación obtenidos para la CH1 y la CH2 fueron entre 86 - 89%, los cuales son considerados altos grados de desacetilación.

Los espectros de ^{13}C RMN de las muestras de quitosana se muestran en la Figura 9. Los valores de DA correspondientes a la CHI y a la CH2 fueron de 0.13 y 0.10, respectivamente. Las señales del metilo y el carbonilo, asociadas con la forma monomérica de la quitina, fueron detectados en la cadena polimèrica de todas las muestras de quitosana, como consecuencia de la desacetilación incompleta de la quitina original. La muestra de quitosana- LMW mostró señales indeseables a 33 ppm debido a las impurezas (proteínas y/o lípidos) que no fueron removidas adecuadamente.

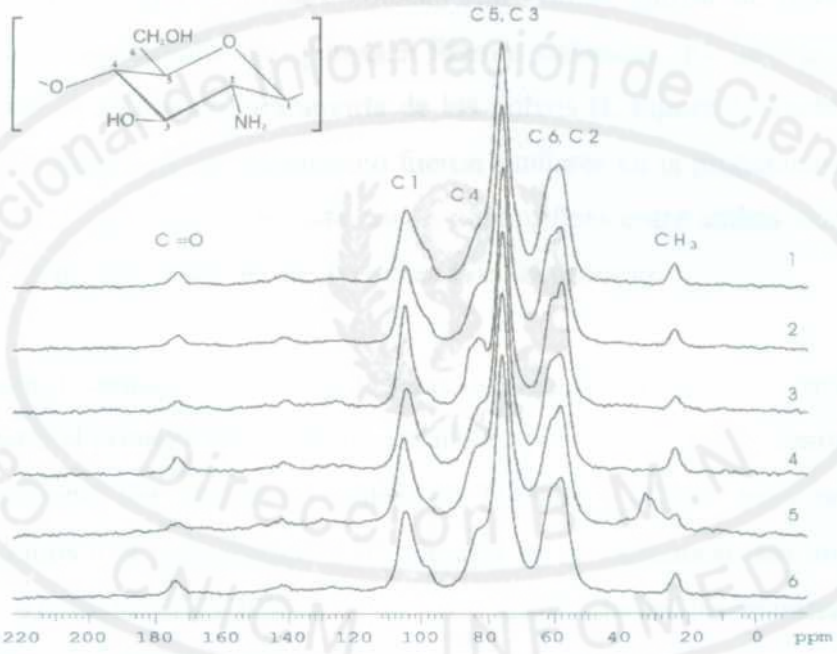

Figura 9. Espectros ^{13}C RMN de las muestras de quitosana. (1) CHI, (2) CH2, (3) Primex, (4) MMW, (5) LMW, (6) HMW.

La dependencia de los valores de desacetilación con el tipo de método analítico (Baxter y col., 1992; Khan, 2002), condiciones experimentales y método de purificación (Sabnis y Block, 1997a) ha sido reportada en la literatura. A pesar de las diferencias en las fuentes de

quitina empleadas para obtener las quitosanas estudiadas, así como los procesos para su obtención, los resultados de las CH1 y CH2 muestran valores adecuados de desacetilación y acetilación (I, Tabla 2). Sin embargo, podemos concluir que los resultados dependieron del método analítico empleado. La correspondencia en las señales de los espectros IR y ^{13}C RMN demostró la similitud estructural entre las quitosanas comerciales y las derivadas de langosta.

Todas las muestras de quitosana mostraron picos de difracción aproximadamente a 10° (20) y 20° (20), antes del molinado, y estaban parcialmente cristalinas (I, Figura 4, Tabla 3). El espectro de XRPD de la CH1 mostró reflexiones correspondientes al polimorfo L-2 a diferencia del resto de las quitosanas estudiadas. Las reflexiones de XRPD de las quitosanas CH2, HMW, MMW, LMW y Primex coincidieron con el patrón de fibra tendón de la quitosana. Cuando las muestras de quitosana fueron molinadas, un halo de difracción fue observado, indicando una estructura amorfa de los polvos (I, Figura 5, Tabla 3). Aunque la temperatura y los tiempos de procesamiento fueron similares en la preparación de las CH1 y CH2, los resultados sugieren que las diferencias polimórficas entre ambas muestras pudieran ser atribuidas a la concentración del álcali empleada en el proceso.

El comportamiento térmico de las quitosanas fúe típico al de un compuesto amorfo hidratado. Durante el primer calentamiento, un amplio pico endotérmico, centrado entre 130- 150°C, fúe observado. De acuerdo al análisis de TGA, los cambios en la pérdida de peso estuvieron atribuidos a la deshidratación, lo que está en concordancia con los resultados de DSC (I, Tabla 4). El segundo fenómeno térmico registrado en las muestras fúe un pico exotérmico de descomposición a 280-300°C.

Las propiedades físicas de las quitosanas evidenciaron la variabilidad entre las muestras (I, Tabla 5). Los valores calculados del índice de Carr y Hausner indicaron excelentes o buenas propiedades de flujo. No hubo diferencias significativas entre las CH1 y CH2 en cuanto a sus densidades de vertido, asentamiento y real y las propiedades de empaquetamiento ($p > 0.05$), mientras que las diferencias en las propiedades de flujo si fueron significativas ($p < 0.05$).

Estudios anteriores, referentes a la caracterización de quitosanas derivadas de langostas han sido realizados por Nieto y col. (1991) y Nieto y col. (1993). El empleo de las técnicas de ^{13}C RMN, difracción de rayos-X de sólidos con temperatura variable, así como la determinación de las propiedades físicas de las muestras de quitosana, incluyendo la utilización de la microscopía electrónica de barrido, se aplican por primera vez en el presente estudio. Por tal motivo, resultan novedosos los estudios de caracterización y comparación con muestras comerciales realizados al respecto.

Los resultados obtenidos para las quitosanas cubanas demuestran la factibilidad de su producción, a partir de exoesqueletos de langostas, con características químico-físicas similares a las muestras comerciales empleadas. El estudio de caracterización evidenció la dependencia de las propiedades con el proceso de obtención y la fuente de quitina empleada como material de partida. Las diferencias polimórficas y en las propiedades de flujo de las CH1 y CH2 requerirán, por tanto, futuras investigaciones del proceso productivo para determinar la reproducibilidad de los resultados logrados en el presente trabajo.

4.2 Propiedades mecánicas y del estado sólido de las películas acuosas de quitosana- amilosa de almidón de maíz (II)

Todas las películas de quitosana-HMW fueron claras y de color amarillo pálido, mostrando una superficie homogénea y continua (II, Figura 2). La concentración del plastificante fue similar (20% m/m basado en el peso del polímero) y suficiente para obtener películas flexibles en todas las muestras estudiadas, excepto aquellas que contenían sorbitol. Remuñán y Bodmeier (1997) sugirieron como rango posible de utilización del glicerol en películas de acetato de quitosana entre el 10-20%, lo que demuestra la concordancia de nuestros resultados con los obtenidos previamente para este plastificante. La incorporación de la amilosa de almidón de maíz *{Hylon VII)* aumentó el espesor de las películas, respecto a las películas simples de quitosana-HMW (II, Tabla 2).

La difracción de rayos-X de la quitosana-HMW mostró su estado cristalino (II, Figura 3). Al procesar la quitosana en películas, fue observado un estado amorfo de las películas

independientemente del tipo de plastificante empleado. Todas las películas de las mezclas binarias de quitosana-*Hylon VII* fueron amorfas.

Los termogramas de DSC de la quitosana y sus películas exhibieron picos exotérmicos a 280 - 300°C indicando la descomposición del polímero. La ausencia de eventos endotérmicos, además del que aparece aproximadamente a 35 - 160°C, demostró que las películas de quitosana eran amorfas. Esto también fue confirmado a través de los resultados de difracción de rayos-X.

El plastificante más adecuado fue el eritritol con los mayores valores de resistencia a la fractura **(II,** Tabla 1). La adición del eritritol aumentó la plastificación y originó una estructura polimèrica en las películas muy amorfa. El incremento de la concentración de *Hylon VII* aumentó los valores de resistencia a la fractura para las películas plastificadas con glicerol y con eritritol, pero a concentraciones mayores del 20% aproximadamente los resultados de la resistencia a la fractura disminuyeron **(II,** Figura 5-6). La concentración de *Hylon VII* no afectó la elongación a la fractura, particularmente en las películas plastificadas con eritritol.

Las películas obtenidas, no reportadas con anterioridad, mostraron propiedades tecnológicas útiles para ser valoradas en el diseño de sistemas orales de liberación controlada, de liberación específica de fármacos, multicapas y en procesos de revestimientos acuosos.

4.3 Estabilidad física y absorción de humedad de las películas acuosas de quitosana- amilosa de almidón de maíz (III)

Una vez estudiadas las propiedades del estado sólido y resistencia mecánica de las películas compuestas por quitosana-HMW y amilosa de almidón de maíz, plastificadas con glicerol y eritritol, fueron sometidas a condiciones extremas de temperatura y humedad para evaluar su estabilidad física durante 3 meses.

Los espectros de difracción de rayos-X y los valores de cristalinidad calculados para las películas plastificadas con eritritol (III, Figura 4a-c, Tabla 1) mostraron claramente cambios en la cristalinidad de las películas durante el estudio, los que parecen ser dependientes de las condiciones de almacenamiento y el plastificante.

Se observó que la capacidad del eritritol como plastificante fue afectada durante el almacenamiento de las películas a 25°C / 60% HR y a 40°C / 75% HR. Las reflexiones del eritritol cristalizado fueron observadas en las películas colocadas a 25°C / 60% HR durante 2 meses (III, Figura 4c). Las reflexiones XRPD se incrementaron haciéndose más visibles a los 3 meses. Durante el almacenamiento el estado amorfo se mantuvo de manera general, indicando que las películas estaban parcialmente cristalinas. La cristalinidad de las muestras comenzó a aumentar después de los 2 meses (III, Figura 4a-c, Tabla 1), siendo mayor en las películas almacenadas a 25°C / 60% HR que a 40°C / 75% HR. Las películas plastificadas con glicerol se mantuvieron totalmente amorfas durante el tiempo y las condiciones de estudio.

Es conocido que un plastificante efectivo debe ser capaz de interactuar y difundir con el polímero dentro del sistema pelicular, con una tendencia mínima a la migración o exudación, en el tiempo. De acuerdo a los resultados obtenidos por rayos-X, los cambios en la cristalinidad de las películas plastificadas con eritritol, mostraron su poca efectividad como agente plastificante. El aumento de la rigidez estructural de las películas, consecuentemente con la disminución de su flexibilidad, provocan una mayor porosidad afectando la resistencia mecánica de las películas y las características de liberación de los fármacos.

Con relación a los estudios de absorción de humedad, las películas acuosas de quitosana- amilosa de almidón de maíz almacenadas a 0, 23, 43, 75, y 95% HR durante 9 días mostraron un incremento sigmoidal en la absorción de humedad con el incremento de la humedad relativa. Las películas de quitosana- *Hylon VII* plastificadas con glicerol absorbieron mayor humedad que el resto de las películas estudiadas; aunque la diferencia en el agua absorbida entre ellas fue muy pequeña, excepto a las humedades relativas del 75% y

el 95% (III, Figura 2b). La absorción de agua de las películas aumentó marcadamente en función del tiempo de almacenamiento a 75% y 95% HR

El NIR mostró bandas de agua en la región de los 1800-2100 nm similares para las películas de quitosana (III, Figura 5a-d) y los materiales de partida. El agua absorbida fue aumentando gradualmente logrando un máximo de absorción a los 1920 nm. Con el incremento del contenido de humedad las bandas de agua en las películas de quitosana-HMW, aumentaron en intensidad y se desplazaron gradualmente desde 1920 hasta 1903 nm denotándose la presencia de agua libre. El análisis de los espectros no evedenció cambios en las películas como consecuencia del almacenamiento a las diferentes humedades relativas.

Los resultados obtenidos para las películas de quitosana-HMW y amilosa de almidón de maíz, recién elaboradas, mostraron al eritritol como un plastificante adecuado al mejorar las propiedades de resistencia mecánica de las mismas. Sin embargo, los estudios realizados en las condiciones de almacenamiento ensayadas demostraron su pobre estabilidad física. Por lo tanto, las respectivas películas plastificadas con glicerol constituyen un sistema con resistencia mecánica y estabilidad física adecuadas para su empleo en procesos de recubrimientos acuosos de interés farmacéutico.

4.4 Recubrimiento pelicular de los pellets en un equipo miniaturizado de revestimiento (IV)

Un reconocido copolímero del ácido metacrílico (Eudragit S), fue empleado como modelo con el objetivo de investigar el proceso de revestimiento pelicular de pellets en un equipo miniaturizado con atomización superior. Los efectos de los principales parámetros del proceso de revestimiento, sobre la resistencia gástrica y calidad de los pellets cubiertos, fueron evaluados y optimizados empleando el método de superficie respuesta.

En el estudio con el equipo miniaturizado de revestimiento, el incremento en la velocidad del flujo de aire produjo un aumento evidente en la eficiencia del recubrimiento (medida de la resistencia acídica de los lotes después del proceso de cobertura). Mientras que la reducción

en la presión del aire de atomización conllevó a una disminución aparente en la eficiencia del proceso (IV, Figura 2).

En la fase preliminar, el flujo de aire y su temperatura, la velocidad de atomización de la solución de recubrimiento y la posición del atomizador fueron los parámetros más importantes que afectaron las variables respuestas estudiadas. La velocidad del flujo de aire ($p < 0.01$) tuvo un efecto negativo claro en la liberación prematura del fármaco en HC1 0.1 N y un efecto positivo sobre la calidad y el rendimiento de los pellets no aglomerados. La posición (altura) del atomizador ($p < 0.05$) y la temperatura del aire ($p < 0.085$) tuvieron efectos contrarios sobre la resistencia gástrica de los pellets cubiertos (IV, Figura 3a,b), pero tuvieron menos influencia (estadísticamente no significativa) sobre la calidad y el incremento de masa de los pellets. Los efectos de la velocidad de atomización de la solución de cubierta sobre la resistencia gástrica y la calidad de los lotes (volumen aparente y número de agregados) no fúeron estadísticamente significativos.

Basados en los resultados de la fase preliminar, los parámetros de temperatura y presión del aire y la velocidad de atomización de la solución de cubierta fueron seleccionados para una subsiguiente fase de optimización (IV, Tabla 3), fijándose la altura (120 mm) y la velocidad del flujo de aire (6.0 m/s). En esta fase, la temperatura del aire ($p < 0.05$) fue estimada el parámetro más crítico que afectaba la resistencia acídica de los pellets cubiertos. El incremento de la temperatura del aire resultó en una disminución de la liberación prematura del fármaco en HC1 0.1 N, confirmando las observaciones realizadas en la fase preliminar. En cuanto al rendimiento y la calidad de los lotes, la temperatura ($p <0.01$) tuvo un efecto positivo claro, mientrás que la velocidad de atomización de la solución tuvo un efecto negativo sobre las variables respuestas estudiadas (IV, Figura 4a,b). El incremento en la temperatura del aire y la disminución de la velocidad de atomización conllevó a una mejor entericidad y uniformidad de los pellets cubiertos. Estos resultados están en concordancia con estudios precedentes sobre recubrimientos peliculares de granulos y pellets por suspensión en aire a gran escala (Wesdyk y col., 1993).

Es evidente, que el sistema de revestimiento a pequeña escala generando un lecho fluido por vibración mecánica y un flujo de aire es muy sensible a la temperatura del aire y a la velocidad de atomización de la solución. El área sombreada mostrada en la Figura 10 ilustra las combinaciones de temperatura y velocidad de atomización que satisfacen los requerimientos de ambos parámetros para una resistencia acídica in vitro (< 5.0%) y un rendimiento de pellets no aglomerados (> 80.0%).

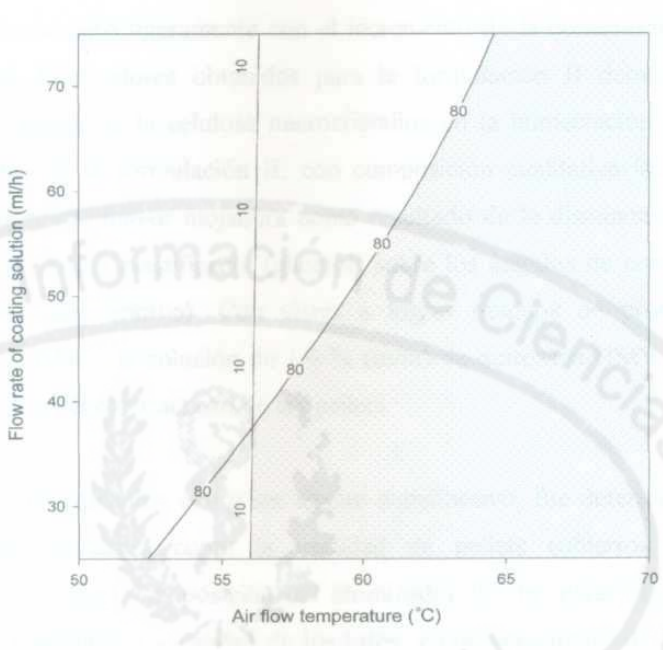

Figura 10. Gráfico de contorno ilustrando la combinación para la temperatura del aire y la velocidad de atomización de la solución de revestimiento para producir una película óptima en un equipo miniaturizado con atomizador superior.

4.5 Revestimiento pelicular acuoso con quitosana (V)

A pesar de las reconocidas propiedades como gelificante y formador de películas de la quitosana, muy poca información se dispone sobre su capacidad como material polimèrico para procesos de revestimientos acuosos. La influencia de la concentración del polisacárido

sobre el grado de humectación de sus soluciones, así como de las variables críticas en los procesos de revestimiento pelicular resultaban desconocidos determinando la necesidad del estudio de estos aspectos para las soluciones acuosas de quitosana-HMW plastificadas con glicerol.

El efecto de la concentración de la quitosana sobre los ángulos de contacto fue evidente (V, Tabla 2). Los resultados mostraron que el ángulo de contacto entre las soluciones y ambos tipos de sustratos aumentó ligeramente con el incremento de la concentración de quitosana en las soluciones. Los valores obtenidos para la formulación II demostraron el efecto positivo de la presencia de la celulosa microcristalina en la humectación del sustrato. Los núcleos de tabletas de la formulación II, con composición cualitativa idéntica a la de los pellets, evidenciaron una mayor mojadura como resultado de la disminución de los ángulos de contacto. El efecto del plastificante (glicerol) sobre los ángulos de contacto fue mínimo (estadíscamente no significativo). Con vistas a lograr tiempos de procesos menores y económicamente factibles, la solución de 1.0 % (m/m) de quitosana-HMW fue seleccionada para el recubrimiento pelicular acuoso de los pellets.

En los experimentos realizados con o sin agente antiadhesivo, fue determinada la eficiencia del recubrimiento expresada como la cantidad de pellets cubiertos no aglomerados (rendimiento) y su calidad. La posición del atomizador fue un parámetro importante que afectaba tanto el rendimiento y calidad de los lotes, y consecuentemente, la adhesividad de los pellets cubiertos con quitosana (V, Figura 1). El incremento en la temperatura del aire mejoró ligeramente la calidad de los pellets cubiertos.

En los experimentos preliminares, tanto el rendimiento como la calidad de los lotes estuvo muy por debajo de la óptima. Estos lotes no fueron muy satisfactorios (V, Tabla 4). La disolución de los pellets cubiertos en buffer fosfato (pH 6.8) fue rápida y no estuvo afectada por el proceso de recubrimiento (los valores de t5o% para todos los lotes fue de 10-12 minutos).

Es conocido que las cargas positivas de la quitosana pueden originar fuertes interacciones electrostáticas con las superficies cargadas negativamente (He y col., 1998). También sus reconocidas propiedades mucoadhesivas y de agente aglutinante (Upadrashta y col., 1992; Patel y col., 1999), pudieran justificar el comportamiento adherente de este polímero durante los procesos de recubrimiento pelicular.

Como puede observarse en la Figura 11, los valores de rendimiento aumentaron con el incremento en la concentración de los antiadhesivos empleados. La incorporación de los agentes antiadhesivos provocó una disminución clara en la adhesividad de las películas. El mecanismo a través del cual los agentes antiadhesivos actúan se basa en la capacidad que tienen para reducir los enlaces de hidrógenos existentes en las películas húmedas, formando simultáneamente un número creciente de enlaces hidrofóbicos en el sistema pelicular.

El estearato de magnesio y el GMS demostraron ser agentes antiadhesivos más efectivos que el SiO_2 y el TiO_2. Petereit y col. (1995) y Wesseling y col. (1999) sugirieron que el GMS era una alternativa prometedora frente al talco en suspensiones de cubierta de polímeros acrílicos y celulósicos siendo más efectivo y menos tóxico. Los resultados obtenidos están en concordancia con los reportados previamente para el GSM.

La mayor eficiencia en la prolongación de la liberación del fármaco debido a la incorporación del estearato de magnesio, comparada con los restantes agentes antiadhesivos, pudo estar atribuida a la interacción iónica entre los grupos amino protonados de la quitosana y los grupos carbonilos del estearato de magnesio (V, Figura 3). Esta interacción electrostática con la formación adicional de la amida y sus efectos como barrera en la prolongación de la liberación fue demostrada con anterioridad (Ritthidej y col., 2000).

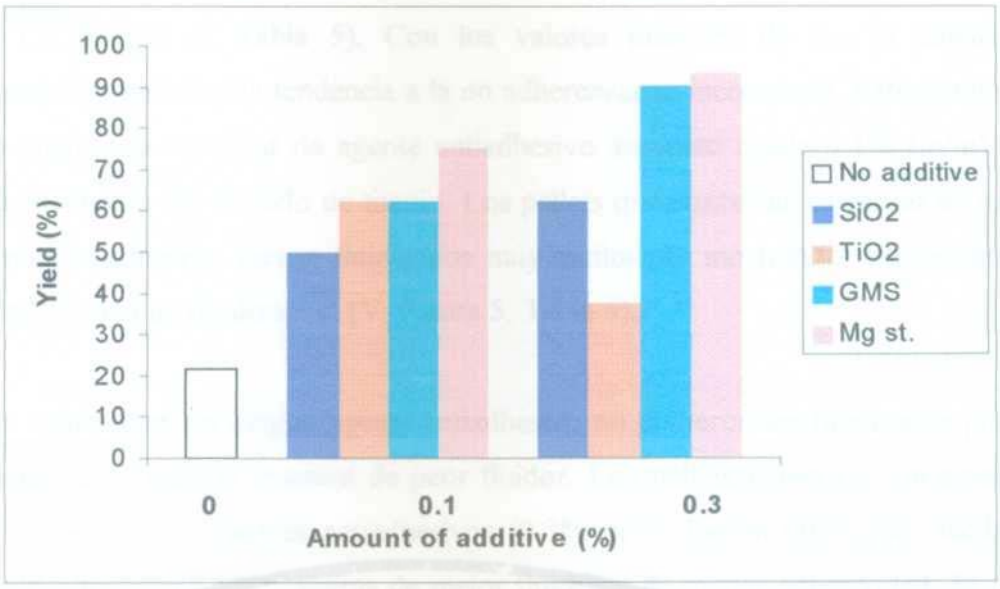

Figura 11. Efecto de los agentes antiadhesivos sobre el rendimiento de los pellets recubiertos con películas de quitosana-HMW.

4.6 Adhesividad de los pellets recubiertos pelicularmente con quitosana (V)

Pocos trabajos han sido reportados sobre métodos para la determinación de la adhesividad de películas poliméricas farmacéuticas. Wesseling y col. (1999) desarrollaron un método en el que las curvas de esfuerzo-deformación fueron utilizadas para medir la adherencia de películas celulósicas y acrílicas.

Un método rápido y novedoso, basado en la determinación de la velocidad mínima de fluidización experimental, *(u*mf) en un lecho fluidizado, fue empleado para evaluar la influencia de los agentes antiadhesivos en la adherencia de las películas acuosas de quitosana-HMW sobre pellets cubiertos.

Los valores más bajos de u_{mf} fueron obtenidos con los pellets no recubiertos utilizados como referencia (V, Figura 4, Tabla 5). Con los valores menores de u_{mf} la capacidad de fluidización de los pellets y la tendencia a la no adherencia se incrementó. Este fenómeno fue observado cuando la cantidad de agente antiadhesivo aumentó desde 0.1% (m/m) a 0.3% (m/m) con excepción del dióxido de titanio. Los pellets que contenían estearato de magnesio como agente antiadhesivo fueron fluidizados muy fácilmente mostrando valores muy bajos de velocidad mínima de fluidización (V, Figura 5, Tabla 5).

Los pellets recubiertos sin ningún agente antiadhesivo no pudieron ser fluidizados por lo que fueron clasificados como la muestra de peor fluidez. Los pellets cubiertos con estearato de magnesio y GMS como agentes antiadhesivos (0.3% m/m) fueron fluidizados fácilmente y fueron clasificados como las muestras de mejor fluidez y de menor adhesividad. El presente método ofrece interesantes posibilidades para la cuantificación de la adherencia de las películas en pellets cubiertos.

Los resultados alcanzados con el estearato de magnesio y el GMS como agentes antiadhesivos, en los procesos de revestimiento acuoso con soluciones de quitosana-HMW plastificadas con glicerol, sugieren la posibilidad de lograr un sistema de revestimiento pelicular a pequeña escala con las películas compuestas de quitosana-*Hylon VII*. Por tal motivo, las condiciones operativas deberán ser investigadas para definir las necesidades de procesamiento final que ofrezcan la mayor calidad y rendimiento de los procesos.

5. Conclusiones

- Las quitosanas CH1 y CH2 derivadas de langosta presentaron propiedades fisicoquímicas similares a las quitosanas comerciales.

- Películas flexibles y resistentes mecánicamente fueron elaboradas con mezclas acuosas binarias de quitosana-HMW y amilosa de almidón de maíz *(Hylon VII)* plastificadas con polioles.

- El eritritol, plastificante mas adecuado para las películas combinadas de quitosana- HMW y amilosa de almidón de maíz *(Hylon VII)* recién elaboradas, no brindó una buena estabilidad física a las películas bajo condiciones extremas de temperatura y humedad a diferencia de las plastificadas con glicerol.

- El proceso de recubrimiento pelicular de pellets en un sistema miniaturizado con atomizador superior, demostró ser sensible fundamentalmente a los parámetros de temperatura del aire y velocidad de atomización de la solución, determinándose sus posibles combinaciones para satisfacer los requerimientos de entericidad y rendimiento de los pellets cubiertos.

- Se desarrolló un nuevo método para la determinación de la adhesividad de las películas en pellets, empleando la velocidad mínima de fluidización, demostrándose su eficiencia para cuantificar la adherencia de los pellets cubiertos a pequeña escala.

- Un novedoso sistema de revestimiento acuoso con quitosana-HMW fue desarrollado, requiriendo de agentes antiadhesivos de los cuales, los mejores resultados se obtuvieron con el estearato de magnesio y el GMS, ambos al 0.3% (m/m).

6. Recomendaciones

- Evaluar las propiedades formadoras de películas de las quitosanas derivadas de langosta.

- Investigar el proceso de revestimiento pelicular a pequeña escala con las películas de quitosana-HMW y amilosa de almidón de maíz

- Evaluar las potencialidades de un sistema multicapas empleando las películas de quitosana-HMW y amilosa de almidón de maíz con fines farmacéuticos.

Referencias Bibliográficas

Aiedeh, K., Gianasi, E., Orienti, I. y **Zecchi, V., 1997.** Chitosan microcapsules as controlled release systems for insulin. J. Microencapsul. 14, 567-576.

Alekseev, V.L., **Kelberg, E.A., Bronnikov,** S.V. y **Evmenenko, G.A., 2001.** Structure and mechanical properties of chitosan-poly(ethylene oxide) blend films. Polym. Sci. Ser. B 43, 281-284.

Alekseev, V.L., **Kelberg, E.A., Evmenenko, G.A.** y **Bronnikov,** S.V., **2000.** Improvement of the mechanical properties of chitosan films by the addition of poly(ethylene oxide). Polym. Eng. Sci. 40, 1211-1215.

Alkan, M.H., Groves, M.J., Roland, C. L., Teng, C.D., Dwyer, E.M. y Patel, M.C., 1988. Small-scale film coating of tablets, pellets, and granules. Pharm. Technol. 12 (6), 98-104

Amadóttir, S.G. y Kristmundsdóttir, T., 1996. Increased dissolution rate by microencapsulation. Eur. J. Pharm. Sci. 4, S134.

Arvanitoyannis, L, Kolokuris, I., Nakayama, A., Yamamoto, N. y Aiba, S., 1997. Physico-chemical studies of chitosan-poly(vinyl alcohol) blends plasticized with sorbitol and sucrose. Carbohydr. Polym. 34, 9-19.

Arvanitoyannis, I.S., Nakayama, A. y Aiba, S., 1998. Chitosan and gelatin based edible films: state diagrams, mechanical and permeation properties. Carbohydr. Polym. 37, 371 - 382.

Aulton, M.E., 1982. Assessment of the mechanical properties of film coating materials. Int. J. Pharm. Tech. Prod. Manuf. 3 (1), 9-16.

Bader, H.G. y **Goritz, D., 1994.** Investigations on high amylose corn starch films. Part 1: Wide-angle X-ray scattering (WAXS). Starch / Starke. 46, 229-232.

Ball, P., 2002. New uses for a dead lobster: crustacean shells could thicken food, paint and makeup. Nature, http://www.nature.com/nsu/020812/020812-1 l.html.

Banker, G.S., **1966.** Film coating theory and practice. J. Pharm. Sci. 55, 81-89.

Baxter, A., Dillon, M., Taylor, K.D.A. y Roberts. G.A.F., 1992. Improved method for I R determination of the degree of N-acetylation of chitosan. Int. J. Biol. Macromol. 14, 166-169.

Begin, A. y **Van Calsteren, M.R., 1999.** Antimicrobial films produced from chitosan. Int. J. Biol. Macromol. 26, 63-67.

Bernkop-Schniirch, A., 2000. Chitosan and its derivatives: potential excipients for peroral peptide delivery systems. Int. J. Pharm. 194, 1-13.

Bjerrun, O.J., 2002. New safe medicines faster: a proposition for a pan-European research effort. Nature Rev. Drug Disscov. 1 (5), 395-398.

Bock, T.K. y **Kraas,** U., **2001.** Experience with the Diosna mini-granulator and assessment of process scalability. Eur. J. Pharm. Biopharm. 52, 297-303.

Bodmeier, R. y **Paeratakul, O., 1994.** Mechanical properties of dry and wet cellulosic and acrylic films prepared from aqueous colloidal polymer dispersions used in the coating of solid dosage forms. Pharm. Res. 11, 882-888.

Bodmeier, R., 1997. Tableting of coated pellets. Eur. J. Pharm. Biopharm. 43, 1-8.

Bodmeier, R., Chen, H.G. **y Paeratakul, O., 1989. A** novel approach to the oral delivery of micro or nanoparticles. Pharm. Res. 6, 413-417.

Brugnerotto, J., Lizardi, J., Goycoolea, F.M., Argiielles-Monal, W., Desbrieres, J. y Rianudo, M., 2001. An infrared investigation in relation with chitin and chitosan characterization. Polymer. 42, 3569-3580.

Chen, R.W. y **Hwa, H.D., 1996.** Effect of molecular weight of chitosan with the same degree of deacetylation on the thermal, mechanical and permeability properties of the prepared membrane. Carbohydr. Polym. 29, 353-358.

Chourasia, M.K. y **Jain, S.K., 2003.** Pharmaceutical approaches to colon targeted drug delivery systems. J. Pharm. Pharmaceut. Sci. 6 (1), 33-66.

Dodane, V. y **Vilivalam, V.D., 1998.** Pharmaceutical applications of chitosan. Pharm. Sci. Technol. Today. Vol. 1, 6, 246-253.

Domszy, J.G. y Roberts, G.A.F., 1985. Evaluation of infrared spectroscopic techniques for analyzing chitosan. Makromol. Chem. 186, 1671-1677.

European Pharmacopoeia, 2002. Council of Europe, Strasbourg. 4th Edition, pp 207-208.

Felt, O., Buri, P. y Gurny, R., 1998. Chitosan: a unique polysaccharide for drug delivery. Drug Dev. Ind. Pharm. 24, 979-993.

Felton, L.A. y McGinity, J.W., 1999. Adhesion of polymeric films to pharmaceutical solids. Eur. J. Pharm. Biopharm. 47, 3-14.

Fernandez-Hervas, M.J. y **Fell, J.T., 1998.** Pectin/chitosan mixtures as coatings for colon- specific drug delivery and in vitro evaluation. Int. J. Pharm. 169, 115-119.

Gocho, H., Shimizu, H., Tanioka, A., Chou, T.-J. y **Nakajima, T., 2001.** Effect of polymer chain end on sorption isotherm of water by chitosan. Carbohydr. Polym. 41, 87-90.

Gupta, K.C. y **Ravi Kumar, M.N.V., 2000.** Semi-interpenetrating polymer network beads of crosslinked chitosan-glycine for controlled release of clorphenaramine maleate. J. Appl. Polym. Sci. 76, 672-683.

Hancock, B.C., Clas, S.-D. y **Christensen, K., 2000.** Micro-scale measurement of the mechanical properties of compressed pharmaceutical powders 2: The elasticity and fracture behavior of microcrystalline cellulose. Int. J. Pharm. 209, 27-35.

Hari, P.R., Chandy, T. y Sharma, C.P., 1996. Chitosan/calcium alginate microcapsules for intestinal delivery of nitrofurantoin. J. Microencapsul. 13, 319-329.

Harish Prashanth. K.V., Kittur, F.S. y **Tharanathan, R.N., 2002.** Solid state structure of chitosan prepared under different N-deacetylating conditions. Carbohydr. Polym. 50, 27-33.

Hasegawa, M., Isogai, A., Onabe, F., Usuda, M. y **Atalla. R.H., 1992.** Characterization of cellulose-chitosan blend films. J. Appl. Polym. Sci. 45, 1873-1879.

Hassan, E.E., **Parish, R.C.** y **Gallo, J.M.,** 1992. Optimized formulation of magnetic chitosan microspheres containing the anticancer agent: oxantrazole. Pharm. Res. 9, 390-397.

He, P., Davis, S.S. y Ilium, L., 1998. In vitro evaluation of the mucoadhesive properties of chitosan microspheres. Int. J. Pharm. 166, 75-88.

Hejazi, R. y **Amiji, M., 2003.** Chitosan-based gastrointestinal delivery systems. **J.** Control. Rel. 89, 151-165.

Hiorth, M., Tho, I. y **Sande, A., 2003.** The formation and permeability of drugs across free pectin and chitosan films prepared by a spraying method. Eur. J. Pharm. Biopharm. 56, 175- 182.

Hoagland, P.D., 1999. Biodegradable laminated films fabricated from pectin and chitosan. U.S. Patent 5, 919, 574, 1-11.

Hoope-Seyler, F., 1894. Ueber chitin und zellulose. Ver. Deut. Chem. Gesell. 27, 3329-3331.

Hosokawa, J., Nishiyama, M., Yoshihara, K. y Kubo, T., 1990. Biodegradable film derived from chitosan and homogenized cellulose. Ind. Eng. Chem. Res. 29, 800.

Hou, W.M., Miyazaki, S., **Takada, M. y Komai, T., 1985.** Sustained release of indomethacin from chitosan granules. Chem. Pharm. Bull. 33, 3986-3992.

Ilango, R., Jayakar, B. y Kavimani, S., 1998. Chitosan a new pharmaceutical excipient The Eastern Pharmacist. 41, 47-49.

Ilango, R., Kavimani, S., **Premila, J., Nair, D.K. y Jayakar, B., 1997.** Studies on tablets of sulfamethoxazole using chitosan. Indian J. Pharm. Sei. 59, 220-224.

Ilium, L., 1998. Chitosan and its use as a pharmaceutical excipient. Pharm. Res. 15, 1326-1331.

Kawashima, Y., **Handa, T., Kassai,** A., **Takenaka, H.** y **Lin,** S.Y., **1985.** The effect of thickness and hardness of the coating film on the drug release rate of theophylline granules coated with chitosan-tripolyphosphate complex. Chem. Pharm. Bull. 33, 2469-2474.

Khan, T.A., 2002. Reporting degree of deacetylation values of chitosan: the influence of analytical methods. J. Pharm. Pharmaceut. Sei. 5 (3), 205-212.

Kim, J.H., Kim, Y., Le, Y.M. y **Kim, K.Y., 1992.** Properties and swelling characteristics of crosslinked PVP/chitosan blend membrane. J. Appl. Polym. Sei. 45, 1711.

Knapczyk, J., Krowcynscki, L., **Krzek, J., Brzeski, M., Nürnberg,** E., **Schenk, D. y Struszczyk, H., 1989.** Requirements of chitosan for pharmaceutical and biomedical applications. In: Skjak-Braek, G., Anthonsen, T., Sandorf, P. (Eds). Chitin and Chitosan- Sources, Chemistry, Biochemistry, Physical Properties and Applications. Elsevier, London, pp 757-764.

Koizumi, T., Ritthidej, G.C. y **Phaechamud, T., 2001.** Mechanistic modeling of drug release from chitosan coated tablets. J. Control. Rel. 70, 277-284.

Kristi, J., Smid-Korbar, J., Struc, E., **Schara, M.** y **Rupprecht, H., 1993.** Hydrocolloids and gels of chitosan as drug carriers. Int. J. Pharm. 99, 13-19.

Kristmundsdottir, T., **Ingvarsdottir, K.** y **Saemundsdottir,** G., 1995. Chitosan matrix tablets: the influence of excipients on drug release. Drug Dev. Ind. Pharm. 21, 1591-1598.

Krogars, K., Heinamaki, J., Karjalainen, M., Niskanen, A., **Leskela, M.** y **Yliruusi, J., 2003.** Enhanced stability of rubbery amylose-rich maize starch films plasticized with a combination of sorbitol and glycerol. Int. J. Pharm. 251, 205-208.

Kurita, K., 1986. Chemical modifications of chitin and chitosan. In: R.A.A. Muzarelli, C. Jeuniaux, G.W. Gooday (Eds). Chitin in Nature and Technology, Plenum, New York, pp 287-293.

Landin, M., York, P., Cliff, M. J., Rowe, R.C. y **Wigmore, A.J., 1996.** Scale-up of a pharmaceutical granulation in a fixed bowl mixer granulator. Int. J. Pharm. 133, 127-131.

Lenaerts, V., Dumoulin, Y. y **Mateescu, M.A., 1991.** Controlled-release of theophylline from cross-linked amylose tablets. J. Control. Rel. 15, 39-46.

Lenaerts, V., Moussa, I., Dumoulin, Y., Mebsout, F., Chouinard, F., Szabo, P., Mateescu, M.A., Cartilier, L. y **Marchessault, R., 1998.** Cross-linked high amylose starch for controlled release of drugs: recent advances. J. Control. Rel. 53, 225-234.

Lever, A.E. **y Rhys, J.A., 1968.** The properties and testing of plastic materials. Temple Press Books, UK. 3rd Ed.

Li, L.C. y **Peck,** G.E., 1989. Water-based silicone elastomer controlled release tablet film coating. I. Free film evaluation. Drug Dev. Ind. Pharm. 15, 65-95.

Lim, L.Y., Wan, L.S.C. y **Thai, P.Y., 1997.** Chitosan microspheres prepared by emulsification and ionotropic gelation. Drug Dev. Ind. Pharm. 23, 981-985.

Lim, LY. y **Wan, L.S.C., 1995.** Heat treatment of chitosan films. Drug Dev. Ind. Pharm. 21 (7), 839-846.

Lippold, B.H., Suiter, B.K. y **Lippold, B.C., 1989.** Parameters controlling drug release from pellets coated with aqueous ethyl cellulose dispersions. Int. J. Pharm. 54, 15-25.

Liu, L.S., Liu, S.Q., Ng, S.Y., Froix, M., Ohno, T. y **Heller, J., 1997.** Controlled release of interleukin-2 for tumour immunotheraphy using alginate/chitosan porous microspheres. J Control. Rel. 46, 65-74.

Lorenzo-Lamasa, M.L., Remuñán-López, C., Vila-Jato, J.L. y **Alonso, M.J., 1998.** Design of microencapsulated chitosan microspheres for colonic drug delivery. J. Control. Rel. 52, 109-118.

Lourdin, D., Della Valle, G. y **Colonna, P., 1995.** Influence of amylose contents on starch films and foams. Carbohydr. Polym. 27, 261-270.

Macleod, G.S., Collett, J.H. y **Fell, J.T., 1999a.** The potential use of mixed films of pectin, chitosan and HPMC for biomodal drug release. J. Control. Rel. 58, 303-310.

Macleod, G.S., Fell, J.T., Collett, J.H., Sharma, H.L. y **Smith, A.M., 1999b.** Selective drug delivery to the colon using pectin: chitosan: hydroxypropyl methylcellulose film coated tablets. Int. J. Pharm. 187, 251-257.

Marechal, P., Chiba, T. y **Inoue, T., 1997.** Melt blending of dissimilar polymers by a small scale mixer: mixing with steel balls. Polymer Networks & Blends. 7 (2), 61-75.

Mehta, A.M., 1997. Processing and equipment considerations for aqueous coatings. In: Aqueous polymeric coatings for pharmaceutical dosage forms. J.W. McGinity (Ed). Marcel Dekker, New York, pp 287-326.

Meshali, M.M. y **Gabr, K.E., 1993.** Effect of interpolymer complex-formation of chitosan with pectin or acacia on the release behavior of chlorpromazine HC1. Int. J. Pharm. 89, 177- 181.

Mi, F.L., Her, N.L., Kaun, C.Y., Wong, T. y **Shyu, S., 1997a.** Chitosan tablets for controlled release of theophylline: effect of polymer drug wet or dry blending and anionic- cationic interpolymer complex. J. Appl. Polym. Sci. 66, 2495-2505.

Mi, F.L., Wong, T.B. y Shyu, S.S., 1997b. Sustained-release of oxytetracycline from chitosan microspheres prepared by interfacial acylation and spray hardening methods. J. Microencapsul. 14, 577-591.

Munjeric, O., Collet, J.H. y **Fell, J.T., 1997.** Hydrogel beads based on amidated pectins for colon-specific drug delivery: the role of chitosan in modifying drug release. J. Control. Rel 46, 273-278.

Murtomaa, M., Rasanen, E., Rantanen, J., Bailey, A., Laine, E., Mannermaa, J.-P. y Yliruusi, J., 2002. Electrostatic measurement on a miniaturized fluidized bed. **J.** Electrostat 57, 91-106.

Muzzarelli R.A.A. y **Peter M.G. (Eds). 1997.** Chitin Handbook. Bremen, Germany: European Chitin Society, pp 437-438

Nakatsuka, S. **y Andrady, A.L., 1992.** Permeability of vitamin B-12 in chitosan membranes. Effect of crosslinking and blending with poly(vinyl alcohol) on permeability. J. Appl. Polym. Sci. 44, 17-28.

Nieto, J.M., Peniche, C. y **Padrón, G., 1991.** Characterization of chitosan by pyrolysis- mass spectrometry, thermal analysis and differential scanning calorimetry. Thermochemica Acta. 176, 63-68.

Nieto, O.M., 1993. Quitina. Su estudio y utilización como fármaco acelerador de la cicatrización. Tesis presentada en opción al grado científico de Dr. en Ciencias Farmacéuticas. IF AL, Universidad de la Habana, Cuba.

Nigalaye, A.G., Adusumilli, P. y Bolton, S., 1990. Investigation of prolonged drug release from matrix formulations of chitosan. Drug Dev. Ind. Pharm. 16, 449-467.

Nogales, A., Ezquerra, T.A., Rueda, D.R., Martínez, F. y **Retuert, J., 1997.** Influence of water on the dielectric behavior of chitosan films. Colloid. Polym. Sci. 275, 419-425.

Nunes, S., Alves, P. y **Galembeck, F., 1990.** A low-cost, small-scale polymer mixer. J. Chem. Education. 67 (11), 982-983.

Nunthanid, J., Puttipipatkhachorn, S., **Yamamoto, K.** y **Peck,** G.E., **2001.** Physical properties and molecular behavior of chitosan films. Drug Dev. Ind. Pharm. 27 (2), 143-157.

Nykanen, P., Lempaa, S., Aaltonen, M.-L., Jurjenson, H., Veski, P. y Marvola, M., 2001. Citric acid as excipient in multiple-unit enteric-coated tablets for targeting drugs on the colon. Int. J. Pharm. 229 (1-2), 155-162.

O'Donnell, P.B. y McGinity, J.W., 1997. Mechanical properties of polymeric films prepared from aqueous polymeric dispersions. In: McGinity, J.W., (Ed). Aqueous Polymeric Coatings for Pharmaceutical Dosage Forms. Marcel Dekker, Inc., New York, pp **517-548.**

Okhamafe, A.O., Amsden, B., Chu, W. y **Goosen, M.F.A., 1996.** Modulation of protein release from chitosan-alginate microcapsules using the pH-sensitive polymer hydroxypropyl methylcellulose acetate succinate. J. Microencapsul. 13 (5), 497-508.

Okutgen, E., Hogan, J.E. y **Aulton, M.E.,** 1995. Quantitative estimation of internal stress development in aqueous HPMC tablet film coats. Int. J. Pharm. 119, 193-202.

Orienti, I., Cerchiara, T., Luppi, B., Bigucci, F., Zuccari, G. y Zecchi, V., 2002.
Influence of different chitosan salt on the release of sodium diclofenac in colon-specific delivery. Int. J. Pharm. 238, 51-59.

Ottoy, M.H., Varum, K.M. y Smidsord, O., 1996. Compositional heterogeneity of heterogeneously deacetylated chitosans. Carbohydr. Polym. 24, 17-24.

Palviainen, P., Heinamaki, J., Myllarinen, P., Lahtinen, R., Yliruusi, J. y Forssell, P.,
2001. Corn starches as film formers in aqueous-based film coating. Pharm. Dev. Technol 6 (3), 351-359.

Parag, K. y **Rangaramanujam, M.K., 2003.** Improvement in ductility of chitosan through blending and copolymerization with PEG: FTIR investigation of molecular interactions Biomacromolecules. 4, 173-180.

Patel, D., Smith, A.W., Grist, N., Barnett, P. y **Smart, J.D., 1999.** An in vitro mucosal model predictive of bioadhesive agents onto the oral cavity. J. Control. Rel. 61, 175-183.

Paul. W. y **Sharma, C.P., 2000.** Chitosan, a drug carrier for the 21st century: a review. S.T.P. Pharma Sci. 10, 5-22.

Peetrs, R. and Kinget, R., 1993. Film-forming polymers for colonic drug delivery: **I.** Synthesis and physical and chemical properties of methyl derivatives of Eudragit S. Int. J. Pharm. 94 (1-3), 125-134.

Petereit, H.U., Assmus, M. y **Lohmann, K., 1995.** Glyceril monostearate as a glidant in aqueous film-coating formulations. Eur. J. Pharm. Biopharm. 41 (4), 219-228.

Polk, A.A., Amsden, B., Yao, K.D., Peng, T. y **Goosen, M.F.A., 1994.** Controlled release of albumin from chitosan-alginate microcapsules. J. Pharm. Sci. 83 (2), 178-185.

Porter, S.C., 1980. The effect of additives on the properties of an aqueous film coating. Pharm. Technol. 67-75.

Portero, A., **Remuñán-López,** C. y **Vila-Jato, J.L., 1998.** Effect of chitosan and chitosan glutamate enhancing the dissolution properties of the poorly water soluble nifedipine. Int. J. Pharm. 175, 75-84.

Puttipipatkhaciiorn, S., **Nunthanid, J., Yamamoto, K.** y **Peck, G.E., 2001.** Drug physical state and drug-polymer interaction on drug release from chitosan matrix films. J. Control. Rel. 75, 143-153.

Rásánen, E., Antikainen, O. y Yliruusi, J., 2003a. A new method to predict flowability using a microscale fluid bed. AAPS Pharm. Sci. Tech. 4 (4). Article 53 (http:// www.aapspharmscitech.org).

Rásánen, E., Rantanen, J., Mannermaa, J.-P., Yliruusi, J. and Vuorela, H., 2003b. Dehydration studies using a novel multichamber microscale fluid-bed dryer with in-line NIR measurement. J. Pharm. Sci. 92 (10), 2074-2081.

Rásánen, E., Rantanen, J., Mannermaa, J.-P. and Yliruusi, J., 2004. The characterization of fluidization behavior using a novel multichamber microscale fluid bed. J. Pharm. Sci. 93 (3), 780-791.

Ravi Kumar, M.N.V., 2000. A review of chitin and chitosan applications. Reactive & Functional Polymers. 46, 1-27.

Rege, P.R. y **Block, L.H., 1999.** Chitosan processing influence of process parameters during acidic and alkaline hydrolysis and effect of the processing sequence on the resultant chitosan's properties. Carbohydr. Res. 321, 235-245.

Rege, P.R., Garmise, R.J. y **Block, L.H., 2003.** Spray-dried chitonosans Part I: preparation and characterization. Int. J. Pharm. 252, 41-51.

Remuñán-López, C. y **Bodmeier, R., 1996a.** Effect of formulation and process variables on the formation of chitosan-gelatin coacervates. Int. J. Pharm. 135, 63-72.

Remuñán-López, C. y **Bodmeier, R., 1996b.** Mechanical and water vapor transmission properties of polysaccharide films. Drug Dev. Ind. Pharm. 22 (12), 1201-1209.

Remuñán-López, C. y **Bodmeier, R, 1997.** Mechanical, water uptake and permeability properties of crooslinked chitosan glutamate and alginate films. J. Control. Rel. 44, 215-225.

Rhodes, C.T. y **Porter,** S.C., **1998.** Coatings for controlled-release drug delivery systems. Drug Dev. Ind. Pharm. 24 (12), 1139-1154.

Rindlav, A., Stading, M., Hermansson, A.-M. y **Gatenholm, P., 1998.** Structure, mechanical and barrier properties of amylose and amylopectin films. Carbohydr. Polym. 36, 217-224.

Ritthidej, G.C. y **Phaechamud, T., 2003.** Effect of anionic water-soluble dyes on film coating properties of chitosan acetate. Drug Dev. Ind. Pharm. 29 (5), 585-594.

Ritthidej, G.C., Chomto, P., Pummangura, S. y **Menasveta, P.,** 1994. Chitin and chitosan as disintegrants in paracetamol tablets. Drug Dev. Ind. Pharm. 20 (13), 2109-2134.

Ritthidej, G.C., **Phaechamud, T.** y **Koizumi, T.,** 2000. Additives in moist-heat-treated chitosan acetate films: a method to extend the release of propranolol hydrochloride-coated tablets. S.T.P. Pharma. Sci. 10(1), 112-119.

Roberts, G.A.F., 1992. Structure of chitin and chitosan. In: G.A.F. Roberts (Ed), Chitin Chemistry, MacMillan Houndmills, pp 1-53.

Rouget, C., **1859.** Des substances amylacies dans le tissu des animaux, spécialement les articulés (chitine). Comp Rend. 48, 792-795.

Rowe, C.R., 2000. Small is beautiful. P.S.**T.T.** 3 **(6), 187-188.**

Rueda, D.R., Secall, T. y Bayer, R.K., 1999. Differences in the interaction of water with starch and chitosan films as revealed by infrared spectroscopy and differential scanning calorimetry. Carbohydr. Polym. 40, 49-56.

Sabnis, S. y **Block, L.H., 1997a.** Improved infrared spectroscopic method for the analysis of degree of N-deacetylation of chitosan. Polym. Bull. 39, 67-71.

Sabnis, S., Rege, P. y Block, L.H., 1997b. Use of chitosan in compressed tablets of diclofenac sodium: inhibition of drug release in an acidic environment. Pharm. Dev. Technol. 2, 243-255.

Sanford, P.A., 1990. Chitosan and alginate: new forms of commercial interest. Am. Chem. Soc. Div. Polym. Chem. 31, 628-629.

Sannan, T., Kurita, K. y **Iwakura, Y., 1976.** Studies on chitin, 2. Effect of deacetylation on solubility. Macromol. Chem. 177, 3589-3600.

Santos, H., Veiga, F., Pina, M., Podczeck, F. y **Sousa, J., 2002.** Physical properties of chitosan pellets produced by extrusion-spheronisation: influence of formulation variables. Int. J. Pharm. 246, 153-169.

Savitzky, A. y Golay, M., 1964. Smoothing and differentiation of data by simplified least square procedures. Anal. Chem. 36, 1627-1639.

Seitz, J.A., Mehta, S. P. y **Yeager, J.L., 1986.** Tablet coating. In: The theory and practice of industrial pharmacy. L. Lachman, H.A. Lieberman, J.L. Kaning (Eds). Lea & Febiger, Philadelphia, pp 346-373.

Senel, S., Ikinci, G., Kas, S., Yousefi-Rad, A., Sargon, M.F. y Hincal, A.A., 2000.
Chitosan films and hydrogels of chlorhexidine gluconate for oral mucosal delivery. Int. J. Pharm. 193, 197-203.

Shimono, N., Takatori, T., Masumi, T., Ueda, M., Mori, M., Higashi, Y. y **Nakamura, Y., 2002.** Chitosan dispersed system for colon-specific drug delivery. Int. **J.** Pharm. 245, 45- 54.

Shimono, N., Takatori, T., Ueda, M., Mori, M. y **Nakamura, Y., 2003.** Multiparticulate chitosan- dispersed system for drug delivery. Chem. Pharm. Bull. 51 (6), 620-624.

Shu, X.Z., Zhu, K.J. y Weihong, S., 2001. Novel pH-sensitive citrate cross-linked chitosan film for drug controlled release. Int. J. Pharm. 212, 19-28

Singla, A.K. y **Chawla, M., 2001.** Chitosan: some pharmaceutical and biological aspects-an update. J. Pharm. Pharmacol. 53, 1047-1067.

Srinivasa, P.C., Ramesh, M.N., Kumar, K.R. y **Tharanathan, R.N., 2003.** Properties and sorption studies of chitosan-polyvinyl alcohol blend films. Carbohydr. Polym. 53, 431-438.

Sukurai, K., Maegawa, T. y **Takahashi, T., 2000.** Glass transition temperature of chitosan and miscibility of chitosan/poly(N-vinyl pyrrolidone) blends. Polymer. 41, 7051-7056.

Synowiecki, J. y Al-khateeb, N.A., 2003. Production, properties and some new applications of chitin and its derivatives. Critical Reviews in Food Science and Nutrition. 43 (2), 145- 171.

Tacharodi, D. y **Panduranga Rao, K., 1993a.** Propranolol hydrochloride release behavior of crosslinked chitosan membranes. J. Chem. Technol. Biotechnol. 58, 177-181.

Tachoridi, D. y Panduranga Rao, K., 1993b. Release of nifedipine through crosslinked chitosan membranes. Int. J. Pharm. 96, 33-39.

Takaya, T., Niwa, K., Muraoka, M., Ogita, I., Nagai, N., Yano, R., Kimura, G., Yashikawa, Y., Yashikawa, H. y Takada, K., 1998. Importance of dissolution process on systemic availability of drugs delivery by colon delivery system. J. Control. Rel. 50 (1-3), **111-122**.

Tapia, C., Buckton, G. y **Newton, J.M., 1993.** Factors influencing the mechanism of release from sustained release matrix pellets produced by extrusion/spheronisation. Int. J. Pharm. 92, 211-218.

Thanou, M., Verhoef, J.C. y **Junginger, H.E., 2001.** Oral drug absorption by chitosan and its derivatives. Adv. Drug Deliv. Rev. 52, 117-126.

Thoma, K., Groning, R. y **Zimmer, T., 1986.** Film-coating method for dosage form development, I: A small scale vortex fluidized-bed coating apparatus. Acta Pharm. Technol. 32 (3), 137-145.

Tozaki, H., kamoike, J., Tada, C., **Maruyama, T., Terabe, A., Suzuki, T., Yamamoto, A. y Muranishi, S., 1997.** Chitosan capsules for colon-specific drug delivery: Improvement of insulin absorption from the rat colon. J. Pharm. Sei. 86, 1016-1021.

Upadrashtra, S.M., Katikaneni, P.R. y Nuessle, N.O., 1992. Chitosan as a tablet binder. Drug Dev. Ind Pharm. 18, 1701-1708.

Wells, J.L y Aulton, M.E., 1998. Preformulation. In: M E. Aulton, Pharmaceutics, the Science of Dosage Form Design. Churchill Livingstone, New York, pp 223-253.

Wesdyk, R., Joshi, Y.M., **De Vincentis, J., Newman,** A.W. **y Jain, N.B.,** 1993. Factors affecting differences in film thickness of beads coated in fluidized bed units. Int. J. Pharm. 93, 101-109.

Wesseling, M., Kuppler, F. y **Bodmeier, R., 1999.** Tackiness of acrylic and cellulosic polymer films used in the coating of solid dosage forms. Eur. J. Pharm. Biopharm. 47, 73-78.

Wiles, J.L., Vergano, P.J., Barron, F.H., Bunn, J.M. y Testin, R.F., 2000. Water vapor transmission rates and sorption behavior of chitosan films. J. Food. Sei. 65, 7, 1175-1179.

WolfT, I.A., Davis, H.A., Cluskey, J.E., Gundrun, L.J. y Rist, C.E., 1951. Preparation of films from amylose. Ind. Eng. Chem. 43, 915-919.

Yao, K.D., Peng, T., Yin, Y.J. y **Xu, M.X., 1995.** Microcapsules/microspheres related to chitosan. J.M.S.-Rev. Macromol. Chem. Phys. C35, 155-180.

Zambito, Y. y **Di Colo, G., 2003.** Preparation and in vitro evaluation of chitosan matrices for colonic controlled drug delivery. J. Pharm. Pharmaceut. Sei. 6 (2), 274-281.

Zhang, H., Ibrahim, A.A. y **Neau, S.H., 2002a.** An in vitro evaluation of a chitosan- containing multiparticulate system for macromolecule delivery to the colon. Int. J. Pharm 239, 197-205.

Zhang, M., Li, X.H., Gong, Y.D., **Zhao, N.M.** y **Zhang, X.F., 2002b.** Properties and biocompatibility of chitosan films modified by blending with PEG. Biomaterials. 23, 2641- 2648

Participación en eventos científicos

> Fernández, M., Krogars, K., Jorgënsën, A., Heinámáki, J., Iraizoz, A, Yliruusi, J. “Chitosan free films plasticized with polyols” (poster). XIII Simposio de la Sociedad de Farmacia Física, 2002, Turku, Finlandia.

> Fernández, M., Krogars, K., Jorgënsën, A., Heinámáki, J., Iraizoz, A., Yliruusi, J. “Aqueous chitosan-amylose starch films plasticized with polyols” (poster). VIII Congreso de la Sociedad Cubana de Farmacia. V Encuentro Iberoamericano sobre las Ciencias Farmacéuticas y Alimentarias CUBAFARMACIA 2002, Ciudad Habana, Cuba.

> Fernández, M., Krogars, K., Jorgënsën, A., Heinámáki, J., Karjalainen, M., Iraizoz, A., Yliruusi, J. “Chitosan free films plasticized with polyols” (póster). Congreso de la AAPS, 2002, Toronto, Canadá.

> Fernández, M., Heinámáki, J., Karjalainen, M., Antikainen, O., Iraizoz, A., Yliruusi, J. “Novel chitosan - amylose starch composite films for pharmaceutical aqueous coat applications” (póster). 2004, Nuremberg, Alemania.

> Fernández, M., Heinámáki, J., Karjalainen, M., Airaksinen, S., Iraizoz, A., Yliruusi, J. “Películas compuestas de quitosana y amilosa para recubrimiento acuoso con fines farmacéutios” (presentación oral). VI Encuentro Iberoamericano de las Ciencias Farmacéuticas y Alimentarias CUBAFARMACIA-ALIMENTOS 2004, Ciudad Habana, Cuba.

Solid-state characterization of chitosans derived from lobster chitin

Fernández Cervera, M., Heinámäki, J., Rásánen, M., Maunu, S.L., Karjalainen. M., Nieto Acosta, O.M., Iraizoz Colarte, A. and Yliruusi, J.

Aceptado para publicar en Carbohydr. Polym (2004)

Available online at www.sciencedirect.com
SCIENCE DIRECT
ELSEVIER
Carbohydrate Polymers xx (xxxx) 1–8
Carbohydrate Polymers
www.elsevier.com/locate/carbpol

Solid-state characterization of chitosans derived from lobster chitin

M. Fernández Cervera[a], J. Heinämäki[b,*], M. Räsänen[c], S.L. Maunu[c], M. Karjalainen[b], O.M. Nieto Acosta[a], A. Iraizoz Colarte[a], J. Yliruusi[b,d]

[a]*Institute of Pharmacy and Food, University of Havana, Cuba*
[b]*Pharmaceutical Technology Division, Faculty of Pharmacy, P.O. Box 56, University of Helsinki, Helsinki FI-00014, Finland*
[c]*Department of Chemistry, P.O. Box 55, University of Helsinki, Helsinki FI-00014, Finland*
[d]*Viikki Drug Discovery Technology Center DDTC, University of Helsinki, Helsinki, Finland*

Received 3 November 2003; revised 26 July 2004; accepted 2 August 2004

Abstract

Two samples of chitosan (CH1 and CH2) of different molecular weights and degrees of deacetylation were prepared from lobster chitin under two different processes. Solid-state properties of CH1 and CH2 were characterized and compared with four commercial chitosans prepared from crab and fresh shrimp shells. Infrared spectroscopy (IR), solid-state CP-MAS ^{13}C NMR, powder X-ray diffraction and differential scanning calorimetric techniques were used to characterize the molecular structure and solid-state properties of the materials. Changes in the crystallinity and polymorphic forms of CH1 and CH2 were attributable to the different process conditions used. The differences in crystallinity were confirmed by powder X-ray diffraction data. The methods of preparation of CH1 and CH2 did not significantly influence the bulk, tap and true densities of the bulk material, but they affected the flow properties of CH1 and CH2. In conclusion, the physicochemical properties of the present chitosans prepared from lobster chitin (CH1 and CH2) are comparable with those of commercial chitosan materials of crab or shrimp shell origin.

Keywords: Chitin; Chitosan; Lobster; Deacetylation; Molecular weight; Solid-state properties; Polymorphism

1. Introduction

Chitin is one of the most abundant natural amino polysaccharide. The main commercial sources of chitin are the shell wastes of shrimp, lobster, krill and crab. Worldwide, millions of tons of chitin are harvested annually (Rha, Rodriguez-Sanchez, & Kienzle-Sterzer, 1984; Roberts, 1992). Chitin is partially deacetylated, usually by alkaline N-deacetylation using industrial processes to produce a variety of polymers (Brugnerotto et al., 2001). When the degree of deacetylation (DD) is 75% or higher, the product is called chitosan (Li, Revol, & Marchessault, 1997). It becomes water-soluble due to the protonation of the $-NH_2$ groups of the glucosamine unit. The production of chitosan from crustacean shells, waste of food industry, is economically feasible (Ravi Kumar, 2000). A lot of chitin-rich food waste is discarded, especially in Asian countries, where people have seafood-rich diets (Ball, 2002). Therefore, the efforts to convert those wastes into a useful product are rational and important.

Chitosan is the N-deacetylated derivative of chitin, although this N-deacetylation is almost never complete. In the last 10 years, chitosan has received much attention because of its extraordinary properties and for its inexpensive and abundant resources (Harish Prashanth, Kittur, & Tharanathan, 2002). Chitosan is biodegradable, biocompatible and non-toxic. The incomplete characterization of chitosans and the variability of commercial chitosans have discouraged the pharmaceutical industry from adopting it as a pharmaceutical excipient or formulation component. The heterogeneity of these chitosans mainly results from the sources of chitin and relatively uncontrolled commercial processing of native chitin involving both N-deacetylation and depolymerization (Rege & Block, 1999; Rege, Garmise, & Block, 2003).

* Corresponding author. Tel.: +358 9 19159158; fax: +358 9 19159144.
E-mail address: jyrki.heinamaki@helsinki.fi (J. Heinämäki).

0144-8617/$ - see front matter © 2004 Published by Elsevier Ltd.
doi:10.1016/j.carbpol.2004.08.017

The characterization of chitin and chitosan derived from crab and shrimp shells has been largely discussed in the literature (Harish Prashanth et al., 2002; Heux, Brugnerotto, Desbrières, Versali, & Rianudo, 2000; Kittur, Haris Prashanth, Udaya Sankar, & Tharanathan, 2002; Saito & Tabeta, 1987). The determinations of the DA as well as its molecular weight (MW) are the two fundamental physical properties of these polymers. In the present study, samples of chitosan from lobster chitin were prepared under two different processes and conditions. Hence, the aim of this study was to characterize and compare the physicochemical properties of those chitosan samples with four commercial chitosans prepared from crab and shrimp shells.

2. Materials and methods

2.1. Materials

Chitosans derived from lobster chitin, i.e. chitosan 1 (CH1) and chitosan 2 (CH2), were prepared industrially in a Cuban enterprise by N-deacetylation of lobster chitin. Chitin was suspended in an alkali solution, 45% NaOH, at 130 °C for 30 min to obtain CH1, whereas CH2 was obtained with 49% NaOH at 130 °C for 30 min. The solids were filtered, intensively washed with distilled water until nearly neutral pH was obtained and dried in vacuum at 40 °C.

Four commercially available chitosan samples derived from crab or fresh shrimp shells varying in MW and degree of deacetylation (% DD) were used as reference materials for CH1 and CH2. High molecular weight chitosan ((HMW), 79.0% DD), medium (MMW, 81.4% DD), and low (LMW, 85.0% DD) MW chitosans (Aldrich Chemical Company Inc., USA) and Primex chitosan (85.6% DD) (Primex Ingredients ASA, Norway) were used. All other reagents and solvents used were of analytical grade.

2.2. Physicochemical material characterization

2.2.1. Molecular weight determination

The viscosity average MW of chitosans was calculated from the classical Mark–Houwink relationship,

$$[\eta] = K_m(\mathrm{MW})^{\alpha}$$

where $[\eta]$, intrinsic viscosity; K_m, 1.81×10^{-3} and α, 0.93 (Ravi Kumar, 2000). The values of constants K_m and α have been determined in 0.1 M acetic acid and 0.2 M sodium chloride solution. Six polymer solutions of known concentrations of CH1 and CH2 were prepared. Relative viscosity was measured in triplicate using an Ubbelohde viscometer kept in a constant-temperature bath at 25 ± 0.1 °C.

2.2.2. Viscosity

Viscosity measurements of solutions of CH1 and CH2 1% in 1% acetic acid were performed on a Brookfield digital viscometer (Model DV-II+, Stoughton, USA) with a LV Spindle Set number 1 at room temperature (25.0 ± 0.1 °C).

2.2.3. Infrared spectroscopy

IR spectra were obtained using the Nicolet 60 SX Fourier Transform Infrared Spectrometer under dry air at room temperature and KBr pellets. Approximately 150 mg of KBr and 2 mg of chitosan powder (particle size ≤ 125 μm) were blended with an agate mortar and pestle for 5 min. The sample pellets were prepared at a pressure of 9 tons for 2 min. The disk was conditioned in an oven at 80 °C for 48 h before analysis.

The IR spectrum was then recorded in the frequency range of 4000–400 cm^{-1}. The absorbances at 1655 cm^{-1} (amide I band), a measure of the *N*-acetyl group content, and 3450 cm^{-1} (hydroxyl band) were determined using the baseline proposed by Baxter, Dillon, Taylor, and Roberts (1992) and the modifications reported by Domszy and Roberts (1985). Three chitosan samples of known DD (HMW, MMW and LMW) were selected for generating the standard curve, and the relationship of absorbance ratio to DD was utilised to determine the DD of unknown chitosans (Fig. 2). Chitosan samples were analysed by calculating their IR absorbance ratios in conjunction with the standard curve in order to determine the corresponding DD, following the procedure described by Sabnis and Block (1997).

2.2.4. Solid-state CP-MAS ^{13}C NMR

The NMR experiments were performed on a Varian Unity Inova spectrometer operating at 300 MHz for ^{1}H frequency, using the combined techniques of proton dipolar decoupling (DD), magic angle spinning (MAS) and cross-polarization (CP). The contact time was 1 ms, the acquisition time 51.2 ms and the recycle delay 4 s. The proton pulse width was 6 μs and 18 kHz spectral window was used. A typical number of 2000 scans was acquired for each spectrum. The chemical shifts were externally referenced by setting the methyl resonance of hexamethylbenzene (HMB) to 17.3 ppm. The samples were contained in a SiN_4 cylindrical rotor which was spun at 5 kHz during measurements.

The degree of acetylation (DA) of chitosan was calculated from the relative intensities of the resonance of the ring carbon ($I_{C_1}, I_{C_2}, I_{C_3}, I_{C_4}, I_{C_5}, I_{C_6}$) and methyl carbon ($I_{CH_3}$) obtained from ^{13}C NMR spectra (Ottoy, Varum, & Smidsord, 1996) by the following equation:

$$\mathrm{DA} = \frac{I_{CH_3}}{I_{C_1} + I_{C_2} + I_{C_3} + I_{C_4} + I_{C_5} + I_{C_6}/6}$$

2.2.5. Powder X-ray diffraction

X-ray diffraction patterns on powders (before and after milling) were obtained by using a variable temperature X-ray diffractometer (D8 Advance Bruker AXS GmbH, Karlsruhe, Germany) (VT-XRPD). The VT-XRPD experiments were performed in symmetrical reflection mode with Cu K_α radiation (1.54 Å) using Göbel Mirror bent gradient multilayer optics. The scattered intensities were measured with

a scintillation counter. The angular range was from 5 to 40° with steps of 0.2°, and the measuring time was 10 s/step. The estimation of the crystallinity was based on the assumption that the experimental XRPD intensity curve is a linear combination of intensities of the crystalline and amorphous component. The crystallinities of the samples were estimated by fitting the intensities of the crystalline and amorphous component to the experimental intensity curve. The diffraction pattern of the totally amorphous ground HMW sample was used as the amorphous model intensity curve and the crystalline one consisted only of the diffraction peaks. The crystallinities were calculated as the ratio of the integrals of the intensities of the crystalline component and the sample studied. The samples of chitosan were subjected to size reduction using a Planetary Mono Mill pulverisette 6 (Fritsch GmbH, Germany).

2.2.6. Differential scanning calorimetry (DSC)

DSC thermograms of chitosan powders were measured using a differential scanning calorimeter (DSC 821^e, Mettler Toledo AG, Schwerzenbach, Switzerland). Samples of 2–3 mg were sealed in an aluminium pan. In this method, the pans were probably not hermetically sealed. A nitrogen purge with a flow rate of 80 ml/min was used in the furnace. The scans were obtained by first heating to 190 °C, cooling to 25 °C and a second heating to 400 °C at a rate of 10 °C/min in order to estimate the glass transition temperature. Each run was performed in triplicate.

2.2.7. Thermogravimetric analysis (TGA)

TGA thermograms of chitosan powders were measured using a thermogravimetric analyser (TGA/SDTA 851^e, Mettler Toledo AG, Schwerzenbach, Switzerland). A nitrogen purge of 50 ml/min was used in the furnace. The sample size of 5 mg was accurately weighed into an aluminium pan. The measurements were obtained at 25–250 °C at a heating rate of 10 °C/min and the weight loss was calculated from three determinations.

2.2.8. Physical powder properties

Bulk, tap and true densities of the powders were determined by the method of European Pharmacopoeia (2002). A standardized tapped density tester (Erweka SVM1, Erweka GmbH, Heusenstamm, Germany) was employed. The volume occupied by the powder was recorded and the bulk density was calculated. For calculating the tapped density the volume occupied after 1250 taps was used. Each sample was measured in triplicate. The true density of materials was measured using a pycnometer (Micrometrics, Model 1305, Norcroos, GA) and helium as an inert gas. The results are averages of three determinations. The Carr index and Hausner ratio were calculated from the tap, bulk and true densities (Wells & Aulton, 1998). The experimental data was analyzed in accordance with the analysis of variance (ANOVA). When a statistically significant difference ($p<0.05$) was obtained, a Tukey HSD test was performed.

3. Results and discussion

3.1. Dependence of viscosity on the molecular weight

Viscometry is a simple and rapid method for the determination of MW, which requires the determination of constants through correlation of $[\eta]$ with MW (Roberts & Domszy, 1982) The MW of CH1 (309,000 g/mol) was slightly higher than that of CH2 (290,000 g/mol). As expected, increasing molar mass corresponds to increasing intrinsic viscosity ($[\eta]_{CH1}=231$ ml/g and $[\eta]_{CH2}=218$ ml/g). This could be attributed to the alkali concentration used in the process. With the increase of the alkaline strength the content of the acetyl group decreases and the nitrogen content increases. Also, the lower viscosity of CH2 compared to CH1 suggests a decrease of MW.

3.2. Degrees of deacetylation and acetylation

The infrared spectra of all chitosan powders (Fig. 1) exhibited broad peaks assigned to OH stretching, indicating intermolecular hydrogen bonding of chitosan molecules. The absence of sharp absorption around 3500 cm^{-1} in all samples indicated that there are no free OH groups. As expected, N-deacetylation is associated with progressive weakening of the band occurring at 1655 cm^{-1} (amide I). A C=O stretching (amide I) peak near the 1655 cm^{-1} and a NH bending (amide II) peak near the 1590 cm^{-1} regions were observed.

The DDs of the samples CH1 and CH2 were obtained from the standard curve that has the following form: $DD=87.8-[3(A_{1655}/A_{3450})]$ ($r^2=0.987$) (Fig. 2). Using extrapolation, the DD values for CH1 and CH2 were roughly 86–89% which show a high degree of deacetylation.

The IR spectroscopic method, commonly used for the estimation of chitosan DDs, has a number of advantages because it is relatively fast and does not require dissolution

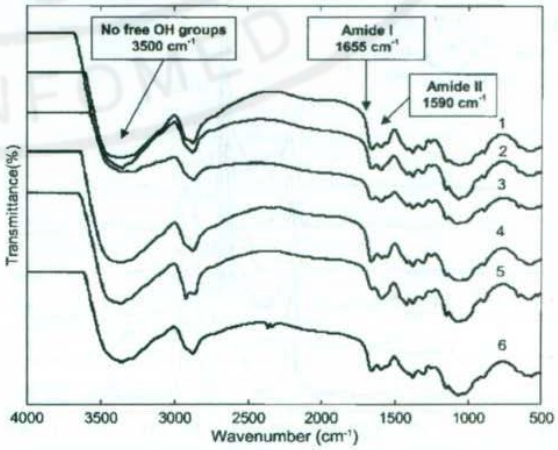

Fig. 1. Transmission infrared spectra of chitosan samples: (1) CH1, (2) CH2, (3) Primex, (4) MMW, (5) LMW, (6) HMW.

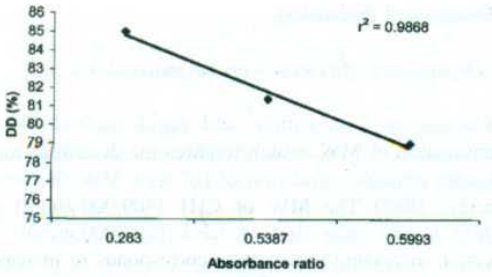

Fig. 2. Standard curve for determination of % DD of CH1 and CH2.

of the sample in an aqueous solvent. However, the sample preparation, the type of instrument used and the experimental conditions may influence the sample analysis (Khan, 2002). Furthermore, since the presence of free water may interfere with the analysis by contributing towards the intensity of the hydroxyl band, the chitosan samples were dried in an oven at 80 °C for 48 h.

Different methods have been applied to determine the acetyl content of chitosan, including infrared spectroscopy (Domszy et al., 1985; Miya, Iwamoto, Yashikawa, & Mima, 1980; Shigemasa, Matsuura, Sashiwa, & Saimoto, 1996), solid-state NMR spectroscopy (Heux et al., 2000; Raymond, Morin, & Marchessault, 1993; Saito et al., 1987), ultraviolet spectrometry (Muzzarelli & Rochetti, 1985), ^{1}H liquid-state NMR (Hirai, Odani, & Nakajima, 1991; Varum, Anthonsen, Grasdalen, & Smidsord, 1991) and elemental analysis (Roberts, 1992). Solid-state ^{13}C NMR appears to be the most reliable for the evaluation of the acetyl content (Heux et al., 2000). It does not need the solubilization of the polymer but needs a high level of purification of the samples studied. ^{13}C CP-MAS NMR spectra of the chitosan samples are shown in Fig. 3. Corresponding chemical shifts and DA values appear in Tables 1 and 2, respectively. The methyl

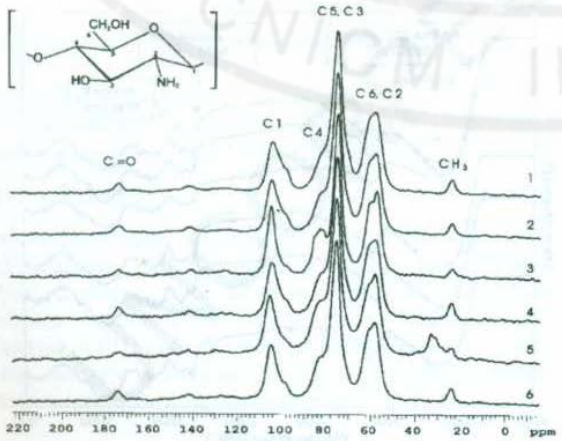

Fig. 3. CP-MAS ^{13}C NMR spectra of chitosan samples: (1) CH1, (2) CH2, (3) Primex, (4) MMW, (5) LMW, (6) HMW.

Table 1
^{13}C chemical shift values (ppm) for chitosan from various sources

Sample	C=O	C_1	C_3/C_5	C_2	CH_3
HMW	173.7	104.8	75.7	58.3	24.3
MMW	174.0	104.5	75.5	58.4	24.0
LMW	*174.1*	*105.4*	*75.7*	*58.2*	*23.6*
Primex	173.4	105.0	75.3	57.7	23.7
CH1	173.7	104.8	75.9	58.9	24.0
CH2	173.5	105.2	75.8	58.1	24.0

and carbonyl signals, associated with the monomeric form of chitin, were detectable in the polymeric chain of all the chitosan samples, showing incomplete deacetylation of the original chitin. The sample of LMW shows undesired signals at 33 ppm due to impurities (proteins and/or lipids) which were not removed adequately.

Solid state CP-MAS ^{13}C NMR is known to be very sensitive to changes in the local structure. The chemical shifts of C-1 and C-4 carbon in 1,4-linked carbohydrates are believed to be highly sensitive to any conformational change at the glycosidic linkage (Tanner, Chanzy, Vincendon, Roux, & Gaill, 1990). As shown in Fig. 3, the C-1 ^{13}C NMRsignal of CH1 is a single peak and the C-4 signal appears as a shoulder which is resolved best for the Primex sample. According to these results, chitosans derived from lobster chitin are similar to those of the commercial samples evaluated.

The dependence of the DD values on the type of analytical methods (Baxter et al., 1992; Khan, 2002) and method of purification (Sabnis et al., 1997) has been reported in the literature. As such, it can be concluded that the values of DD depend on the analytical method employed. This should be noticed when comparisons of chitin and chitosans of different sources are made.

3.3. Polymorphism

Figs. 4 and 5 show the powder X-ray diffraction patterns of chitosan samples. All chitosan powders showed diffraction peaks at approximately 10° (2θ) and 20° (2θ) before milling (Fig. 4). All types of chitosan powders were partly crystalline (Table 3).

Table 2
Properties of chitosans from various sources

Sample	Viscosity (mPa)	Degree of deacetylation (% DD)	Degree of acetylation (DA) ^{13}C NMR
HMW	1.77[a]	79.0[b]	0.11
MMW	286.0[a]	81.4[b]	0.15
LMW	53.0[a]	85.0[b]	0.02
Primex	59.0[a]	85.6[c]	0.08
CH1	10.2	86–89[d]	0.13
CH2	9.6	86–89[d]	0.10

[a] Suppliers' data.
[b] Determined by colorimetric assay (reference method).
[c] Determined by potentiometric titration.
[d] Determined by IR.

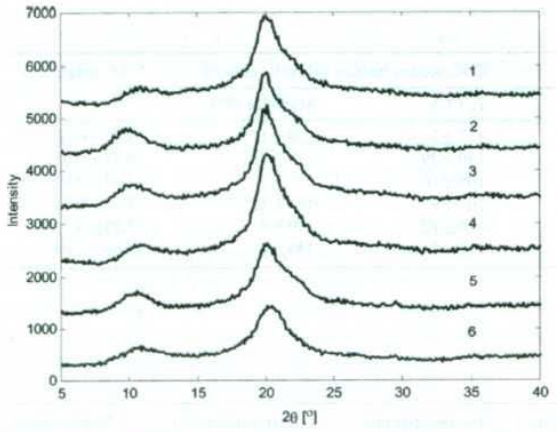

Fig. 4. X-ray diffraction patterns of chitosan samples before milling: (1) Primex, (2) HMW, (3) MMW, (4) LMW, (5) CH2, (6) CH1.

Six polymorphs have been proposed for chitosan: 'tendon chitosan' (Clark & Smith, 1936), 'annealed' (Saito et al., 1987), '1-2', 'L-2' (Saito et al., 1987), 'form I' and 'form II' (Samuels, 1981). The X-ray powder pattern of CH1 showed that it is polymorph 'L-2' and differed from the other chitosans studied. The two peaks having lattice angles of 10.8 and 20.4° corresponds to the respective equatorial (100) and (020) reflections of the 'L-2' polymorph of chitosan. XRPD diffraction of the CH2, HMW, MMW, LMW and Primex of chitosan coincides with tendon chitosan: the reflections corresponded to the equatorial (200), (020) and (220) reflections of the tendon chitosan.

As shown in Fig. 5, when the chitosan samples were milled, halo diffraction patterns were observed, indicating an amorphous state of the powders (Table 3). However, the reflections at approximately 12° (2θ) and 20.2° (2θ) were observed at low intensity in LMW chitosan.

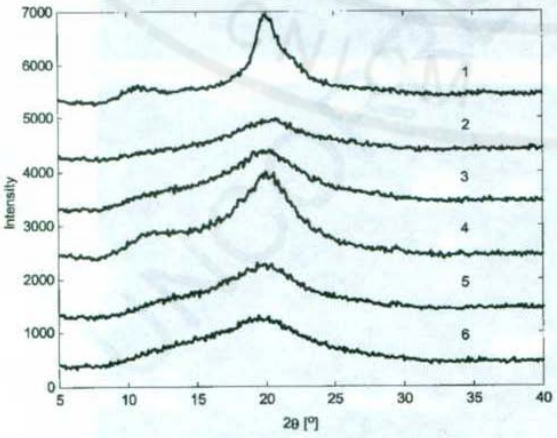

Fig. 5. X-ray diffraction patterns of chitosan samples after milling: (1) Primex, (2) HMW, (3) MMW, (4) LMW, (5) CH2, (6) CH1.

Table 3
Crystallinities of chitosans from various sources

Sample	Crystallinity (% ± 10)	
	No milling	Milling
HMW	43	0
MMW	50	0
LMW	49	43
Primex[a]	–	46
CH1	39	0
CH2	45	0

[a] Milled sample.

3.4. Thermal behaviour of chitosan powders

The thermal data of the chitosan samples are listed in Table 4. During the first heating run, a broad endothermic peak, centred at 130–150 °C was observed. According to TGA analyses, the changes in weight loss were attributed to dehydration, which is in agreement with the DSC results. Therefore, these results support the view that water evaporation occurred during the first DSC scan. The differences in the position and shape of the endotherm peak indicate differences in the water holding capacity and strength of water–polymer interaction (Kittur et al., 2002; Sakurai, Maegawa, & Takahashi, 2000). CH2 showed higher ΔH values than CH1, indicating a high DD value; i.e. it has more hydrophilic centres (amine groups) in the polysaccharide chain to bind more water molecules and to increase the content of bound water. The commercial chitosans do not show clear differences. The fact that the SD was increased indicates that the samples were less homogeneous. In addition, chitosan is not a completely crystalline polymer, so differences in the mobility of water molecules could be expected.

As reported by Sakurai et al. (2000), two cycles of heating and cooling runs were performed to eliminate the effect of moisture. Careful examination of the second heating run allows estimation of the glass transition temperature of the samples. The results of the second heating run obtained in the present study are shown in Table 4. Sakurai et al. employed chitosan films (chitosan with 96% of DD) and assigned a value of 205 °C to the glass transition temperature. In the present study, chitosan samples as a powder form and with a lower % of DD were used. Different properties such as crystallinity, amount of water, degree of deacetylation and OH- or amine-groups in the chain of the macromolecule, can be associated with glass transition and its variability. The second thermal change registered for the chitosan samples in the present study was an exothermic decomposition peak with onset at 280–300 °C.

3.5. Particle and powder properties

The physical properties of the chitosan samples are listed in Table 5. The Carr index and Hausner ratio widely used in characterising flow properties of pharmaceutical excipients,

Table 4
Thermal transitions of chitosan samples

Sample	DSC/first heating (endotherm)			DSC/second heating (glass transition)		TGA weight loss (%)
	T_o (°C)	T_p (°C)	ΔH (J/g)	T_o (°C)	Midpoint (°C)	
HMW	121±11	142±6	78±22	117±7	129±11	9.91±0.03
MMW	130±6	135±5	70±5	130±29	133±18	8.53±0.03
LMW	136±1	139±1	61±3	105±16	113±7	7.64±0.07
Primex	139±9	142±8	69±20	107±9	121±12	8.30±0.01
CH1	146±2	147±2	64±2	116±12	139±4	7.29±0.21
CH2	127±3	133±2	92±9	112±5	130±4	10.66±0.09

T_o, onset temperature; T_p, peak temperature; ΔH, enthalpy; mean±SD; $n=3$.

Table 5
Physical properties of chitosans

Sample	Bulk density (g/cm^3)	Tap density (g/cm^3)	True density (g/cm^3)	Packing fraction	Carr's index (%)	Hausner ratio
HMW	0.223 ± 0.012^a	0.246 ± 0.016^a	1.446 ± 0.007^a	0.157^a	9.5^a	1.10^a
MMW	0.180 ± 0.017^b	0.206 ± 0.019^b	$1.426\pm0.007^{a,b}$	0.125^b	12.7^a	1.14^b
LMW	0.311 ± 0.014^c	0.351 ± 0.019^c	1.434 ± 0.000^a	0.226^c	9.2^a	1.10^a
CH1	0.195 ± 0.007^b	0.211 ± 0.005^b	1.407 ± 0.004^c	$0.139^{a,b}$	7.8^b	1.08^a
CH2	0.186 ± 0.002^b	0.216 ± 0.002^b	$1.413\pm0.004^{b,c}$	0.131^b	14.1^c	1.16^b

Letters a–d illustrate the statistical difference ($p<0.05$) of the results based on ANOVA and Tukey tests. For example in bulk density code 'a' means that HMW is not statistically equivalent with any of the others. In the same column, MMW, CH1 and CH2 all having code 'b' are not statistically differing from each other.

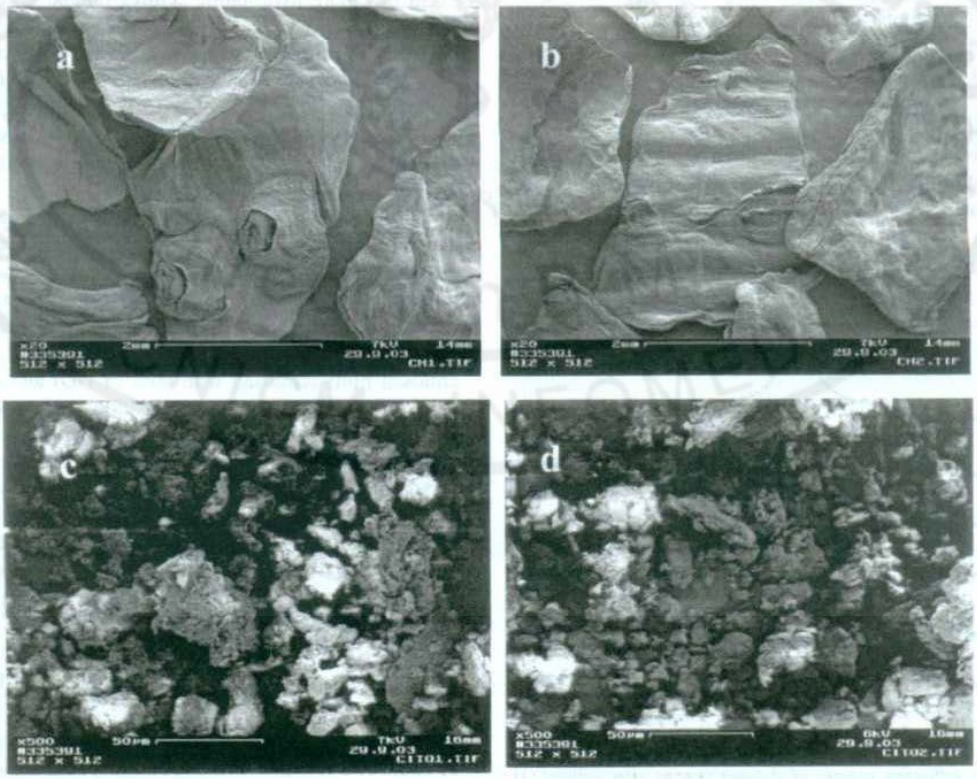

Fig. 6. Scanning electron micrographs (SEMs) on (a) native unmilled CH1, (b) native unmilled CH2, (c) milled CH1 and (d) milled CH2.

indicated that the present chitosan powders had an excellent or good flowability. Table 5 provides evidence of the variability encountered in the chitosans. The significant differences ($p<0.05$) are supported by the results of the Tukey HSD test. There were no significant differences in the bulk, tap and true densities and the packing properties ($p>0.05$) of CH1 and CH2, whereas the differences in flow properties were significant ($p<0.05$).

The scanning electron micrographs (SEMs) of both native and milled CH1 and CH2 are shown in Fig. 6. The chitosans prepared from lobster chitin consisted of amorphous particles of rather irregular size and shape. The particle sizes of native unmilled and milled chitosans (CH1 and CH2) were 2000 and 20 μm, respectively.

4. Conclusions

The properties of chitosans are very much dependent on the degree of deacetylation, which depends on the synthesis of chitosan as well as the source of the starting material (i.e. chitin). Powder X-ray diffraction permitted the analyses of the polymorphs of chitosan. The synthesis process does not significantly influence the bulk, tap and true densities and packing properties of chitosan powders of lobster origin. The method of synthesis significantly affects the flow properties of the present materials. The chitosans (CH1 and CH2) prepared by N-deacetylation from lobster chitin have physico-chemical properties that are similar to the commercial chitosans of crab or shrimp shell origin.

Acknowledgements

The authors wish to thank the Centre for International Mobility for Foreign Students (CIMO) for financial support of the present study. We gratefully acknowledge Leena Christiansen, PhD (Pharm.) for her suggestions related to thermal study, Saara Tiittanen, MSc (Orion Pharma, Espoo, Finland) for her assistance in DSC and TGA measurements and Simo Siiriä for technical drawings.

References

Ball, P. (2002). New uses for a dead lobster: Crustacean shells could thicken food, paint and makeup. *Nature* http//www.nature.com/nsu/020812/020812-11.html.

Baxter, A., Dillon, M., Taylor, K. D. A., & Roberts, G. A. F. (1992). Improved method for i.r. determination of the degree of N-acetylation of chitosan. *International Journal of Biological Macromolecules, 14*, 166–169.

Brugnerotto, J., Lizardi, J., Goycoolea, F. M., ArgÜelles-Monal, W., Desbrières, J., & Rianudo, M. (2001). An infrared investigation in relation with chitin and chitosan characterization. *Polymer, 42*, 3569–3580.

Clark, G. L., & Smith, A. F. (1936). X-ray diffraction studies of chitin, chitosan and derivatives. *Journal of Physical Chemistry, 40*, 863.

Domszy, J. G., & Roberts, G. A. F. (1985). Evaluation of infrared spectroscopic techniques for analyzing chitosan. *Makromolecules Chemistry, 186*, 1671–1677.

European Pharmacopoeia (2002). *Council of Europe Strasbourg* (4th ed) pp. 207–208.

Harish Prashanth, K. V., Kittur, F. S., & Tharanathan, R. N. (2002). Solid state structure of chitosan prepared under different N-deacetylating conditions. *Carbohydrate Polymers, 50*, 27–33.

Heux, L., Brugnerotto, J., Desbrières, J., Versali, M. F., & Rianudo, M. (2000). Solid State NMR for determination of degree of acetylation of chitin and chitosan. *Biomacromolecules, 1*, 746–751.

Hirai, A., Odani, H., & Nakajima, A. (1991). Determination of degree of deacetylation of chitosan by ^{1}H NMR spectroscopy. *Polymer Bulletin, 26*, 87–94.

Khan, T. A. (2002). Reporting degree of deacetylation values of chitosan: The influence of analytical methods. *Journal of Pharmaceutics and Pharmaceutical Sciences, 5*(3), 205–212.

Kittur, F. S., Haris Prashanth, K. V., Udaya Sankar, K., & Tharanathan, R. N. (2002). Characterization of chitin, chitosan and their carboxymethyl derivatives by differential scanning calorimetry. *Carbohydrate Polymers, 49*, 185–193.

Li, J., Revol, J. F., & Marchessault, R. H. (1997). Effect of degree of deacetylation of chitin on the properties of chitin crystallites. *Journal of Applied Polymer Sciences, 65*(2), 373–380.

Miya, M., Iwamoto, R., Yashikawa, S., & Mima, S. (1980). IR spectroscopic determination of CONH content in highly deacetylated chitosan. *International Journal of Biological Macromolecules, 2*, 323–324.

Muzzarelli, R. A. A., & Rochetti, R. (1985). Determination of the degree of acetylation of chitosans by first derivative ultraviolet spectrophotometry. *Carbohydrate Polymers, 5*, 461–472.

Ottoy, M. H., Varum, K. M., & Smidsord, O. (1996). Compositional heterogeneity of heterogeneously deacetylated chitosans. *Carbohydrate Polymers, 24*, 17–24.

Ravi Kumar, M. N. V. (2000). A review of chitin and chitosan applications. *Reactive and Functional Polymers, 46*, 1–27.

Raymond, L., Morin, F. G., & Marchessault, R. H. (1993). Degree of deacetylation of chitosan using conductimetric titration and solid-state NMR. *Carbohydrate Research, 243*, 331–336.

Rege, P. R., & Block, L. H. (1999). Chitosan processing influence of process parameters during acidic and alkaline hydrolysis and effect of the processing sequence on the resultant chitosan's properties. *Carbohydrate Research, 321*, 235–245.

Rege, P. R., Garmise, R. J., & Block, L. H. (2003). Spray-dried chitosans part I: Preparation and characterization. *International Journal of Pharmaceutics, 252*, 41–51.

Rha, C. K., Rodriguez-Sanchez, D., & Kienzle-Sterzer, C. (1984). Novel applications of chitosan. In R. R. Colwell, E. R. Pariser, & A. J. Sinskey (Eds.), *Biotechnology of marine polysaccharides* (pp. 284–311). Washington: Hemisphere.

Roberts, G. A. F. (1992). Structure of chitin and chitosan. In G. A. F. Roberts (Ed.), *Chitin chemistry*1st ed (pp. 1–100). New York: Macmillan Press.

Roberts, G. A. F., & Domszy, J. G. (1982). Determination of the viscosimetric constants for chitosan. *International Journal of Biological Macromolecules, 4*, 374–377.

Sabnis, S., & Block, L. H. (1997). Improved infrared spectroscopic method for the analysis of degree of N-deacetylation of chitosan. *Polymer Bulletin, 39*, 67–71.

Saito, H., & Tabeta, R. (1987). High-resolution solid-state ^{13}C NMR study of chitosan and its salts with acids: Conformational characterization of polymorphs and helical structures as viewed from the conformation-dependent ^{13}C chemical shifts. *Macromolecules, 20*, 2424–2430.

Sakurai, K., Maegawa, T., & Takahashi, T. (2000). Glass transition temperature of chitosan and miscibility of chitosan/poly(*N*-vinyl pirrolidone) blends. *Polymer, 41*, 7051–7056.

Samuels, R. J. (1981). Solid state characterization of the structure of chitosan films. *Journal of Polymer Sciences, 19*, 1081–1105.

Shigemasa, Y., Matsuura, H., Sashiwa, H., & Saimoto, H. (1996). Evaluation of different absorbance ratios from infrared spectroscopy for analyzing the degree of deacetylation in chitin. *International Journal of Biological Macromolecules, 18*, 237–242.

Tanner, S. F., Chanzy, H., Vincendon, M., Roux, J. C., & Gaill, F. (1990). High-resolution solid-state carbon-13 nuclear magnetic resonance study of chitin. *Macromolecules, 23*, 3576–3583.

Varum, K. M., Anthonsen, M. W., Grasdalen, H., & Smidsord, O. (1991). Determination of the degree of N-acetylation and the distribution of N-acetyl groups in partially N-deacetylated chitins (chitosans) by high-field NMR spectroscopy. *Carbohydrate Research, 211*, 17–23.

Wells, J. I., & Aulton, M. E. (1998). Preformulation. In M. E. Aulton (Ed.), *Pharmaceutics, the science of dosage form design* (pp. 223–253). New York: Churchill Livingstone.

Solid-state and mechanical properties of aqueous chitosan-amylose starch films plasticized with polyols

II

Fernández Cervera, M., Heinámaki, J., Krogars, K., Jorgensen A., Karjalainen, M., Iraizoz Colarte, A. and Yliruusi, J.

AAPS Pharm. Sci. Tech. 2004, 5(1) Article 15 (hltp://www.aapspharmscitech.org) 1-6.

AAPS PharmSciTech 2004; 5 (1) Article 15 (http://www.aapspharmscitech.org).

Solid-State and Mechanical Properties of Aqueous Chitosan-Amylose Starch Films Plasticized With Polyols

Submitted: October 6, 2003; Accepted: December 19, 2003

Mirna Fernández Cervera,[1] Jyrki Heinämäki,[2] Karin Krogars,[2] Anna C. Jörgensen,[2] Milja Karjalainen,[2] Antonio Iraizoz Colarte,[1] and Jouko Yliruusi[2,3]

[1]Institute of Pharmacy and Food, University of Havana, Havana, Cuba
[2]Pharmaceutical Technology Division, Department of Pharmacy, FIN-00014 University of Helsinki, Finland
[3]Viikki Drug Discovery Technology Center DDTC, University of Helsinki, Finland

ABSTRACT

The film-forming ability of chitosan and binary mixtures of chitosan and native amylose corn starch (Hylon VII) was evaluated with free films prepared by a casting/solvent evaporation method. Unplasticized and plasticized free chitosan films in aqueous acetic acid and respective films containing a mixture of chitosan and native amylose starch in acetic acid were prepared. Glycerol, sorbitol, and i-erythritol were used as plasticizers. Solid-state and mechanical properties of the films were studied by powder x-ray diffractometry (XPRD), differential scanning calorimetry (DSC), and a materials testing machine. The films composed of a mixture of chitosan and native amylose starch in acetic acid were clear and colorless. A plasticizer concentration of 20% wt/wt (of the polymer weight) was sufficient to obtain flexible films with all samples tested. X-ray diffraction patterns and DSC thermograms indicated an amorphous state of the films independent of the type of plasticizer used. In conclusion, incorporation of native amylose corn starch into chitosan films improves the consistency and the mechanical properties of the films.

KEYWORDS: chitosan, amylose corn starch, erythritol, free films, plasticizer

INTRODUCTION

Chitosan (Figure 1) is a cationic natural polysaccharide generally considered as a safe, biocompatible and biodegradable material.[1] During the past 20 years, chitosan has been evaluated for numerous pharmaceutical applications(eg, as a direct compression diluent, wet granulation excipient, wetting agent, gel and emulsion agent, and most recently as a film-coating agent. Higher molecular weight chitosans have been reported to have good film-forming properties as a result of intra- and intermolecular hydrogen bonding.[2] The chitosan film characteristics, however, varied from one report to another. Differences in the sources of chitin used to produce chitosan, chitosan material properties, solvents used, methods of film preparation, and types and amounts of copolymers and plasticizers used may affect the quality of the films.[3-6]

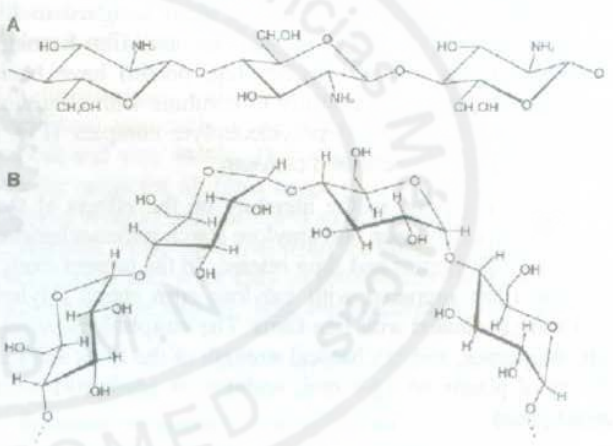

Figure 1. Chemical structure of chitosan (A) and native amylose corn starch (Hylon VII) (B).

Another natural polysaccharide, amylose starch (Figure 1), has also been investigated by several researchers using starch-based films cast from a solution or gel.[7-11] Wolff and collaborators[12] prepared self-supporting amylose films with and without glycerol plasticization. The influence of amylose content on the mechanical properties of cast films was studied by Lourdin et al.[8] They studied mixed amylose-amylopectin films and found slightly higher stress at break for plasticized amylose films but lower stress at break for plasticized amylopectin films with a glycerol/polymer ratio of 0.2. Moreover, according to Rindlav et al,[9] the functional

Corresponding Author: Jyrki Heinämäki, Pharmaceutical Technology Division, Department of Pharmacy, FIN-00014 University of Helsinki, Finland;
Tel: +358-9-19159158; Fax: +358-9-19150144;
Email: jyrki.heinamaki@helsinki.fi

Table 1. Effect of Plasticizer on the Thickness, Tensile Strength, and Percentage Elongation of Free Films (n = 5)

Property	Type of Plasticizer			
	Unplasticized	Glycerol	Erythritol	Sorbitol*
Thickness mm ± SD	0.019 ±0.003	0.031 ±0.004	0.028 ± 0.002	0.030 ±0.004
Tensile Strength N/mm^2 ± SD	26.8 ±2.0	27.2 ± 1.9	44.2 ± 2.0	-
Percentage Elongation at Break % ± SD	4.6 ± 1.9	5.4 ±0.1	5.9 ± 1.6	-

*The films plasticized with sorbitol were very brittle and cracking.

properties of amylose films were, in general, slightly better than those of amylopectin films, regarding both film strength and barrier properties. More recently it was discovered that cross-linked starches possess unique features as an excipient for the manufacture of the controlled-release solid oral dosage form of drugs.[13,14]

Chitosan has also been assessed for its potentiality in the development of controlled-release systems and for its propensity for targeting drugs to specific sites.[15,16] Numerous control or sustained delivery systems with chitosan have been described in the literature.[17-21] The potentiality of chitosan in sustained-release systems has been assigned to its polymeric character, including its gel- and film-forming properties. Other polysaccharides (eg, pectin) have been evaluated for their susceptibility to combine with chitosan; there exists a potential of polyelectrolyte complex (PEC) formation between pectin and chitosan.[22,23]

There are no reports in the literature on the effects of the combination of chitosan and amylose starch polysaccharides on the film properties and drug release. In the present study, chitosan films prepared with amylose corn starch (Hylon VII) were evaluated with free films. The morphology, solid-state properties, and mechanical strength of the films and the effects of plasticizer (glycerol, sorbitol, or erythritol) were investigated.

MATERIALS AND METHODS

Materials

The film-coating materials studied were high molecular weight chitosan (Aldrich Chemical Company Inc., Milwaukee, WI, U.S.A) and amylose-rich corn starch, Hylon VII (National Starch & Chemical GmbH, Neustadt, Germany). Glycerol (European Pharmacopeia [PhEur]), sorbitol (PhEur), and i-erythritol (Sigma-Aldrich Chemie GmbH, Steinheim, Germany), 20% wt/wt of the polymer weight, were used as plasticizers, and acetic acid (Riedel-de Haën, Seelze, Germany) and purified water as solvents.

Preparation of Free Films

Unplasticized and plasticized polymeric solutions (1% wt/wt) were prepared by dissolving chitosan in a diluted acetic acid (1%) solution at room temperature (21°C ± 2°C). The plasticizers (plasticizer content based on polymer weight = 20% wt/wt) employed were glycerol, sorbitol, and erythritol.

The aqueous polymer solutions contained 2% (wt/wt) of film former (mixture of chitosan and Hylon VII), glycerol or erythritol as a plasticizer (20% wt/wt of the polymer weight), acetic acid (1%), and purified water. The compositions of the chitosan-Hylon VII solutions studied were as follows: 100:0%, 80:20%, 60:40%, and 50:50% with glycerol; 100:0%, 80:20%, and 60:40% with erythritol.

Hylon VII solutions were prepared in a high-pressure reactor. In order to obtain the Hylon solutions, the suspensions were heated to 157°C, cooled down below 95°C, and filtrated. Details of the procedure are described elsewhere.[11] Hylon solutions were mixed with the chitosan solutions at ~50°C to 60°C.

For preparing free films, 8.0 g of the polymer solution was poured into polytetra-fluoroethylene (Teflon) molds (11 × 3.0 cm). A total of 10 to 12 molds per composition were originally made. The films were air dried for 4 hours at 60°C and allowed to stabilize in a desiccator for at least 24 hours at 21°C ± 2°C and 60% relative humidity (RH) before testing. The dry thickness of the films was measured at 5 locations (center and 4 corners) using a digital micrometer (Sony U30-F, Sony Magnescale Inc, Tokyo, Japan), and the mean thickness was calculated. The total number of replicates was 5. The results are summarized in Tables 1 and 2.

The cross sections of free films were studied by scanning electron microscopy (SEM). Samples for SEM were prepared by attaching the free films to double-sided carbon tape and coated 20 nm platinum with a sputter coater (Agar sputter coater B7340, Agar Scientific Ltd, Stansted, UK). The micrographs were taken with a Zeiss DSM 820 (Carl Zeiss, Oberkochen, Germany) SEM. An accelerated voltage of 10 kV and secondary electrons was used for all micrographs.

Table 2. Thickness of Free Chitosan

Type of Chitosan Films	Thickness (mm ± SD)
Chitosan-Hylon VII (100: 0%), glycerol	0.054 ± 0.003
Chitosan-Hylon VII (80: 20%), glycerol	0.051 ± 0.005
Chitosan-Hylon VII (60: 40%), glycerol	0.040 ± 0.001
Chitosan-Hylon VII (50: 50%), glycerol	0.039 ± 0.002
Chitosan-Hylon VII (100: 0%), erythritol	0.082 ± 0.003
Chitosan-Hylon VII (80: 20%), erythritol	0.043 ± 0.001
Chitosan-Hylon VII (60: 40%), erythritol	0.042 ± 0.002

Powder X-Ray Diffraction

Powder x-ray diffraction patterns on powders and free films were obtained by using an x-ray diffractometer (D8 Advance Bruker AXS GmbH, Karlsruhe, Germany) with CuKα radiation (1.54 Å). The samples were scanned from 5° to 40° (2θ) with an increment of 0.02° and measurement time of 10 s/increment. Determination of crystallinity was based on the assumption that the experimental intensity curve is a linear combination of a crystalline component and an amorphous component. The crystallinity of the samples was estimated by fitting the intensity of the crystalline component and the amorphous material to the experimental curve, and it was obtained as the ratio between the integrals of the intensities of the crystalline component and the studied sample.

Differential Scanning Calorimetry

Differential Scanning Calorimetry (DSC) thermograms of chitosan powder and free films were measured using a differential scanning calorimeter (model 910 DSC, TA Instruments, New Castle, DE). Samples of 2 to 5 mg were accurately weighed into solid aluminum pans without seals. The measurements were obtained at a heating rate of 10°C/min and scanning from 60°C to 400°C.

Mechanical Strength Measurements

A Lloyd LRX materials testing machine (Lloyd Instruments Ltd, Fareham, UK) was used to determine the mechanical properties of free films. The films were cut into 11 × 1.5 cm strips for testing. The measurements were performed using a 2000 N load cell and a cross-head speed of 5 mm/min. Five parallel determinations were made for each sample. The tensile stress was plotted against the percentage of elongation to give a stress-strain curve, and the ultimate tensile strength as well as the percentage of elongation at break was reported.

RESULTS AND DISCUSSION

Scanning electron micrographs of cross-sections of free films are presented in Figure 2. These figures indicate that the structure of films was homogeneous and continuous and thus the films were suitable for further evaluation.

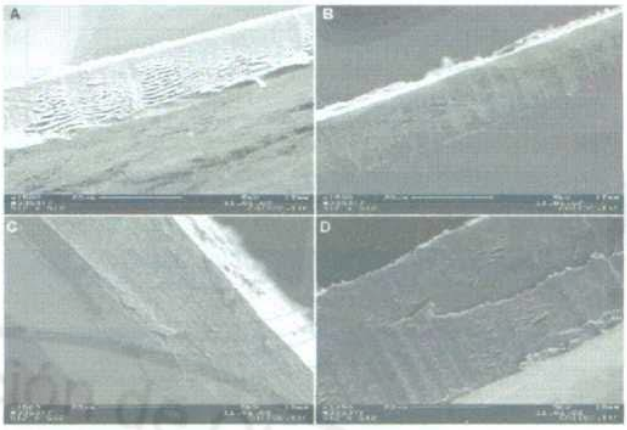

Figure 2. Scanning electron micrographs on cross-sections of free chitosan films containing glycerol (A), erythritol (B), chitosan and Hylon VII (60:40) and glycerol (C), as well as chitosan and Hylon VII (80:20) and erythritol (D).

All chitosan films were clear and colorless to pale yellow. The films, especially those prepared with sorbitol, were smooth and very brittle. The plasticizer concentration used was the same for all films tested (20% wt/wt based on the polymer weight) and sufficient to obtain flexible films with all samples. Films produced from the unplasticized solutions were thinner and were easy to remove from the mold. The incorporation of amylose corn starch increased the thickness of the films.

Solid-State Properties and Thermal Behavior

As seen in Figure 3, the powder x-ray diffraction pattern of chitosan powder showed diffraction peaks at ~10° (2θ) and 20° (2θ). The high molecular weight chitosan was in crystalline state. When processing chitosan powder into films, an amorphous state of the films independent of the type of plasticizer used was observed. The intensity of the hydrated crystal peak at ~20° (2θ) was higher than that at ~10° (2θ).

Amylose is known to recrystallize into the type-B crystalline form from a dilute solution. Gidley[24] proposed that the origin of amylose gelation lies in the formation and subsequent aggregation of interchain type-B double helices. Figure 4 shows the effect of incorporation of Hylon VII to chitosan films. The free films maintain an amorphous state. None showed any specific diffraction peaks at 2θ to type B (5.6°, 15°, 17°, 22°, and 24°),[25] thus Hylon VII remained in an

amorphous state. It may be concluded that all films of binary mixtures of chitosan and Hylon VII were in an amorphous state. Nunthanid et al[6] found that the chitosan (lower and higher molecular weight) films prepared by casting from aqueous acetic solution were in amorphous to partially crystalline form.

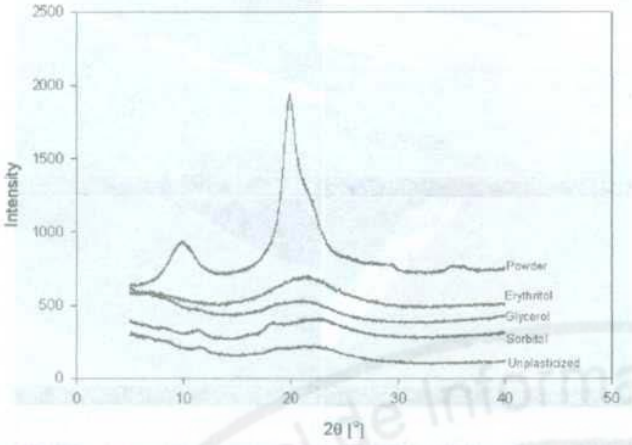

Figure 3. X-ray diffraction patterns of chitosan powder and chitosan films. From bottom to top: unplasticized films, films plasticized with sorbitol, glycerol, and erythritol, and high molecular weight chitosan powder.

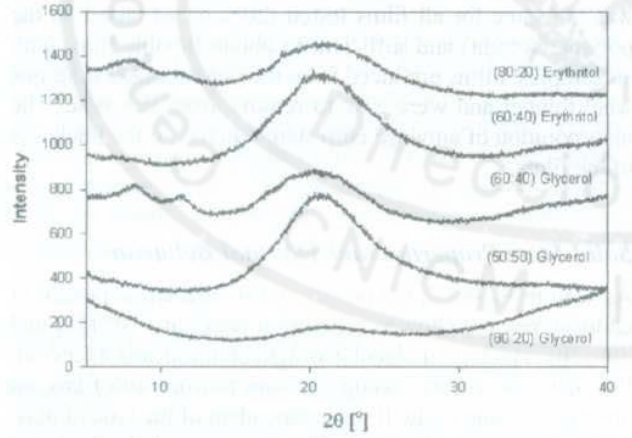

Figure 4. X-ray diffraction patterns of chitosan-Hylon films (80:20) and glycerol, (50:50) and glycerol, (60:40) and glycerol, (60:40) and erythritol, and (80:20) and erythritol.

DSC thermograms of chitosan powder and films exhibited exothermic peaks at 280°C to 300°C, indicating polymer decomposition. Processing of chitosan powder into films resulted in degradation at a lower temperature. The endothermic peaks that occur over a large temperature range (~35°C-160°C), attributable to water loss, represent the energy required to vaporize water present in the film samples. Lim and Wan[3] reported the exothermal decomposition peaks of chitosan flakes and films. Nunthanid et al[6] reported that all chitosan films were degraded at <280°C to 300°C, which agrees well with the results of our study. Chitosan molecules have a strong affinity for water molecules. Chitosan films have a higher affinity for water compared with the powder, probably because the chitosan molecules in the films are protonated, rendering the films more hydrophilic than the powder.[3]

The absence of other endotherms in the DSC thermograms, besides the one at ~35°C to 160°C, implied that the chitosan films were amorphous. This was also confirmed by the x-ray diffraction results.

Mechanical Properties

The tensile strength and the elongation at break of free chitosan films are summarized in Table 1. The most suitable plasticizer was erythritol with the greatest tensile strength. Erythritol decreases the rigidity of the network, producing a less ordered film structure and increasing the ability of movement of polymer chains. Films of suitable toughness and flexibility may thus be obtained. The addition of erythritol enhanced the plasticization and resulted in a highly amorphous polymer film structure. Chitosan films plasticized with sorbitol were very brittle and cracking. In general, the crystallinity of a film structure promotes intermolecular forces, thus increasing the rigidity and brittleness of the film, and the crystallinity of sorbitol-plasticized films was the highest. The mechanical properties of chitosan/polyvinyl alcohol (PVA)/H_2O and chitosan/gelatine with or without polyols, sorbitol, and sucrose were studied by Arvanitoyannis et al.[26,27] The tensile strength decreased proportionally to the plasticizer content, whereas the percentage elongation increased considerably, particularly in the case of sorbitol.

Studies on the effect of molecular weight on the chitosan film characteristics have reported that the mechanical strength of the film increased with increasing molecular weight of chitosan.[6] This finding might be attributable to an entanglement network forming during film formation of higher molecular weight chitosan. Glycerol is a commonly used plasticizer in chitosan acetate films. It improves the mechanical properties of free films.[4] Remuñán-López and Bodmeier[4] reported that films made of chitosan acetate were significantly less flexible than those made of chitosan glutamate at any investigated glycerol content (0%-30%), thus they were better plasticized by glycerol.

As shown in Figures 5 and 6, the increase of Hylon VII concentration increased the values of tensile strength for both

glycerol- and erythritol-plasticized films, but at concentrations higher than ~20% the results of tensile strength decreased. The Hylon VII concentration did not affect the elongation at break, particularly in the films plasticized with erythritol. Free films containing 50% wt/wt of Hylon VII were soft, weak, and difficult to remove from the molds; consequently, this was the maximum concentration of Hylon VII evaluated to obtain flexible films. The variations in the percentage of elongation of films with erythritol were lower compared with the results obtained with glycerol.

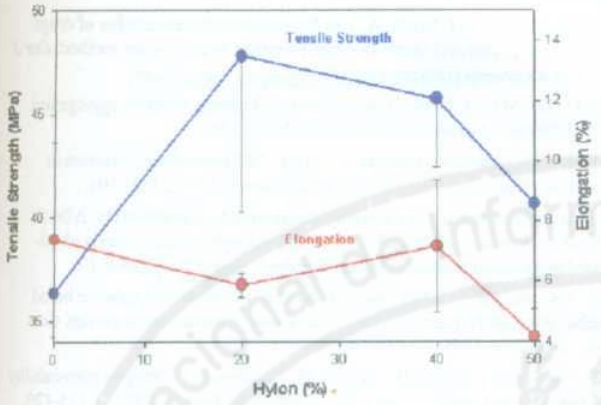

Figure 5. Tensile strength and elongation profiles of free chitosan films containing Hylon VII 0%-50% and glycerol as a plasticizer (n = 5).

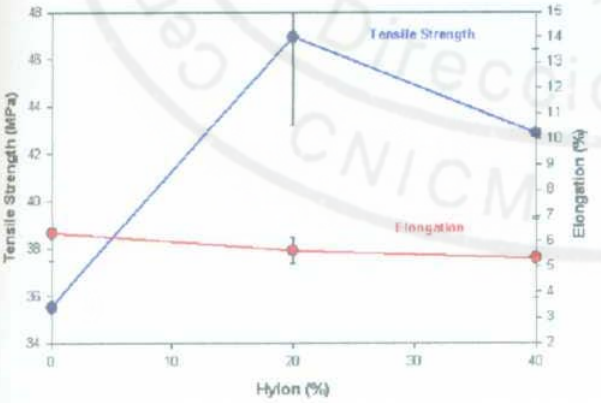

Figure 6. Tensile strength and elongation profiles of free chitosan films containing Hylon VII 0%-40% and erythritol as a plasticizer (n = 5).

Although, DSC and powder x-ray diffraction techniques confirmed that all films of binary mixtures of chitosan and Hylon VII were in an amorphous state, according to x-ray diffraction patterns of chitosan, Hylon VII (50:50) films plasticized with glycerol and (60:40) plasticized with erythritol showed a higher degree in molecular arrangement around 20° (2θ) (Figure 4). Therefore, it is evident that the molecules of film formers start to rearrange and probably crystallize, consequently affecting the mechanical properties of the films. It is expected that erythritol is a promising plasticizer to be used with the film coatings of the present binary mixtures. However, more information is needed, for example, on the physical stability of the present films plasticized with polyols.

The present films can be used, for example, in special, multilayered, complex, controlled-release systems for oral site-specific drug delivery. Another application could be the film coatings to obtain enhanced oxygen and gas barrier properties as amylose starch has been shown to form films with a high resistance to oxygen.[28]

CONCLUSION

Flexible and mechanically strong films can be prepared with aqueous binary mixtures of chitosan and amylose corn starch (Hylon VII) plasticized with polyols. The film properties such as morphology, mechanical strength, and crystallinity are dependent on the film former to film former ratio and on the plasticizer (polyol) used.

ACKNOWLEDGEMENTS

The Centre for International Mobility for Foreign Students (CIMO) is gratefully acknowledged for financial support of the present study. The authors would like to thank Simo Siiriä, Department of Pharmacy, University of Helsinki, Finland, for technical drawings.

REFERENCES

1. Karlsen JJ. Excipient properties of chitosan. *Manuf Chemist*. 1991;62:18-19.

2. Muzzarelli RAA, Peter MG, eds. *Chitin Handbook*. Bremen, Germany: European Chitin Society; 1997:437-438.

3. Lim LY, Wan SC. Heat treatment of chitosan films. *Drug Dev Ind Pharm*. 1995;21:839-846.

4. Remuñán-López C, Bodmeier R. Mechanical and water vapour transmission properties of polysaccharide films. *Drug Dev Ind Pharm*. 1996;22:1201-1209.

5. Bégin A, Van Calsteren MR. Antimicrobial films produced from chitosan. *Int J Biol Macromol*. 1999;26:63-67.

6. Nunthanid J, Puttipipatkhachorn S, Yamamoto K, Peck GE. Physical properties and molecular behavior of chitosan films. *Drug Dev Ind Pharm*. 2001;27:143-157.

7. Bader HG, Göritz D. Investigations on high amylose corn starch films. Part 1: Wide-angle X-ray scattering (WAXS). Starch / Stärke. 1994;46:229-232.

8. Lourdin D, Della Valle G, Colonna P. Influence of amylose contents on starch films and foams. *CarbohydPolym.* 1995;27:261-270.
9. Rindlav A, Stading M, Hermansson A-M, Gatenholm P. Structure, mechanical and barrier properties of amylose and amylopectin films. *Carbohydr Polym.* 1998;36:217-224.
10. Palviainen P, Heinämäki J, Myllärinen P, Lahtinen R, Yliruusi J, Forssell P. Com starches as film formers in aqueous-based film coating. *Pharm Dev Technol.* 2001;6:351-359.
11. Krogars K, Heinämäki J, Karjalainen M, Niskanen A, Leskelä M, Yliruusi J. Enhanced stability of rubbery amylose-rich maize starch films plasticized with a combination of sorbitol and glycerol. *Int J Pharm.* 2003;251:205-208.
12. Wolff 1A, Davis HA, Cluskey JE, Gundrun LJ, Rist CE. Preparation of films from amylose. *Ind Eng. Chem. Res.* 1951;43:915-919.
13. Lenaerts V, Dumoulin Y, Mateescu MA. Controlled-release of theophylline from cross-linked amylose tablets. *J Control Release.* 1991;15:39-46.
14. Lenaerts V, Moussa 1, Dumoulin Y, et al. Cross-linked high amylose starch for controlled release of drugs: recent advances. *J Control Release.* 1998;53:225-234.
15. Felt O, Buri P, Gumy R Chitosan: a unique polysaccharide for drug delivery. *Drug Dev Ind Pharm.* 1998;24:979-993.
16. Paul W, Sharma CP. Chitosan, a drug carrier for the 21st century: a
review. *S. T.P. Pharm. Sci.* 2000;10:5-22.
17. Hou WM, Miyazaki S, Takada M, Komai T. Sustained release of in- domelhacin from chitosan granules. *Chem Pharm Bull (Tokyo).* 1985;33:3986-3992.
18. Mi FL, Her NL, Kaun CY, Wong T, Shyu S. Chitosan tablets for controlled release of theophylline: effect of polymer drug wet or dry blending and anionic-cationic interpolymer. *JAppl Polym Sci.* 1997;66:2495-2505.
19. Gupta KC. MNV. Ravi Kumar. Semi-interpenetrating polymer network beads of crosslinked chitosan-glycine for controlled release of clor- phenaramine maleate. *J App! Polym Sci.* 2000;76:672-683.
20. Ritthidej GC, Phaechamud T, Koizumi T. Additives in moist-heat- treated chitosan acetate films: a method to extend the release of propranolol hydrochloride coated tablets. *S T.P. Pharma Sci.* 2000; 10:112- 119.
21. Shu XZ. Zhu KJ, Weihong Song. Novel pH-sensitive citrate cross- linked chitosan film for drug controlled release. *IntJPharm.* 2001:212:19-
28.
22. Macleod GS, Collett JH, Fell JT. The potential use of mixed films of pectin, chitosan and HPMC for biomodal drug release. *J Control Release.* 1999;58:303-310.
23. Hiorth M, Tho 1, Sande A. The formation and permeability of drugs across free pectin and chitosan films prepared by a spraying method. *Eur J Pharm Biopharm* 2003;56:175-182.
24. Gidley MJ. Molecular mechanisms underlying amylose aggregation and gelation. *Macromolecules.* 1989;22:351-358.
25. Bail PLe. Bizot H, Buleon, A "B " to "A" type phase transition in short amylose chains. *Carbohydrate Polymers.* 1993;21:99-104.
26. Arvanitoyannis I, Kolokuris 1, Nakayama A, Yamamoto N, Aiba S. Physico-chemical studies of chitosan-poly(vinyl alcohol) blends plasticized with sorbitol and sucrose. *Carbohydr Polym.* 1997;34:9-19.
27. Arvanitoyannis 1, Nakayama 1, Aiba S. Chitosan and gelatine based edible films:state diagrams, mechanical and permeation properties. *Carbohydr Polym.* 1998;37:371-382.
28. Forssell P, Lahtinen R, Lahelin M, Myllärinen P. Oxygen permeability of amylose and amylopectin films. *Carbohydr Polym.* 2002;37:125-129.

Physical stability and moisture sorption of aqueous chitosan-amylose starch films plasticized with polyols

III

Fernández Cervera, M.. Karjalainen, M., Airaksinen, S., Rantanen, J., Heinämäki. J., Iraizoz Colarte, A. and Yliruusi, J.

Eur. J. Pharm. Biopharm. 2004, 58, 69-76.

Available online at www.sciencedirect.com
SCIENCE DIRECT
ELSEVIER
European Journal of Pharmaceutics and Biopharmaceutics 58 (2004) 69–76
European Journal of Pharmaceutics and Biopharmaceutics
www.elsevier.com/locate/ejpb

Research paper

Physical stability and moisture sorption of aqueous chitosan–amylose starch films plasticized with polyols

Mirna Fernández Cervera[a], Milja Karjalainen[b], Sari Airaksinen[b], Jukka Rantanen[b], Karin Krogars[b], Jyrki Heinämäki[b,*], Antonio Iraizoz Colarte[a], Jouko Yliruusi[b,c]

[a]*Institute of Pharmacy and Food, University of Havana, Havana, Cuba*
[b]*Pharmaceutical Technology Division, Faculty of Pharmacy, University of Helsinki, Helsinki, Finland*
[c]*Viikki Drug Discovery Center DDTC, University of Helsinki, Helsinki, Finland*

Received 24 November 2003; accepted in revised form 17 March 2004

Abstract

The short-term stability and the water sorption of films prepared from binary mixtures of chitosan and native amylose maize starch (*Hylon VII*) were evaluated using free films. The aqueous polymer solutions of the free films contained 2% (w/w) film formers, glycerol, or erythritol as a plasticizer, as well as acetic acid (1%) and purified water. Characterization of the present fresh and conditioned film formers and free films was done using X-ray diffraction analysis, determination of moisture sorption isotherms, and near infrared spectroscopy. The results indicated that clear changes in the crystallinity of the films are evident within a 3-month period of storage, and the changes in the solid state are dependent on the plasticizer and storage conditions. When stored at ambient conditions for 3 months, the aqueous chitosan–amylose starch films plasticized with erythritol exhibited a partly crystalline structure. This was as a result of sugar recrystallisation due to the high hydrogen bonding. The respective films plasticized with glycerol and stored at 25 °C/60% relative humidity (RH) or at 40 °C/75% RH remained flexible and amorphous for at least 3 months. The water sorption of the free films greatly increased as a function of storage time at 75 and 95% RH. The second derivative spectra of starting material and free films were capable of distinguishing the internal water from the free water after storage at different relative humidities. Free water resulted in a separate band at a lower wavelength (1903 nm) in comparison to the structured absorbed water band at 1920 nm, in the case of films the free water resulted in a band around 1900 nm.

Keywords: Amylose starch; Chitosan; Free films; Physical stability; Polyols; Water sorption

1. Introduction

Chitosan is a cationic natural polysaccharide derived by deacetylation of chitin. Chitosan meets the important requirements of excipients in drug delivery, i.e. biocompatibility and biodegradability. Due to these favorable properties the interest in chitosan and its derivatives as excipients in drug delivery has increased in recent years [1,2]. Higher molecular weight chitosans have been reported to have good film-forming properties as a result of intra- and intermolecular hydrogen bonding [3].

Recent studies on pharmaceutical and food chitosan film coatings have often examined the permeability to water vapor and moisture sorption of chitosan films [4–7]. The influence of molecular weight as well as degree of deacetylation on the moisture sorption behavior, swelling properties, and water vapor transmission rates have also been evaluated [5,7]. In most studies the films were produced from blends of chitosan and other polymers such as cellulose, polyvinyl alcohol, or polyvinyl pyrrolidone [4]. To date, only little attention has been paid to the effects of storage conditions on the stability of chitosan films.

The mechanism for the prediction of water transport through hydrophilic films like chitosan films is extremely complex. The complexity is due to nonlinear water sorption isotherms and water content dependent diffusivities [8]. The water vapor transmission of hydrophilic films varies nonlinearly with water vapor pressure. If the films are cationic and strongly hydrophilic, water interacts with

* Corresponding author. Address: Pharmaceutical Technology Division, Faculty of Pharmacy, P.O. Box 56, FIN-00014 University of Helsinki, Helsinki, Finland. Tel.: +358-970859158; fax: +358-970859144.
E-mail address: jyrki.heinamaki@helsinki.fi (J. Heinämäki).

0939-6411/$ - see front matter © 2004 Elsevier B.V. All rights reserved.
doi:10.1016/j.ejpb.2004.03.015

the polymer matrix and increases the permeation for water vapor [9].

In our previous study, chitosan films prepared with amylose corn starch (*Hylon VII*) as a co-film-forming agent were evaluated using free films [10]. Erythritol was found as a plasticizer of choice for these composite films improving mechanical strength of the films. This study therefore aimed to investigate the physical stability and sorption behavior of the present chitosan films prepared with amylose corn starch (*Hylon VII*) as a co-film-forming agent. The effects of type and molecular weight of chitosan, type of plasticizer, and storage humidity conditions were evaluated.

2. Materials and methods

2.1. Materials

High, medium, and low molecular weight chitosans (Aldrich Chemical Company Inc., Milwaukee, WI, USA) were used in this study. Amylose-rich corn starch (*Hylon VII*) (National Starch and Chemical GmbH, Neustadt, Germany) was used as a co-film former, and glycerol (Ph.Eur) and i-erythritol (Sigma-Aldrich Chemie GmbH, Steinheim, Germany) as plastizers. Acetic acid (Riedel-de Haën, Germany) and purified water were employed as solvents.

2.2. Free films and stability testing

The aqueous polymer solutions contained 2% (w/w) film former (mixture of high molecular weight chitosan and *Hylon VII*), glycerol, or erythritol as a plasticizer (20% w/w of the polymer weight), as well as acetic acid (1%) and purified water. The ratios of the chitosan–*Hylon VII* solutions plasticized with glycerol or erythritol were 80:20 and 60:40.

Hylon VII solutions were prepared in a high-pressure reactor equipped with a blade mixer (VTT Automation, Espoo, Finland). *Hylon* was first dispersed in cold water. Once loaded in the reactor chamber, the starch dispersion was gradually heated to 160 °C and the pressure in the vessel reached 3.0 bar. The starch solution obtained was cooled down to approximately 90 °C and filtered. The *Hylon* solution was mixed with the chitosan solution at approximately 60 °C, and the temperature of the solution for preparing free films was maintained above 50–60 °C. The plasticizer was added at a concentration of 20% (w/w) of the total dry weight. For preparing free films, the polymer solution was poured into polytetrafluoroethylene (Teflon®) molds, and the films were air dried for 4 h at 60 °C.

Films of binary mixtures of chitosan and *Hylon VII* were stored at 25 °C/60% RH (relative humidity) and 40 °C/75% RH for 3 months.

2.3. Characterization of materials and free films

2.3.1. XRD measurements

X-ray diffraction patterns of all the samples were measured using X-ray powder diffraction (XRPD) theta–theta diffractometry (Bruker AXC D8, Karlsruhe, Germany). The XRPD experiments were performed in symmetrical reflection mode using Cu K_α radiation (1.54 Å) and Göbel Mirror bent gradient multilayer optics. The scattered intensities were measured with a scintillation counter. The pure materials were measured at an angular range from 2 to 40° (2θ) with steps of 0.1° and a measuring time of 5 s/step. The X-ray diffraction patterns of high, medium, and low molecular weight chitosan, native amylose corn starch (*Hylon VII*), glycerol, and erythritol are shown in Fig. 1.

The diffraction pattern of erythritol included the strongest reflections at about 14.7, 20.2, 21, 24.6, 27.9, 29.7, 30.5, 31.3, and 32.9° (2θ). These reflections agreed with earlier reported reflections of erythritol [11]. The diffraction patterns of chitosan have the clearest reflections at about 10 and 20° and resemble closely the earlier presented chitosan form II [12]. The diffraction pattern of *Hylon VII* included weak reflections at about 17.2 and 20°, corresponding to the earlier reported structure of B-type starch [13]. No reflections are seen in the diffraction pattern of glycerol, indicating that the material is totally amorphous.

X-ray diffraction patterns of the film samples (15 days, 1, 2, and 3 months) were measured at angles ranging from 5 to 40° in 2θ with steps of 0.02° and a measuring time of 10 s for each angular step. The determination of crystallinity was based on the assumption that the experimental intensity curve is a linear combination of intensities of a crystalline and an amorphous component.

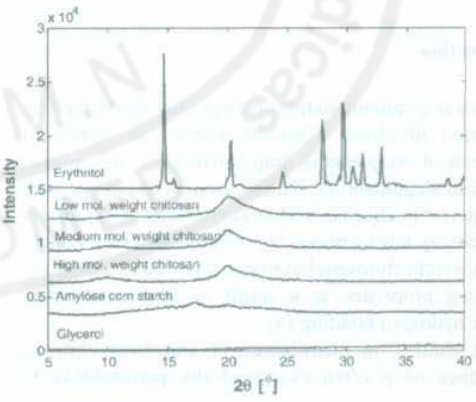

Fig. 1. X-ray diffraction patterns of pure film-forming polymers and plasticizers. From bottom to top: glycerol, native amylose corn starch (*Hylon VII*), high molecular weight chitosan, medium molecular weight chitosan, low molecular weight chitosan, and erythritol.

The crystallinity of the samples was estimated by fitting the intensity of the crystalline component and the intensity of the amorphous component to the experimental intensity curve. The crystallinity of the samples was obtained as the ratio of the integrals of the intensities of the crystalline component and the studied sample. The intensity curves of totally amorphous samples were used as the amorphous background of the samples. The experimental intensity curve, where the amorphous background was subtracted, was used as the crystalline model intensity curve.

2.3.2. Moisture sorption isotherms

Water sorption isotherms were determined by placing powders and films of binary mixtures of chitosan and *Hylon VII* into a controlled humidity environment at a constant temperature until equilibrium. After drying at 40 °C and 160 mbar for 24 h in a vacutherm (Heraeus VT 6025, Kendro Laboratory Products GmbH, 63450 Hanau, Germany), the dried powders and films were placed into environments of various relative humidities above salt solutions in desiccators. The relative humidities were 0% RH (silica gel), 11% RH (lithium chloride), 23% RH (potassium acetate), 33% RH (magnesium nitrate), 43% RH (potassium carbonate), 52% RH (magnesium nitrate), 59% RH (sodium bromide), 75% RH (sodium chloride), 85% RH (potassium chloride), and 95% RH (disodium hydrogen phosphate). All the salts were of reagent grade. Three types of chitosan powder, amylose-rich corn starch, and erythritol were placed into each condition while placing the films into 0, 23, 43, 75, and 95% of relative humidities.

Completely dry samples in weighing bottles were stored in desiccators for 9 days at 21 ± 2 °C. The bottles with samples were removed from the desiccator for quick weighing. After weighing, the bottles were replaced in the desiccators. The weight gain of the powders and the films were recorded at predetermined time intervals (2, 5, and 9 days). The measurement was made in triplicate. Moisture sorption isotherms were calculated as the equilibrium of moisture sorption (EMC), and experimental monolayer water values were determined from the adsorption isotherm using BET equations (Brunauer, Emett, and Teller's multilayer adsorption theory; Eq. (1)) [14] and GAB equations (Guggenheim, Andersen, and de Boer monolayer sorption theory; Eq. (2)) [15–17] for modelling moisture sorption isotherms.

$$a_w/(1 - a_w)m = 1/m_0C + a_w(C - 1)/m_0C \quad (1)$$

$$m = C_1km_0a_w/(1 - ka_w)(1 - ka_w + C_1ka_w) \quad (2)$$

where

m, moisture content
a_w, water activity
m_0, monolayer moisture content
C, constant related to excess enthalpy of sorption
C_1 and k are constants.

2.3.3. Near infrared spectroscopy

The near-infrared (NIR) spectra were measured with a Fourier Transform (FT)-NIR spectrometer (Bomem MD-160 DX, Hartmann and Braun, Que., Canada) using Bomem-GRAMS software (v. 4.04, Galactic Industries Inc., Salem, NH, USA) and Teflon as reference (99% reflective Spectralon, Labsphere me., North Sutton, NH, USA). The spectra were measured through the bottom of the glass vial containing the sample. The measurements were carried out in triplicate. The spectra were recorded over a range of 10,000–4000 cm^{-1} with a resolution of 16 cm^{-1} and averaged over 32 scans. Second derivative transformations of absorbance, $\log(1/R)$, were performed with 11-point Savitzky–Golay smoothing [18] using Matlab software (v. 5.3, MathWorks Inc., Natick, MA, USA).

3. Results and discussion

3.1. Moisture sorption properties of starting materials

The association of pharmaceutical solids with water can result in significant changes in, e.g. chemical stability, physical solid state properties, crystal growth and dissolution, dispersibility and wetting, caking, and flow.

The steady-state moisture in the starting materials was measured after 9 days of storage of the samples at different relative humidities. As seen in Fig. 2a, the moisture increase of low molecular weight chitosan was lower than that of high and medium molecular weight chitosan at a relative humidity of 95%. The moisture increase of *Hylon VII* was lower than that of other starting materials from relative humidities of 52–95%.

The storage of the erythritol at a high humidity resulted in a significant increase in water uptake, causing a liquefaction of the substance even higher than that of chitosans. Starch and chitosan are hydrophilic and retain a considerable amount of water. The amount depends on the relative humidity. At least in chitosan there exist three predominant absorption sites such as the hydroxyl group, the amino group, and the polymer chain end. The polymer chain end is supposed to be composed of a hydroxyl group or an aldehyde group [7]. Usually the amine content increases with increasing molecular weight. In the case of chitosan, the water is bound to the hydroxyl group more strongly than to the amine group. Therefore, the release of water molecules could preferentially occur via the amine group [19]. Modelling of the moisture sorption isotherms was done using the BET equation, and the experimental monolayer water values were 5.5 g water/100 g dry material (d.m.) for high molecular weight chitosan, 6.0 g water/100 g d.m. for medium molecular weight chitosan, and 5.0 g water/100 g d.m. for low molecular weight chitosan. Using the GAB equation, the monolayer values were 7.0, 7.4, and 6.2 g/100 g d.m. for high, medium, and low molecular weight chitosan, respectively. In the case of *Hylon VII*,

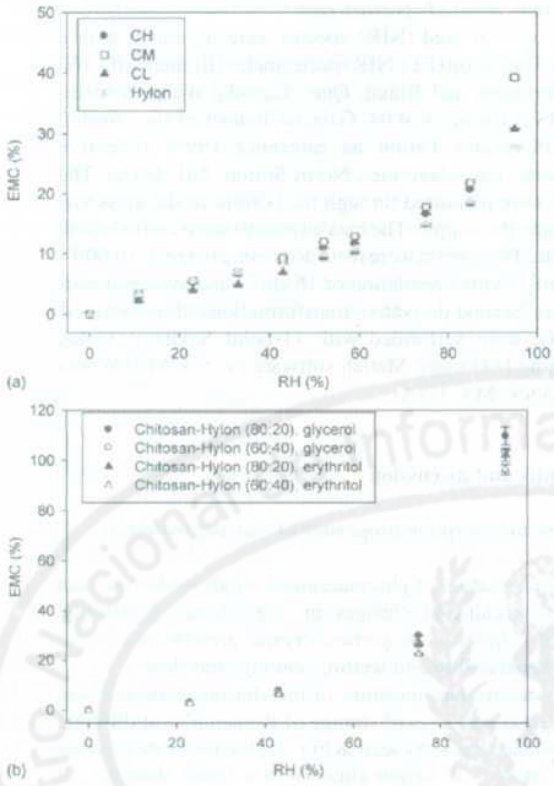

Fig. 2. Equilibrium moisture content (EMC%) of high molecular weight chitosan (CH), medium molecular weight chitosan (CM), low molecular weight chitosan (CL), amylose corn starch (*Hylon VII*) starting materials (a), and chitosan–*Hylon VII* films (b) stored at different relative humidities for 9 days.

the value by the BET equation was 4.9 g water/100 g d.m. and by the GAB equation 6.5 g water/100 g d.m.

A series of NIR spectra for high molecular weight chitosan and *Hylon VII* with increasing RH (following 9 days of storage with the saturated salt solution) are shown in Fig. 3a–d. With increasing moisture content the water bands of the starting material increased in size and shifted gradually from 1920 to 1903 nm. The second derivative spectra of the starting material were capable of distinguishing the absorbed water from the free water. The free water resulted in a separated band at a lower wavelength (1903 nm) in comparison to the structured absorbed water band at 1920 nm. The intensity of the water bands increased with increasing water content. The NIR spectra collected for the samples did not show any change that was induced during the storage at different humidities.

3.2. Effects of storage on solid-state properties of free films

X-ray diffraction patterns and calculated values for crystallinity of various film samples plasticized with erythritol are shown in Fig. 4a–c and Table 1, respectively. There are clear changes in the crystallinity of the films during storage, and the changes seem to be dependent on the storage conditions and the plasticizer. The yellow tint of all the films studied became more evident as the films were stored in higher temperature and relative humidity (40 °C/75% RH). Furthermore, the films became more flexible and less brittle when stored at a high relative humidity. When stored at 25 °C/60% RH, however, the aqueous chitosan–amylose starch films plasticized with erythritol exhibited white spots on the surface, and they were very brittle.

The diffraction patterns of the films plasticized with glycerol and stored at 25 °C/60% RH included only diffuse maxima with no reflections in the patterns. This means that the films are totally amorphous. The same films stored at 40 °C/75% RH were also amorphous. The effect of erythritol as a plasticizer was demonstrated by storing the films at 25 °C/60% RH and at 40 °C/75% RH. The reflections of crystalline erythritol were observed in the films stored for 2 months at 25 °C/60% RH (Fig. 4c). The reflections increased and became clearer at 3 months, but the amorphous background also increased, indicating that the films were partly crystalline.

Although all the 15-day-old samples were totally amorphous, the diffraction patterns of the films differed slightly. The diffraction pattern of the chitosan–*Hylon VII* (80:20) sample has a diffuse maximum at about 20° (2θ) (Fig. 4c), while the pattern of the chitosan–*Hylon VII* (60:40) (Fig. 4a and b) sample has two diffuse maxima at about 19.6 and 20° (2θ). This indicates that the macroscructure of the samples was different.

The effect of water was demonstrated by storing the films at 75% RH (40 °C) (Fig. 4b). The films became mechanically very weak. As seen in Fig. 4a; the crystalline peaks appeared only in the films of chitosan–Hylon VII (60:40) plasticized with erythritol after 2 months of storage. The rest of the films analysed were amorphous.

As seen in Fig. 4a–c and Table 1, the crystallinity of the samples started to increase after 2 months. The crystallinities of the films stored at 25 °C/60% RH were higher than those of the respective films stored at 40 °C/75% RH. The diffraction pattern of the 40 °C/75% RH sample (Fig. 4b) after 2 months has a strong amorphous background and only two reflections of crystalline erythritol at about 24.6 and 28.32° (2 theta). Until 3 months, the diffraction pattern has a strong amorphous background and three reflections at about 19.6, 20.3, and 37.5° (2 theta). While the diffraction patterns of the 25 °C/60% RH samples after 2 and 3 months showed a slightly amorphous background and almost all of reflections of crystalline erythritol. The diffraction patterns differed due to the preferred orientation of the 40 °C/75% RH samples. So the storing has a tendency to increase the crystallinity of the samples, but the films stored at 25 °C/60% RH remain more isotropic.

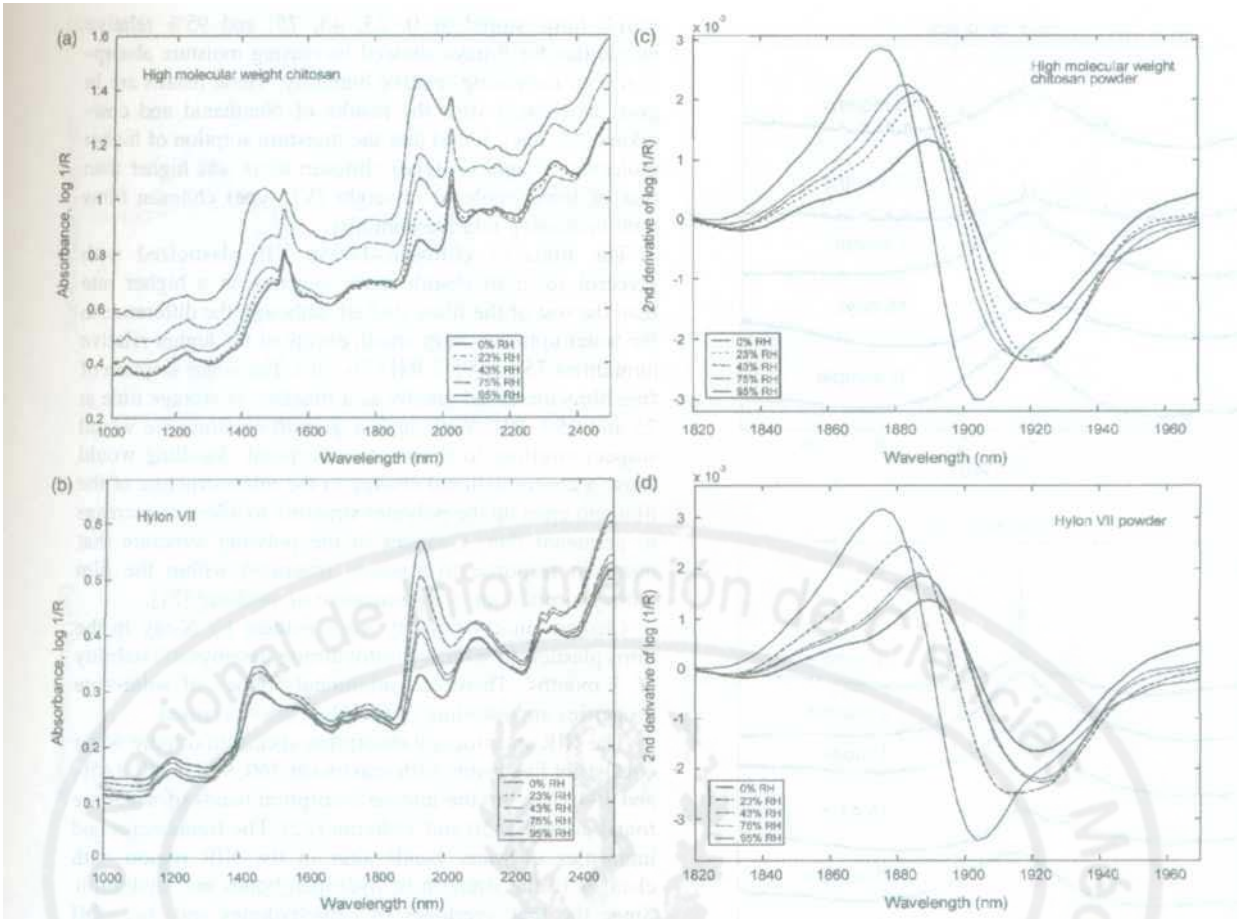

Fig. 3. NIR absorbance spectra (log(l//?)) and second derivative of log(l/Æ) of the starting materials studied. Absorbance 1000-2500 nm, (a) high molecular weight chitosan, (b) *Hylon VII*. Second derivative of log(l/Æ) 1820-1970 nm, (c) high molecular weight chitosan, (d) *Hylon VII*.

Independent of the ratio of chitosan and native starch in the films and the storage conditions, none of the films studied showed reflections specific to B-type starch (5.6, 15, 17, 22, and 24, 26) [20], indicating that *Hylon VII* remained amorphous.

3.3. Effects of storage on moisture sorption of free films The equilibrium moisture contents (EMC %) of chitosan -*Hylon VII* films stored at different relative humidities for 9 days are shown in Fig. 2b. Aqueous chitosan-amylose

Table 1
Crystallinities of chitosan and *Hylon VII* films plasticized with erythritol

Storage time (days)	Storage conditions	Samples	Ciystallinity ± 10%
15	25 °C/60% RH	Chitosan: *Hylon VII* (60:40)	0
		Chitosan: *Hylon VII* (80:20)	0
	40 °C/75% RH	Chitosan: *Hylon VII* (60:40)	0
30	25 °C/60% RH	Chitosan: *Hylon VII* (60:40)	0
		Chitosan: *Hylon VII* (80:20)	0
	40 °C775% RH	Chitosan: *Hylon VII* (60:40)	0
60	25 °C/60% RH	Chitosan: *Hylon VII* (60:40)	35
		Chitosan: *Hylon VII* (80:20)	29
	40 °C/75% RH	Chitosan: *Hylon VII* (60:40)	12
90	25 °C/60% RH	Chitosan: *Hylon VII* (60:40)	35
		Chitosan: *Hylon VII* (80:20)	33
	40 °C/75% RH	Chitosan: *Hylon VII* (60:40)	20

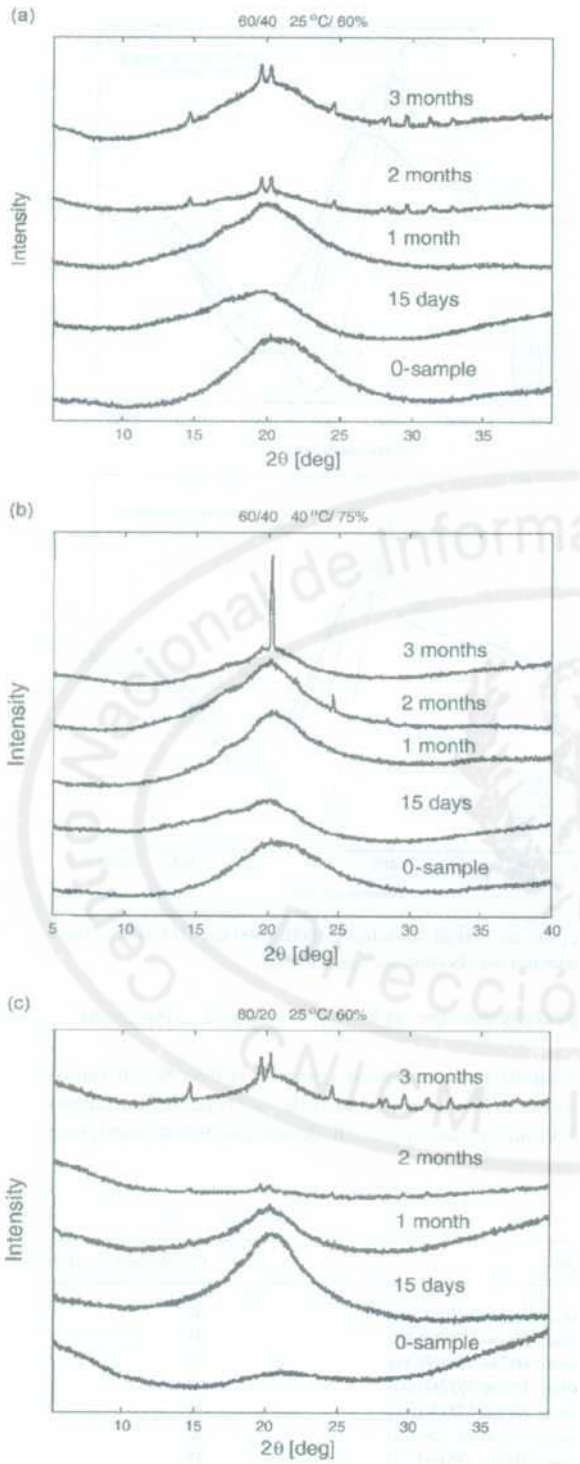

Fig. 4. X-ray diffraction patterns of fresh and aged chitosan-*Hylon VII* free films plasticized with erythritoL Key: (a) chitosan *Hylon VII* (60:40) stored at 25 °C/60% RH, (b) chitosan-ffyfon *VII* (60:40) stored at 40 °C/75% RH, and (c) chitosan-//y/wi *VII* (80:20) stored at 25 "C/60% RH.

starch films stored at 0, 23, 43, 75, and 95% relative humidities for 9 days showed increasing moisture absorption with increasing relative humidity. These results are in good agreement with the results of Nunthanid and coworkers [6], They found that the moisture sorption of higher molecular weight (H-type) chitosan films was higher than that of lower molecular weight (VL-type) chitosan films with increasing relative humidity.

The films of chitosan-Hylon VII plasticized with glycerol seem to absorb more moisture at a higher rate than the rest of the films studied; although the difference in the water uptake is very small, except at the higher relative humidities 75 and 95% RH (Fig. 2b). The water sorption of free films increased greatly as a function of storage time at 75 and 95% RH. With such a gain in moisture we would suspect swelling to occur at some point. Swelling would cause a conformational change in the microstructure of the film and open up the polymer structure to allow an increase in permeant flux. Changes in the polymer structure that occur in response to stresses generated within the film during sorption are a consequence of swelling [21],

Changes in crystallinity were evident by X-ray in the films plasticized with erythritol during the physical stability of 3 months. Therefore, additional studies of solid-state properties and swelling of the films are warranted.

The NIR spectrocopy absorption spectrum of pure water consists of five bands with maxima at 760, 970, 1190, 1450, and 1940 nm, but the intense absorption bands of water are found around 1450 and 1940 nm [22], The frequencies and intensities of water bands alter in the NIR region with changes in the strength of hydrogen bonds and hydration. Since the first overtones of carbohydrates and the -OH groups of water overlap at the same wavelengths (around 1450 nm), the combination band (around 1940 nm) provides a better selectivity for water and, hence, is the most important absorption band in the NIR region [23].

The same water bands at the 1800-2100 nm region were identified by NIR from the chitosan films (Fig. 5a-d) as described before. The absorbed water was seen as a gradually increasing absorption maximum at 1920 nm. With increasing moisture content the water bands of chitosan films shifted gradually from 1920 to 1903 nm. Free water resulted in a separate band at around 1900 nm.

4. Conclusions

The changes in the physical stability of aqueous chitosan-amylose starch films are dependent on the storage conditions and the type of plasticizer. Until 3 months, storing had a tendency to increase the crystallinity of the films plasticized with erythritol in addition to the changes on their film surface. The respective films plasticized with glycerol remained amorphous. Although in the beginning the quality of the present films plasticized with erythritol was very good, stability of the films was poor. The films

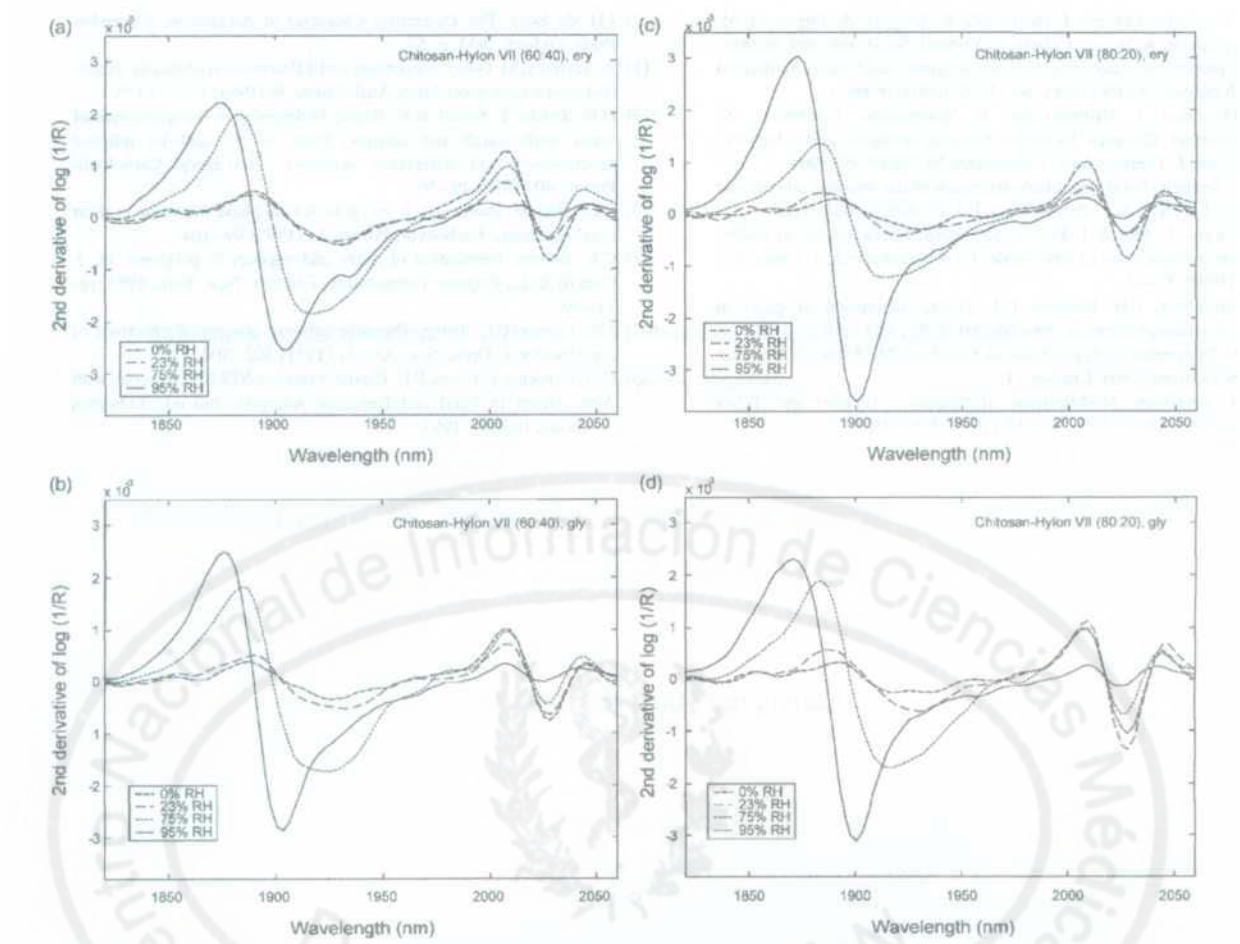

Fig. 5. Near infrared (NIR) reflectance spectra of (a) chitosan *Hylon VII* (60:40) films with erythritol, (b) chitosan *Hylon VII* (60:40) films with glycerol, (c) chitosan-Wy/on *VII* (80:20) films with erythritol, and (d) chitosan *Hylon VII* (80:20) films with glycerol. Second derivative of absorbance, log(l/R), at 1820-2060 nm.

prepared from binary mixtures of chitosan and *Hylon VII* plasticized with glycerol are a promising system for use in the coating process.

Acknowledgements

The Centre for International Mobility for Foreign Students (CIMO) and the Finnish Cultural Foundation are gratefully acknowledged for financial support of the present study.

References

[1] L. Ilium, Chitosan and its use as a pharmaceutical excipient, Pharm. Res. 15(1998) 1326-1361.
[2] V. Dodane, V.D. Vilivalum, Pharmaceutical applications of chitosan, Pharm. Sci. Technol. Today 1 (1998) 246-253.
[3] R.A. Muzzarelli, M.G. Peter (Eds.), Chitin Handbook, Europen Chitin Society, 1997, pp. 437-438.
[4] C. Remunan, R. Bodmeier, Mechanical and water vapor transmission properties of polysaccharide films, Drug. Dev. Ind. Pharm. 12 (1996) 1201-1209.
[5] J.L. Wiles, P.J. Vergano, F.H. Barron, J.M. Bunn, R. Testin, Water vapor transmission rates and sorption behavior of chitosan films, J. Food. Sci. 7 (2000) 1175-1179.
[6] J. Nunthanid, S. Puttipipatkhachom, K. Yamamoto, G. Peck, Physical properties and molecular behavior of chitosan films, Drug. Dev. Ind. Pharm. 2 (2001) 143-157.
[7] H. Gocho, H. Shimizu, A. Tanioka, T.-J. Chou, T. Nakajima, Effect of polymer chain end on sorption isotherm of water by chitosan, Carbohydr. Polym. 41 (2001) 87-90.
[8] H.C. Swartzberg, Modeling of gas and vapor transport through hydrophilic films, in: M. Mathlouthi (Ed.), Food Packaging and Preservation: Theory and Practice, Elsevier, London, 1986, pp. 115-135.
[9] B. Pascat, Study of some factors affecting permeability, in: M. Mathlouthi (Ed.), Food Packaging and Preservation: Theory and Practice, Elsevier, London, 1986, p. 7.

[10] M. Fernandez Cervera, J. Heinämäki, K. Krogars, A. Jörgensen, M. Karjalainen, A. Iraizoz Colarte, J. Yliruusi, Solid-state and mechanical properties of aqueous chitosan-amylose starch films plasticized with polyols, AAPS Pharm. Sci. Tech. (2004) in press.
[11] L.M. Zhou, J. Sirithunyalug, E. Yonemochi, T. Oguchi, K. Yamamoto, Complex formation between erythritol and 4-hexylie-sorcinol, J. Thermal Anal. Calorimetry 59 (2000) 951-960.
[12] R.J. Samuels, Solid state characterization of the structure of chitosan films, J. Polym. Sci.: Polym. Phys. Ed. 19 (1981) 1081-1105.
[13] P. Cairns, L. Sun, V.J. Morris, S.G. Ring, Physicochemical studies using amylose as an in vitro model for resistant starch, J. Cereal Sci. 21 (1995) 37-47.
[14] S. Brunauer, P.H. Emmett, EJ. Teller, Adsorption of gases in multimolecular layers, J. Am. Soc. 60 (1938) 309-319.
[15] E.A. Guggenheim, Application of Statistical Mechanics, Clarendon Press, Oxford, 1966, Chapter 11.
[16] R.B. Anderson, Modifications of Brunauer, Emmett and Teller Equation, J. Am. Chem. Soc. 68 (1946) 686-691.
[17] J.H. de Boer, The Dynamical Character of Adsorption, Clarendon Press, Oxford, 1953, p. 57.
[18] A. Savitzky, M. Golay, Smoothing and differentiation of data by simplified least square procedures, Anal. Chem. 36 (1964) 1627-1639.
[19] D.R. Rueda, T. Secall, R.K. Bayer, Differences in the interaction of water with starch and chitosan films as revealed by infrared spectroscopy and differential scanning calorimetry, Carbohydr. Polym. 40 (1999) 49-56.
[20] P.Le. Bail, H. Buleon, A. Bizot, B to A type phase transition in short amylose chains, Carbohydr. Polym. 21 (1993) 99-104.
[21] C.E. Rogers, Permeation of gases and vapours in polymers, in: J. Comyn (Ed.), Polymer Permeability, Elsevier, New York, 1985, pp. 11-69.
[22] J.A. Cursio, C.C. Petty, The near infrared absorption spectrum of liquid water, J. Optic. Soc. Am. 41 (1951) 302- 304.
[23] B.G. Osborne, T. Feam, P.H. Hindle, Practical NIR Spectroscopy with Applications in Food and Beverage Analysis, 2nd ed., Longman Scientific, Harlow, 1993.

Effective optimization of enteric film coating of pellets with a miniaturized top-spray coater

Fernández Cervera, M, Heinámáki. J., Salgado-Rodríguez, E., Antikainen, O., Iraizoz Colarte, A. and Yliruusi, J.

Pharm. Ind. 2004 (en prensa).

IV

17-06-04 14:50:58 PI04$$0941

Eiliger Abzug der Korrektur
Urgent proof

Rücksendung eines genehmigten Abzuges erbeten an:
Please return one corrected copy to:

ECV · Editio Cantor Verlag · Postfach/P.O.B. 12 55
88322 Aulendorf (Germany)
Fax + 49 (0) 75 25-94 01 27 · Tel. + 49 (0) 75 25-94 00
e-mail: redaktion.pi@ecv.de

PI

PI04$$0941

Effective Optimization of Enteric Film Coating of Pellets with a Miniaturized Top-Spray Coater

Mirna Fernández Cervera[a], Jyrki Heinämäki[b], Elena Salgado Rodriguez[d], Osmo Antikainen[b], Antonio Iraizoz Colarte[a], and Jouko Yliruusi[b,c]

Institute of Pharmacy and Food, University of Havana[a], Havana City (Cuba), Pharmaceutical Technology Division, Department of Pharmacy[b] and Viikki Drug Discovery Technology Center DDTC[c], University of Helsinki, Helsinki (Finland), and Department of Pharmacy, University of Complutense de Madrid[d], Madrid (Spain)

Summary

Enteric film coating of pellets was studied and optimized using a miniaturized Caleva top-spray film coating system. Each small-scale batch coated comprised 20.0 g of pellets and methacrylic acid copolymer (Eudragit® S), plasticized with dibutyl phthalate, was applied as an enteric coating material for the pellet cores. A face-centered central composite design (CCD) was used to evaluate the coating parameters of potential importance with respect to the final film coating properties of the enteric pellets. The parameters (i.e. independent variables) studied were inlet air temperature, atomizing air pressure and flow rate of coating solution. The total number of coatings, including the preliminary screening and final optimization batches, was approximately 40.

The results indicated that an air flow top-spray film coating procedure of pellets in a small scale is sensitive to the flow rate of the coating solution, inlet air flow rate and air flow temperature. These parameters are critical, affecting both in vitro acidic resistance and batch quality (i.e. bulk appearance) of the methacrylic acid copolymer enteric-coated pellets. As regards in vitro acidic resistance, position (height) of the spraying nozzle also seems to be an important coating parameter. The present miniaturized film coating system used for preparing en-

– Spalte 2 –

teric (or colon-specific) Eudragit S-coated pellets was successfully optimized by using the response surface method.

Zusammenfassung

Effektive Optimierung von enteral filmbeschichteten Pellets mit einer miniaturisierten Topspray-Beschichtungsmaschine

Die enterale Filmbeschichtung von Pellets wurde durch die Verwendung einer miniaturisierten Caleva-Topspray-Beschichtungsmaschine untersucht und optimiert. Jeder zu beschichtende Durchsatz bestand aus 20,0 g Pellets und Methacrylsäure-Copolymer (Eudragit® S), mit Dibutylphthalat plastifiziert, als enterales Beschichtungsmaterial für die Pelletkerne. Ein Central Composite Design (CCD) wurde zur Evaluierung der die endgültigen Filmbeschichtungseigenschaften der enteralen Pellets beeinflussenden Beschichtungsparameter angewandt. Die untersuchten Parameter (unabhängige Variablen) waren die Zulufttemperatur, der Sprühdruck und die Fließgeschwindigkeit der Beschichtungsflüssigkeit. Die Gesamtanzahl der Beschichtungen, inklusive Screening-Versuche und Optimierungsdurchläufe, betrug ca. 40.
Die Ergebnisse zeigen, daß das Coating bzw. Beschichten der Pellets in kleinem Umfang sehr empfindlich auf Änderungen der Fließgeschwindigkeit der Beschichtungsflüssigkeit, der Strömungsgeschwindigkeit der Zuluft und der Temperaturänderungen reagiert. Diese Parameter sind kritisch, denn sie beeinflussen sowohl die In-vitro-Magensaftresistenz der enteralen Pellets als auch die Optik und Qualität des jeweiligen Durchsatzes, wenn Methacrylsäure-Copolymer als Beschichtungsmaterial verwendet wird. In Hinblick auf die In-vitro-Säureresistenz der enteralen Pellets scheint auch die Lage und die Höhe der Sprühdüse ein wichtiger Beschichtungsparameter zu sein. Das jetzige zur Fertigung von enteralen (oder kolon-spezifischen) Eudragit S-beschichteten Pellets eingesetzte miniaturisierte Filmbeschichtungssystem wurde erfolgreich durch die Verwendung dreidimensionaler Diagramme (Response Surface Method) optimiert.

Key words

- Enteric film coating
- Eudragit® S
- Fluid bed
- Methacrylic acid copolymer
- Miniaturized coater
- Pellets

Pharm. Ind. 66, No ■, ■–■

1. Introduction

With a rapidly increasing number of new expensive drug candidates, there has been a growing interest in developing and designing miniaturized manufacturing equipment for early-stage drug product development and formulation. In recent years, such novel small-scale equipment have been introduced for a variety of applications, including mixing/blending operations [1–3], wet granulation and pelletization [1, 4–8], as well as tablet compression [9]. The miniaturized or small-scale manufacturing systems can offer several advantages, including high throughput screening technique (for effective pharmaceutical formulation development), economic considerations and safety issues, thus accelerating the final breakthrough of a new drug candidate.

Film coating is an important pharmaceutical process stage in the manufacture of solid dosage forms affecting e.g. the appearance, masking, stability and drug release properties of the final drug product. In a larger scale, film coatings are generally performed by using either air-suspension (fluid-bed) or side-vented pan coating techniques. To date, very little attention has been paid to the development of miniaturized or small-scale film coating systems and only few papers are available in the literature [10, 11]. This is obviously because of the great challenges to understanding the thermodynamic phenomena and relationships existing in small-scale film coating and the difficulties in controlling multivariate side-vented pan or fluid-bed coating processes at a very small scale. An interesting recent approach in this area is the miniaturized Caleva top-spray film coating apparatus that generates a fluid bed of spheroids by mechanical vibration and air flow.

An increasing number of new drug candidates are either acid-labile compounds or require a specific absorption site in the distal parts of the gastrointestinal (GI) tract. Enteric-coated dosage forms are designed to resist the acidic environment of the stomach and to rapidly disintegrate in a higher pH environment of the intestinal fluid or in the colon. Polymers for enteric coating are usually applied to small spheroids (i.e. pellets, granules or microcapsules) since multiple-unit preparations are reliable and independent of the fed state as regards their GI transit. Anionic polymers based on methacrylic acid and methacrylic acid esters (i.e. Eudragit® L and S) are today widely used enteric polymers, and the higher-pH-sensitive Eudragit S methacrylic acid copolymer (the ratio of carboxyl groups to ester units 1:2) is also applied for colon-specific drug delivery [12–14].

The aim of the present study was to investigate an enteric film coating of pellets prepared by a miniaturized top-spray coating system. An established methacrylic acid copolymer (Eudragit S) was used as a coat-

1. Introduction

With a rapidly increasing number of new expensive drug candidates, there has been a growing interest in developing and designing miniaturized manufacturing equipment for early-stage drug product development and formulation. In recent years, such novel small-scale equipment have been introduced for a variety of applications, including mixing/blending operations [1–3], wet granulation and pelletization [1, 4–8], as well as tablet compression [9]. The miniaturized or small-scale manufacturing systems can offer several advantages, including high throughput screening technique (for effective pharmaceutical formulation development), economic considerations and safety issues, thus accelerating the final breakthrough of a new drug candidate.

Film coating is an important pharmaceutical process stage in the manufacture of solid dosage forms affecting e.g. the appearance, masking, stability and drug release properties of the final drug product. In a larger scale, film coatings are generally performed by using either air-suspension (fluid-bed) or side-vented pan coating techniques. To date, very little attention has been paid to the development of miniaturized or small-scale film coating systems and only few papers are available in the literature [10, 11]. This is obviously because of the great challenges to understanding the thermodynamic phenomena and relationships existing in small-scale film coating and the difficulties in controlling multivariate side-vented pan or fluid-bed coating processes at a very small scale. An interesting recent approach in this area is the miniaturized Caleva top-spray film coating apparatus that generates a fluid bed of spheroids by mechanical vibration and air flow.

An increasing number of new drug candidates are either acid-labile compounds or require a specific absorption site in the distal parts of the gastrointestinal (GI) tract. Enteric-coated dosage forms are designed to resist the acidic environment of the stomach and to rapidly disintegrate in a higher pH environment of the intestinal fluid or in the colon. Polymers for enteric coating are usually applied to small spheroids (i.e. pellets, granules or microcapsules) since multiple-unit preparations are reliable and independent of the fed state as regards their GI transit. Anionic polymers based on methacrylic acid and methacrylic acid esters (i.e. Eudragit® L and S) are today widely used enteric polymers, and the higher-pH-sensitive Eudragit S methacrylic acid copolymer (the ratio of carboxyl groups to ester units 1:2) is also applied for colon-specific drug delivery [12–14].

The aim of the present study was to investigate an enteric film coating of pellets prepared by a miniaturized top-spray coating system. An established methacrylic acid copolymer (Eudragit S) was used as a coat-

ing material for the pellets. The effects of major coating parameters were evaluated and critical parameters affecting gastric resistance and batch quality of the coated pellets were identified and optimized by using the response surface method.

2. Materials and methods

The basic coating solution contained 7.5 % (w/w) enteric film former (anionic polymer based on methacrylic acid and methacrylic acid esters, Eudragit S 100, Röhm Pharma, Darmstadt, Germany), dibutyl phthalate (Fluka Chemie, Buchs, Switzerland) as a plasticizer (10 % w/w of the polymer weight), absolute ethanol (Primalco, Rajamäki, Finland) and purified water at a ratio of 9:1 as a solvent system. The composition of the core pellets used in the coating experiments was as follows: theophylline anhydrate (Ph.Eur.) 5 %, lactose monohydrate (Pharmatose® 80M, DMV International, Veghel, The Netherlands) 35 %, and microcrystalline cellulose (Emcocel® 90M, Penwest Pharmaceuticals, Mendell, Patterson, NY, USA) 60 %. The pellets were produced using a NICA extrusion-spheronisation apparatus (NICA System AB, Mölndal, Sweden). Purified water was used as a granulating liquid. The pellets were dried for at least 48 h at room temperature (21 ± 2 °C), and the pellet size fraction ranging from 1.0 to 1.25 mm was used in the subsequent coating experiments. The physical properties of the core pellets are summarized in Table 1.

■ **Tab. 1** ■

The size and size distribution of the core pellets were determined by sieve analysis with a set of sieves consisting of screens with a number 1250, 1000, 710, 500, 315, 250, 125 and a collector. The moisture content of pellet cores was determined as a loss of weight using an infrared apparatus (Sartorius Thermol Control, Sartorius, Göttingen, Germany). All measurements were made in triplicate.

The coatings were applied using a miniaturized top-spray air-suspension coating apparatus (Caleva Mini Coater, Caleva Process Solutions, Dorset, UK). The apparatus generates a fluid bed by the simultaneous application of heated air flow and mechanical vibration of the coating cone (Fig. 1). In the present study, each small-scale batch coated comprised 20.0 g of pellets. The theoretical amount of coating was 20 % (w/w) of the total weight of the pellets.

■ **Abb. 1** ■

In the preliminary screening phase, the aim was to identify the coating factors affecting the present type of miniaturized film coating of pellets. Five independent coating parameters of potential importance with respect to the final enteric film coating quality of pellets were evaluated using a fractional factorial (resolution V) design. The parameters studied were air flow temperature, X_1 (30, 40 and 50 °C), atomizing air pressure, X_2 (0.2, 0.3 and 0.4 bar), flow rate of coating solution, X_3 (25, 40 and 55 ml/h), inlet air flow rate, X_4 (4.0, 5.0 and 6.0 m/s), and position (height) of spraying nozzle, X_5 (120, 140 and 160 mm). The effects of the independent variables were modeled by using the polynomial equation:

$$y = a_0 + a_1X_1 + a_2X_2 + a_3X_3 + a_4X_4 + a_5X_5 + a_6X_1X_2 + a_7X_1X_3 + a_8X_1X_4 + a_9X_1X_5 + a_{10}X_2X_3 + a_{11}X_2X_4 + a_{12}X_2X_5 + a_{13}X_3X_4 + a_{14}X_3X_5 + a_{15}X_4X_5$$

Main effects and all two-factor interactions were included in the model. The model was simplified with a multi-linear backwards, step-wise regression technique. The least significant terms were excluded from the model as long as the predictive

power (Q^2) of the model was increasing. The modeling was performed using Modde for Windows (Version 3.0, Umetrics, Umeå, Sweden). The total number of experiments (performed in a randomized order) was 19.

Based on the results of the preliminary screening phase, air flow temperature, atomizing air pressure and flow rate of coating solution were further characterized. A face-centered central-composite experimental design (CCD) was applied to optimize the present small-scale top-spray coating procedure. The experimental conditions for the batches and the matrix of the CCD are shown in Tables 2 and 3, respectively. The levels of fixed coating parameters, i.e. inlet air flow rate and nozzle height, were adjusted to 6.0 m/s and 120 mm, respectively. The effects of the independent variables were modeled as described in the previous chapter. The total number of experiments (performed in a randomized order) was 17. Five additional coating batches were prepared at the lowest flow rate of coating solution (25 ml/min) to further optimize the coating procedure.

■ **Tab. 2, 3** ■

The responses evaluated with enteric-coated pellets were in vitro acidic resistance, expected yield and batch quality (i.e. film coating appearance). The in vitro dissolution tests were performed using a USP apparatus 1 (basket method). The acidic test medium was 900 ml of 0.1 N hydrochloride acid (HCl) maintained at 37 ± 0.3 °C. Phosphate buffer solution pH 7.5 was used (at 37 ± 0.3 °C) for testing the final dissolution of the selected preparations. The basket rotation speed was 50 rpm. The samples were filtered and assayed by UV spectrophotometry (Perkin Elmer Lambda2S, Perkin-Elmer Analytical Instruments, Norwalk, CT, USA) at 273 nm for theophylline. The expected yield was obtained by gently sieving the film-coated batches through a 1.8 mm sieve and weighing the mass of the pellets that passed this sieve. The physical appearance of the coated pellets was determined by visual inspection (assigning rank scores from 1 to 10 based on visual inspection).

3. Results and discussion

In the present study with a miniaturized apparatus, the increase in inlet air flow rate produced a clear increase in coating efficiency (measured as acid resistance of the batches after the coating procedure), while the reduction in atomizing air pressure produced an apparent decrease in the coating efficiency (Fig. 2). It seems that application of mechanical vibration combined with air flow (to generate a fluid bed) does not completely prevent the impact of changes in the atomizing air pressure. With the present miniaturized top-spray coating procedure, a properly selected ratio (balance) between the two above-mentioned parameters seems to be of major importance.

■ **Abb. 2** ■

According to the literature, fluidized patterns in the top-spray coating technique (like the present one) are more random than in the conventional bottom spray (Wurster column) or tangential spray modes [15, 16]. The random nature of the fluid bed in the top-spray mode may limit the potential for segregation or differences in bead velocities, thus affecting the film coating quality. Furthermore, solubilization of core components into the film can contribute in the top-spray mode to

the greater variation in the film coating thickness [16].

In the preliminary screening phase, the present miniaturized top-spray coating procedure was characterized with respect to coating variables of potential importance to batch performance and final enteric film coating quality of the pellets. The inlet air flow rate and temperature, flow rate of coating solution and position of spraying nozzle were found to be the most important parameters affecting the film coating responses studied. Inlet air flow rate ($p < 0.01$) had a clear negative effect on the premature drug release in 0.1 N HCl and a positive effect on the batch quality and yield (Fig. 3). Position (height) of spraying nozzle ($p < 0.05$) and air flow temperature ($p < 0.085$) had an effect on the acidic resistance of the coated pellets (Fig. 3), but they had less influence (not statistically significant) on the batch quality and mass increase of the pellets. The effects of flow rate of coating solution on acidic resistance and batch quality (i.e. bulk appearance and number of clumps) were not statistically significant.

Based on the results of the preliminary screening phase, the most critical coating parameters were further optimized in the present small-scale coating procedure. Since the position (height) of the spraying nozzle and inlet air flow rate were adjusted to the maximum level available in the coater to obtain the most satisfactory coatings, other relevant parameters including air flow temperature, atomizing air pressure and flow rate of coating solution were selected for the subsequent optimisation phase (CCD design; Table 3). In this phase, air flow temperature ($p < 0.05$) was found the most critical parameter affecting the acidic resistance of the coated pellets prepared in a miniaturized top-spray coater. Increasing the air flow temperature resulted in a decrease of the premature drug release in 0.1 N HCl, and this result confirms the earlier observation made in the preliminary screening phase. As regards yield and batch quality, air flow temperature ($p < 0.01$) had a clear positive effect, while the flow rate of coating solution had a negative effect on the present responses studied (Fig. 4). This implies that by increasing the air flow temperature and by decreasing the flow rate of coating solution, more acidic resistance and uniform enteric-coated pellets can be produced in the present small-scale coating system. These results are also in accordance with earlier studies on larger-scale air-suspension film coatings of granules and pellets [16].

■ **Abb. 3, Tab. 3, Abb. 4** ■

It is evident that a small-scale coating system generating a fluid bed by mechanical vibration and air flow is very sensitive to both the air flow temperature and the flow rate of the coating solution. If the air flow temperature is too low and the flow rate of the coating solution is too high, over-wetting of the batch with subsequent clump formation may easily occur, thus impairing the film coating properties of the final products. The shaded area shown in Fig. 5 illustrates the combinations of air flow temperature and flow rate of coat-

ing solution that yield the optimal enteric coating results in the present small-scale coating procedure. The contour plots obtained allowed the selection of combinations of the above-mentioned two coating parameters that satisfy the given requirements for both in vitro acidic resistance (< 5.0 %) and expected yield (> 80.0 %). In order to achieve target values for the selected responses, air flow temperature should be set over 55 °C and flow rate of coating solution should be increased, taking into account the applied level of air flow temperature.

Fig. 6 shows photographs on the small-scale batches of enteric-coated pellets representing the best (i.e. batch quality rank score of 9), higher medium (rank score of 7), lower medium (rank score of 5) and the lowest (rank score of 1) batch quality. The main parameters affecting the batch quality (i.e. physical appearance and number of clumps) and yield were air flow temperature and flow rate of coating solution. Air flow temperature had a clear positive effect and flow rate of coating solution a negative effect on the batch quality in a miniaturized coating procedure.

■ **Abb. 5, 6** ■

4. Conclusions

The top-spray film coating procedure of pellets in a small scale is sensitive to the inlet air flow rate, air flow temperature and flow rate of coating solution. These parameters are important to be considered with enteric coatings since they have a great influence on the in vitro acidic resistance and batch quality of coated pellets. Furthermore, the balance between inlet air flow rate and atomizing air pressure as well as position (height) of spraying nozzle should be carefully adjusted and controlled. A miniaturized top-spray coating system is a useful tool for high throughput screening in early-stage pharmaceutical formulation development of film-coated products.

5. References

[1] Rowe, C. R., Small is beautiful, P.S.T.T. 187 (2000)

[2] Nunes, S., Alves, P., Galembeck, F., A low-cost, small-scale polymer mixer, J. Chem. Education **67**, 982 (1990)

[3] Marechal, P., Chiba, T., Inoue, T., Melt blending of dissimilar polymers by a small scale mixer: mixing with steel balls, Polymer Networks Blends **7**, 61 (1997)

[4] Landin, M., York, P., Cliff, M. J. et al., Scale-up of a pharmaceutical granulation in a fixed bowl mixer granulator, Int. J. Pharm. **133**, 127 (1996)

[5] Bock, T. K., Kraas, U., Experience with the Diosna minigranulator and assessment of process scalability, Eur. J. Pharm. Biopharm. **52**, 297 (2001)

[6] Murtomaa, M., Räsänen, E., Rantanen, J. et al., Electrostatic measurement on a miniaturized fluidized bed, J. Electrostat. **57**, 91 (2002)

[7] Räsänen, E., Rantanen, J., Mannermaa, J.-P. et al., Dehydration studies using a novel multichamber microscale fluid-bed dryer with in-line NIR measurement, J. Pharm. Sci. **92**, 2074

449 (2003)
450 [8] Räsänen, E., Rantanen, J., Mannermaa, J.-P. et al., The
451 characterization of fluidization behavior using a novel multi-
452 chamber microscale fluid bed, J. Pharm. Sci. (2003), in press
453 [9] Hancock, B. C., Clas, S.-D., Christensen, K., Micro-scale
454 measurement of the mechanical properties of compressed
455 pharmaceutical powders, 2: The elasticity and fracture be-
456 havior of microcrystalline cellulose, Int. J. Pharm. **209**, 27
457 (2000)
458 [10] Thoma, K., Groning, R., Zimmer, T., Film-coating
459 method for dosage form development, I: A small scale vortex
460 fluidized-bed coating apparatus, Acta Pharm. Technol. **32**, 137
461 (1986)
462 [11] Alkan, M. H., Groves, M. J., Roland, C. L. et al., Small-
463 scale film coating of tablets, pellets, and granules, Pharm. Tech-
464 nol. **12**, 98 (1988)
465 [12] Peeters, R., Kinget, R., Film-forming polymers for co-
466 lonic drug delivery, I. Synthesis and physical and chemical
467 properties of methyl derivatives of Eudragit S, Int. J. Pharm. **94**,
468 125 (1993)
469 [13] Takaya, T., Niwa, K., Muraoka, M. et al., Importance of
470 dissolution process on systemic availability of drugs delivered
471 by colon delivery system, J. Controlled Release. **50**, 111 (1998)
472 [14] Nykanen, P., Lempaa, S., Aaltonen, M.-L. et al., Citric
473 acid as excipient in multiple-unit enteric-coated tablets for tar-
474 geting drugs on the colon, Int. J. Pharm. **229**, 155 (2001)
475 [15] Mehta, A. M., Valazza, M. J., Abele, S. E., Evaluation of
476 fluid-bed processes for enteric coating systems, Pharm. Tech-
477 nol., April 1986, pp. 46
478 [16] Wesdyk, R., Joshi, Y. M., De Vincentis, J. et al., Factors
479 affecting differences in film thickness of beads coated in fluid-
480 ized bed units, Int. J. Pharm. **93**, 101 (1993)
481

482 **Acknowledgements**

483 The Centre for International Mobility for Foreign Students
484 (CIMO) is gratefully acknowledged for financial support of the
485 present study.

486 **Correspondence:**
487 Dr. Jyrki T. Heinämäki, Ph.D. (Pharm),
488 Department of Pharmacy,
489 Pharmaceutical Technology Division,
490 P.O. Box 56,
491 00014 University of Helsinki (Finland),
492 Fax: +358-9-19 15 91 44,
493 e-mail: jyrki.heinamaki@helsinki.fi

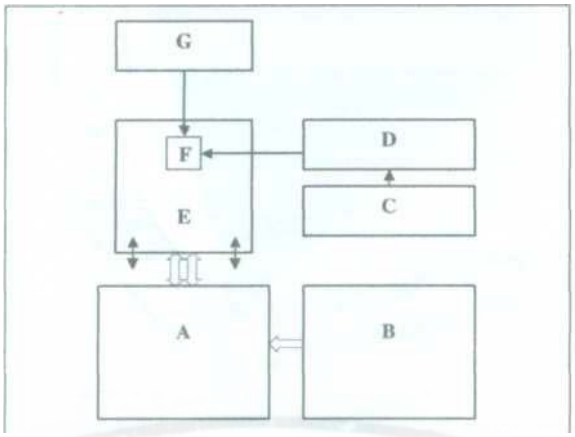

Fig. la: Block diagram of a miniaturized Caleva top-spray coating apparatus. A: heater unit, B: flow air supplier, C: microprocessor syringe pump, D: syringe, E: mechanically vibrating cone, F: spraying nozzle, G: low-pressure compressed air supplier.

Fig. 1b: Miniaturized top-spray coater.

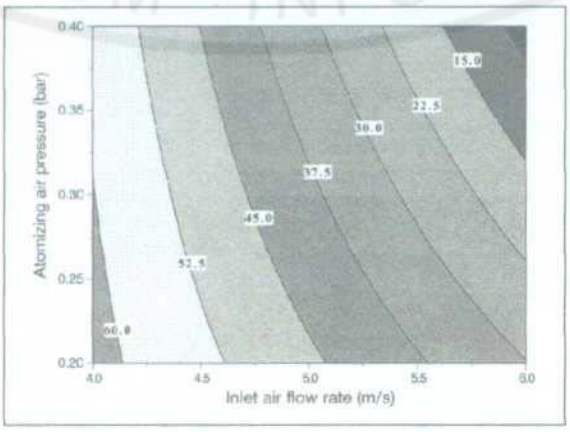

Fig. 2: Contour plots showing the effects of inlet air flow rate and atomizing air pressure on premature drug release in 0.1 N HC1 of the enteric-coated pellets prepared in a miniaturized top-spray coater.

Table 1: Physical properties of the core pellets.

Property	
Mean size (mm)	0.920
Bulk density (g/cm^3)	0.802 ± 0.006
Tap density (g / cm^3)	0.858 ± 0.007
Carr index (%)	6.5
Hausner ratio	1.1
Moisture content (%)	2.3 ± 0.2

Table 2: Levels of the face-centered central composite experimental design (CCD).

Factor	Level -1	Level 0	Level 1
Air flow temperature (°C)	50	60	70
Atomizing air pressure (bar)	0.4	0.5	0.6
Flow rate of coating solution (ml/h)[a.]>	25	55	75

[a)] The lower levels tested were -1 (i.e. 25 ml/h) and -0.6 (i.e. 35 ml/h).

Table 3: Matrix of the face-centered central composite experimental design (CCD) and results.

Experiment		Coating parameter			Response		
Exp. no.	Run order	X,	X_2	X_3	A	B	C
1	1	-1	-1	-0.6	73.1	38.4	2
2	14	+1	-1	-0.6	1.2	78.8	7
3	16	-1	+1	-0.6	1.2	93.8	7
4	5	+1	+1	-0.6	1.2	99.9	9
5	9	-1	-1	+ 1	13.7	42.9	1
6	13	+1	-1	+ 1	11.5	81.9	5
7	12	-1	+1	+ 1	31.5	9.6	1
8	3	+1	+1	+1	33	88.6	6
9	11	-1	0	0	87.9	25.9	1
10	8	+1	0	0	9.0	66.9	6
11	4	0	-1	0	1.8	70.7	6
12	7	0	+1	0	2.2	77.4	4
13	6	0	0	-0.6	2.4	64.5	3
14	17	0	0	+ 1	3.1	79.0	5
15	2	0	0	0	3.7	74.0	4
16	10	0	0	0	1.1	91.7	8
17	15	0	0	0	2.5	96.6	8
18	18	+1	+1	-1	3.6	86.0	5
19	19	-1	-1	-1	2.5	76.7	4
20	20	-1	+1	-1	3.2	78.9	3
21	21	+1	-1	-1	2.6	91.4	7
22	22	0	0	-1	2.9	88.1	6

A: Amount of drug released after 1-hour treatment in 0.1 N HC1 (%).
B: Yield (%). C: Batch quality rank score.

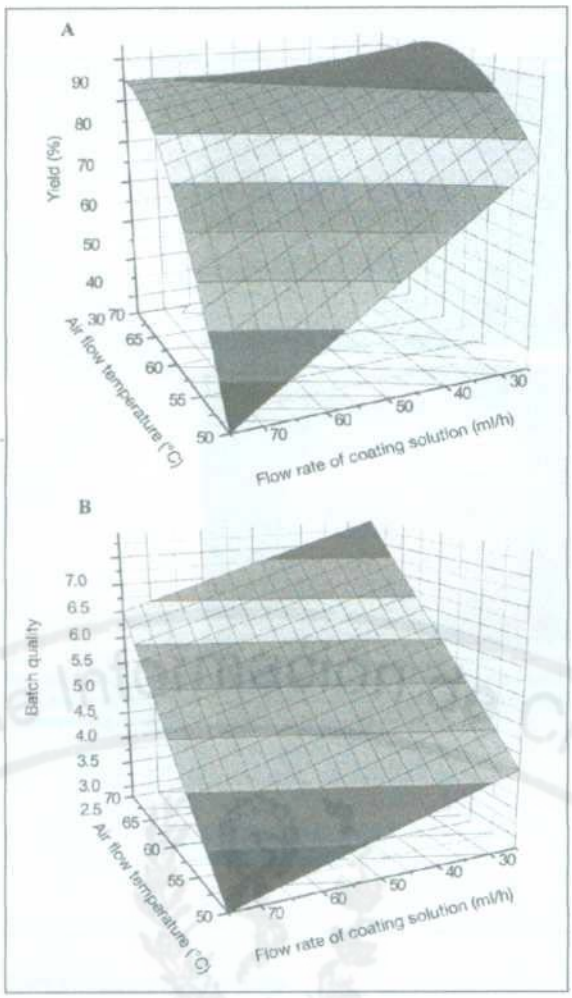

Fig. 4: Surface plot showing the effects of air flow temperature and flow rate of coating solution on yield (A) and batch quality (B) of the enteric-coated pellets prepared in a miniaturized top- spray coater.

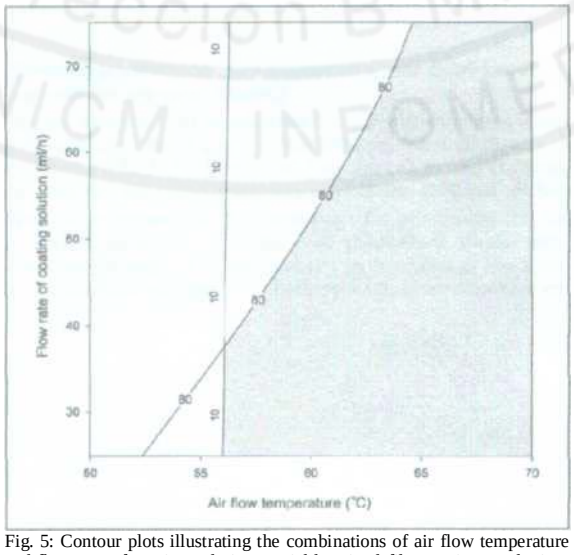

Fig. 5: Contour plots illustrating the combinations of air flow temperature and flow rate of coating solution to yield optimal film coating results in a miniaturized top-spray coater. The shaded area corresponds to combinations that satisfy the given constraints for in vitro acidic resistance (< 5.0 %) and batch yield (> 80 %).

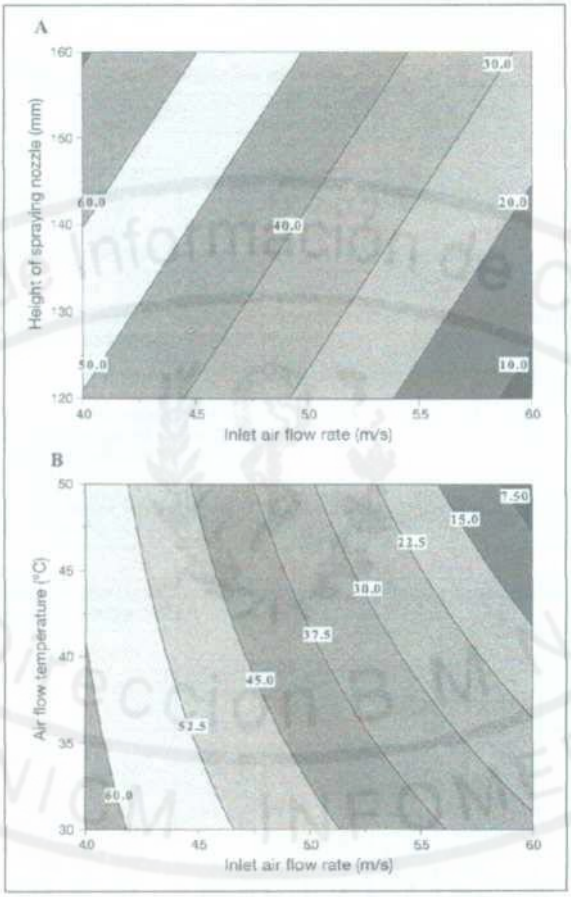

Fig. 3: Contour plots showing the effects of inlet air flow rate, height of spraying nozzle (A) and air flow temperature (B) on premature drug release in 0.1 N HCl of the enteric-coated pellets prepared in a miniaturized top-spray coater.

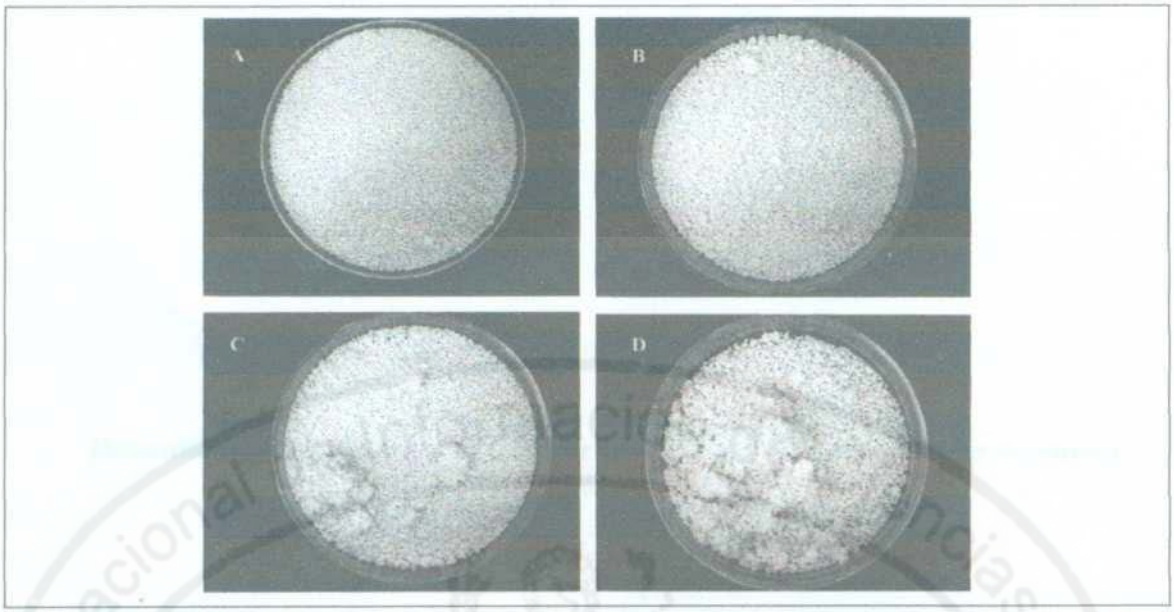

Fig. 6: Photographs on batches of enteric-coated pellets prepared in a miniaturized top-spray coater. A: batch no. 4 representing quality rank score of 9. B: batch no. 3 representing quality rank score of 7. C: batch no. 6 representing quality rank score of 5. D: batch no. 5 representing quality rank score of 1.

Nach Erledigung der Korrektur:
After completing corrections:

☐ zum Druck frei / Imprimatur

☐ neuer Abzug erbeten / new galley proof requested

Datum / Date

Unterschrift / Signature

Determination of tackiness of chitosan film-coated pellets exploiting minimum fluidization velocity

Fernández Cervera, M., Heinámáki. J., Rásánen, E., Antikainen, O., Nieto Acosta, O.M., Iraizoz Colarte, A. and Yliruusi, J.

Int. J. Pharm. 2004, 281, 119-127.

V

Available online at www.sciencedirect.com
SCIENCE DIRECT®
ELSEVIER
International Journal of Pharmaceutics 281 (2004) 119–127
international journal of pharmaceutics
www.elsevier.com/locate/ijpharm

Determination of tackiness of chitosan film-coated pellets exploiting minimum fluidization velocity

M. Fernández Cervera [a], J. Heinämäki [b,*], E. Räsänen [b], O. Antikainen [b], O.M. Nieto [a], A. Iraizoz Colarte [a], J. Yliruusi [b,c]

[a] *Institute of Pharmacy and Food, University of Havana, Havana, Cuba*
[b] *Pharmaceutical Technology Division, Faculty of Pharmacy, University of Helsinki, P.O. Box 56, FIN-00014 Helsinki, Finland*
[c] *Viikki Drug Discovery Technology Center DDTC, University of Helsinki, Helsinki, Finland*

Received 22 January 2004; received in revised form 27 May 2004; accepted 3 June 2004

Abstract

The tackiness of aqueous chitosan film coatings and effects of anti-sticking agents on sticking tendency, were evaluated. A novel rapid method exploiting minimum fluidization velocity to determine tackiness was introduced and tested. The pressure difference over the miniaturized fluidized-bed was precisely recorded as a function of velocity of fluidization air. High molecular weight chitosan plasticized with glycerol was used as a film-forming agent. Magnesium stearate, titanium dioxide, colloidal silicon dioxide and glyceryl-1-monostearate (GMS) were studied as anti-sticking agents. Film coatings were performed in a miniaturized top-spray coater. The incorporation of anti-sticking agents led to a clear decrease in tackiness of the chitosan films, and magnesium stearate and GMS were shown the most effective. Film-coated pellets containing magnesium stearate and GMS as an anti-sticking agent were very easily fluidized (showing very low values of minimum fluidization velocity) and were thus classified as the best flowing and the least sticking samples. Both these additives were found anti-sticking agents of choice for aqueous chitosan film coatings. Determination of the experimental minimum fluidization velocity in a fluidized bed, is a useful and sensitive method of measuring the tackiness tendency of film-coated pellets.

Keywords: Chitosan; Aqueous film coating; Pellets; Tackiness; Anti-sticking agents; Minimum fluidization velocity

1. Introduction

Chitosan, a polysaccharide derived by partial deacetylation of chitin, has been reported as an excipient of choice for a number of pharmaceutical applications (Illum, 1998; Paul and Sharma, 2000). Due to the unique dissolution and gelation characteristics, chitosan has been succesfully exploited in wet granulation as a binding agent, in direct compression as a diluent, in tabletting as a disintegrating agent and in sustained-release matrices as a retarding agent. Its use in novel drug delivery of, e.g., gene and peptide-type drugs and in colon targeting, has been described in recent review articles (Dodane and Vilivalam, 1998; Singla and Chawla, 2001). In spite of well-known gel and film forming characteristics of chitosan, little attention has been paid so far to the potential film coating applications of this poly-

* Corresponding author. Tel.: +358-9-19159158; fax: +358-9-19159144.
E-mail address: jyrki.heinamaki@helsinki.fi (J. Heinämäki).

0378-5173/$ – see front matter © 2004 Elsevier B.V. All rights reserved.
doi:10.1016/j.ijpharm.2004.06.004

meric material (Ritthidej et al., 2000; Koizumi et al., 2001).

The tackiness of films during coating procedure is a material- and process-related limitation that can result in extensive agglomeration of substrates. This may increase the number of coating defects and impair the yield and quality of the coated batch. Since chitosan has been reported to possess strong binding and mucoadhesive potential (Upadrashtra et al., 1992; Patel et al., 1999), it can be expected that the tackiness or sticking behaviour of this polymer during film coating is evident. It is also known that positive charges of chitosan could give rise to strong electrostatic interactions with negatively charged surfaces (He et al., 1998) . During coating with other cellulosic or acrylic polymers, unwanted and irreversible agglomeration due to tackiness of the batch has been reported. This phenomenon was mainly due to the influences of the type of polymer as well as type and concentration of plasticizer (Wesseling et al., 1999). Therefore, effective anti-sticking agents are needed to improve the film coating (Petereit et al., 1995; Wesseling et al., 1999).

Little work has been done on methods that can be used for determining the tackiness or sticking behavior of pharmaceutical polymer films. Wesseling et al. (1999) developed a method, in which force-displacement curves of the detachment process of polymer films were used as a measure for tackiness. The method was suitable to measure the tackiness of cellulosic and acrylic polymer films.

The aim of the present study was to investigate aqueous chitosan film coating of pellets in a miniaturized top-spray coating system with special reference to the effects of anti-sticking agents on tackiness of film coatings. The sticking tendency of the chitosan films was evaluated using a novel rapid method which exploits minimum fluidization velocity.

2. Materials and methods

2.1. Materials

The coating solutions contained high molecular weight chitosan (HMW-chitosan, Sigma-Aldrich, USA), hydroxypropyl methylcellulose (HPMC, Methocel E5, Dow Chemical, USA), acetic acid (Riedel- de Haen, Germany) and glycerol (Ph. Eur.) in purified water. Magnesium stearate (Ph. Eur.), titanium dioxide (TÍO2, Ph. Eur.), colloidal silicon dioxide, Aerosil (SÍO2, Ph. Eur.) and glyceryl-1-monostearate (GMS, Genay, France) were used in the film coating formulations as anti-sticking agents. Polyoxyethylenesorbitan monooleate 80 (Tween 80, Ph. Eur.) was used to enhance the dispersability of GMS in water. The pellet cores for film coatings were prepared by using microcrystalline cellulose (MCC, Emcocel, type 90M, E. Mendell, Nastola, Finland) and lactose monohydrate (LM, Pharmatose, type 80M, DMV International, Veghel, The Netherlands) as fillers, theophylline anhydrous (Ph. Eur.) as a model drug, and purified water as a granulation liquid. For preparing core tablets for contact angle measurements, the following excipients were used: microcrystalline cellulose (MCC, Emcocel, type 90M, E. Mendell, Nastola, Finland), lactose monohydrate (LM, Pharmatose, type 80M, DMV International, Veghel, The Netherlands) as filler materials and magnesium stearate (Ph. Eur.) as a pre-lubricating agent in the die.

2.2. Contact angle measurements

For contact angle measurements, both unplasticized and plasticized aqueous solutions of chitosan at concentrations of 0.5, 1.0 and 1.5% were prepared by dissolving chitosan in diluted acetic acid solution with glycerol. HPMC at 10% (w/w) aqueous solution plasticized with glycerol was used as a reference solution. Two types of tablet preparations with a qualitative composition identical to that of pellet cores were compressed in a Korsch EK-0 single-punch tablet machine (Erweka Apparatebau, Germany) equipped with 13 mm flat-faced-punches and a compression force of 20 kN (Table 1). The tablet height under load was kept constant.

Table 1
Compositions of substrates (core tablets) used in contact angle measurements

Formulation	Composition of core tablets (%)	
	Formulation I	Formulation II
Lactose monohydrate (LM)	99.0	49.5
Microcrystalline cellulose (MCC)	-	49.5
Magnesium stearate	1.0	1.0

Table 2
Matrix of the experimental design and results of contact angles

Experiment no.	Chitosan (%)	Plasticizer“ (%)	Contact angles (°)	
			Formulation I	Formulation II
1	0.5	0	44.0 ± 2.3	36.1 ± 2.4
2	1.5	0	54.6 ± 1.9	53.1 ± 1.4
3	0.5	20	44.2 ± 2.6	35.9 ± 2.2
4	1.5	20	53.7 ± 0. 9	52.6 ± 1.8
5	1	0	47.6 ± 2.2	43.2 ± 2.1
6	1	20	51.6 ± 1.3	47.4 ± 0.8
7	1	20	54.7 ± 2.5	51.5 ± 2.7
8	1	20	53.7 ± 2.1	49.1 ± 2.0
9	1	20	53.7 ± 1.8	51.5 ± 1.8
Reference solution (HPMC/glycerol)		20	59.7 ± 3.5	53.8 ± 2.7

[a] Percentage (w/w) of the polymer weight.

The contact angles between the solutions and the core tablets were determined by the sessile drop method (Optical Contact Angle Meter CAM 200, KSV Instruments Ltd.). The measurements were repeated ten times for each experiment according to the complete two factorial experimental design (Table 2).

2.3. Film coating of pellets

2.3.1. Preparation of core pellets

The composition of core pellets was as follow: 5% (w/w) theophylline anhydrous, 60% (w/w) MCC and 35% (w/w) LM. Pellets were made with the extrusion/spheronization technique (Nica M6L mixer/granulator; Nica El70 extruder; Nica S320 spheronizer; Nica System AB, Molndal, Sweden). The pellets were dried for 48 h at room temperature (21 ± 2 °C), and the size fraction ranging from 1.0 to 1.25 mm was used in the subsequent coating experiments. The physical properties of the core pellets are shown in Table 3.

Table 3
Physical properties of core pellets

Property	
Mean size (mm)	0.940
Bulk density (g/cm^3)	0.802 ± 0.001
Tap density (g/cm^3)	0.837 ± 0.007
Carr index (%)	4.2
Hausner ratio	1.0
Moisture content (%)	1.1 ± 0.2

The size and size distribution of the core pellets were determined by sieve analysis with a set of sieves with 1250, 1000, 710, 500, 315, 250 and 125(1111 screens and a collector. The moisture content of pellet cores was determined as a loss of weight using an infrared apparatus (Sartorius Thermol Control, Sarto- rius GmbH, Germany). All measurements were made in triplicate. The Carr index and Hausner ratio were calculated from the tap and bulk densities (Wells and Aulton, 1998).

2.3.2. Film coating experiments

The basic composition of the coating solution was 1.0% of chitosan in aqueous acetic acid (1%) plasticized with glycerol (20% (w/w) of the polymer weight). The coating solutions were applied using a miniaturized top-spray air-suspension coating apparatus (Caleva Mini Coater, Caleva Process Solutions Ltd., UK). Each small-scale batch coated comprised 8.0 g of pellets.

A full 3^2 factorial design was used as a study design (Table 4). The levels of position (height) of spraying nozzle, *X*\ (120, 140 and 160 mm) and inlet air temperature, *Xo* (50, 60 and 70 °C) were varied. The levels of coating solution flow rate, inlet air flow and atomizing air pressure were adjusted to 15 ml/h, 6.0m/s and 0.5 bar, respectively. The theoretical amount of coating was 3% (w/w) of the total weight of the pellets. The present film coating batches of pellets prepared without any anti-sticking agents were used as a reference

Table 4
Matrix of the complete 3^2 experimental design and results

Experiment no.	Coating parameter		Response	
	A:,	*2	A	B
1	-1	-1	29.8	5
2	+ 1	-1	36.5	4
3	-1	+1	24.6	6
4	+ 1	+1	41.3	7
5	-1	0	18.2	5
6	+ 1	0	39.4	6
7	0	-1	19.4	6
8	0	+1	30.1	6
9	0	0	22.8	6
10	0	0	24.3	6
11	0	0	17.4	5

Key: (A) Expected yield (%) and (B) batch quality rank score.

batches for those obtained by applying anti-sticking agents.

Eight coating batches were prepared to investigate the effects of four anti-sticking agents on the tackiness of pellets during the coating process. Magnesium stearate, titanium dioxide, colloidal silicon dioxide and GMS (0.1 and 0.3%) were added to the plasticized solution of chitosan. GMS was added in the form of suspension in an aqueous 0.08% Tween 80 solution. The polymer dispersions were sprayed according to the conditions of central level used in the experimental design described above. After spraying the same temperature (60 °C) was maintained for an additional lOmin in the drying phase. Film-coated pellets were placed in plastic bottles for further evaluation.

Expected yield and quality (i.e. film coating appearance) were used as indicators of film tackiness. The expected yield was obtained by gently sieving the film-coated batches through a 1.8 mm and weighing the mass of the pellets passing this sieve. The physical appearance of the coated pellets (batch quality) was determined by visual inspection (assigning rank scores from 1 to 10 based on visual inspection). Furthermore, the in vitro release test for uncoated and coated pellets was performed using a USP apparatus I (basket method). The dissolution medium was 900 ml of phosphate buffer pH 6.8 or 7.4 maintained at 37.0 ± 0.1 °C. The basket rotation speed was kept at 50 rpm. The samples were filtered through a filter and assayed by UV spectrophotometry (Perkin-Elmer, Perkin-Elmer GmbH, Germany) at 273 nm for theophylline.

2.4. Film tackiness measurements

2.4.1. Theoretical considerations of minimum fluidization velocity

The minimum or incipient fluidization velocity (wmf) **represents the point of transition between the fixed and the fluidized states. Several authors have published models for predicting the u_mf in different conditions (Wen and Yu, 1966; Saxena and Vogel, 1977; Chitester et al., 1984; Noda et al., 1986; Lippens and Mulder, 1993; Rao and Bheemarasetti, 2001). The w_mf describes universally the velocity when the buoyancy of the upward moving gas counterbalances the weight of the bed of solid particles. For design and scaling-up purposes it is important to be able to calculate the value of w_mf precisely and thus to keep the number of experiments low.**

When a gas passes through a bed of solid particles at a low velocity, the gas fluid first percolates through the void spaces between the particles. This stage is called the fixed bed (Davidson et al., 1985; Kunii and Levenspiel, 1991). When the velocity is increased, particles begin to vibrate and the pressure drop across the bed increases. This is the expanded bed and at this stage the bed performance is fairly similar to that of a fixed bed. An insignificant increase in the void fraction in the bed is then observed. At a certain velocity the buoyancy of upward moving gas counterbalances the weight of the bed (interparticle forces denied). This stage is referred to as a bed at minimum fluidization or an incipiently fluidized bed. The bed starts to behave like a dense fluid. At this point the pressure drop across the bed equals the weight of the bed. After the bed has been fluidized and the velocity of air increase, the pressure drop across the bed remains constant but the height of the bed continues to increase.

2.4.2. Film tackiness measurements exploiting minimum fluidization velocity

A microscale fluid-bed apparatus (Ariacon Oy, Helsinki, Finland) was used to study the tackiness (sticking) tendency and flow properties of coated pellets. The present fluidized-bed system and experimental setup have been described earlier in detail (Rasanen et al., 2003). The accuracy of the method

was improved using a rubber 0-ring just above the bed of pellets. In each test, the pressure difference over the bed was recorded as a function of velocity of fluidization air. Experimental minimum fluidiza- tion velocity (w_mf) was measured from increasing and decreasing flow rates. The sample size of the pellets was 5 ml equal to 2-4 g, and the pellets were fluidized by increasing air flow rate slowly up to 400 ml/s. The pellets were fluidized 1 min at constant velocity (400 ml/s) and the fluidization occurred mainly at the lower part of the chamber. Thereafter the velocity of the fluidization air was gradually decreased to zero. Uncoated pellets were used as a reference sample representing a readily flowing (unsticking) product. The measurements were identical. The reference sample was measured triplicate, other samples once.

3. Results and discussion

3.1. Wettability of MCC-containing substrates by chitosan solutions

In granulation, pelletization and film coating uniform wetting of the solids is necessary. In the present study, the contact angle measurements were used to characterize the wettability of MCC-containing substrates that were qualitatively identical with the core pellets used in subsequent film coatings. The contact angles between chitosan solutions and core tablets are shown in Table 2. Aqueous HPMC solution (10% (w/w)) was used as a reference solution.

The effect of chitosan concentrations on the contact angles of the substrates was evident. The results showed that the contact angle between the solutions and both types of MCC-containing substrates increases slightly with increasing amount of chitosan in the solutions. On the other hand, the effect of plas- ticizer (glycerol) on the contact angles measured was minimal (not statistically significant). On the basis of the present results, the solution with 1.0% (w/w) chitosan was selected for aqueous film coating of pellets.

3.2. Effect of position of spraying nozzle and inlet air temperature on film coating

Coating experiments were first performed with chitosan solutions without any anti-sticking agents. In these experiments, the coating efficiency expressed as amount of non-agglomerated coated pellets (expected yield) and batch quality was quantified. The position of the spraying nozzle was found an important parameter affecting both expected yield and batch quality and, consequently, tackiness of chitosan film-coated pellets (Fig. 1). It is obvious that by increasing the height of the spraying nozzle, excessive overwetting and subsequent irreversible agglomeration (sticking) of pellets are avoided due to partial spray drying of the coating solution droplets. As shown in Fig. 1, increasing the air flow temperature improved slightly the batch quality.

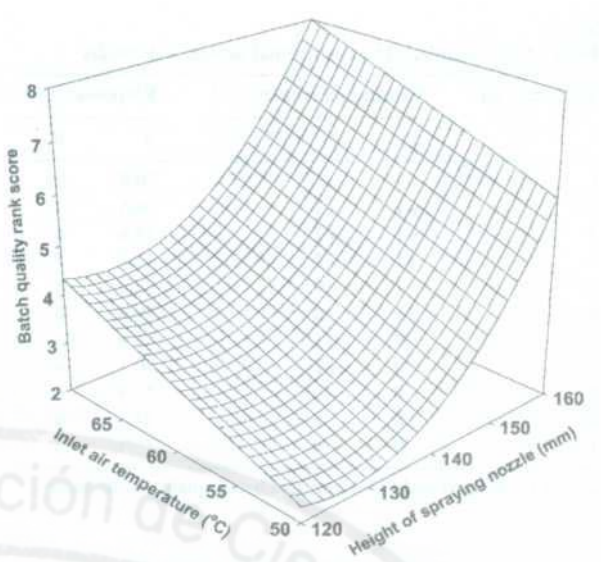

Fig. 1. Effect of height of spraying nozzle and inlet air temperature on batch quality of pellets coated with chitosan films.

In these preliminary experiments, expected yield and batch quality were far below the optimal. Thus, the batches were not very satisfactory (Table 4). The dissolution of the chitosan-coated pellets in phosphate buffer (pH 6.8) was rapid and unaffected by the coating process (t50% values for all batches were 10-12 min). It was concluded that chitosan film coatings lacking anti-sticking adjuvants are prone to evident irreversible agglomeration of pellets thus impairing the performance of film coating.

3.3. Effect of anti-sticking agents on the film coating

For various coating applications, a low stickiness is desirable. As seen in Fig. 2, the expected yield

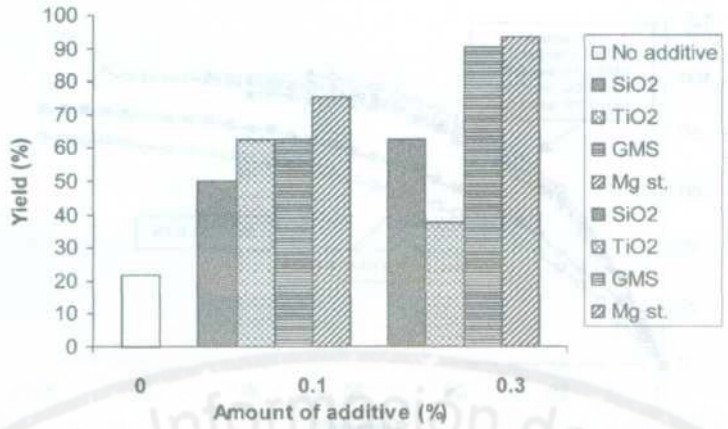

Fig. 2. Effect of anti-sticking agents on the yield of pellets coated with chitosan films.

values increased with increasing concentration of anti-sticking additives used. The incorporation of the anti-sticking agents led to a clear decrease in tackiness of films, and magnesium stearate and GMS were shown more effective than SiC>2 and Ti02- In aqueous chitosan film coating, water-accelerated formation of hydrogen bonds is evident due to a great number of hydroxyl groups and protonated amino groups existing in chitosan molecule (primary amine) (Kienzle-Sterzer et al., 1982; Peng et al., 1994). Since hydrogen bonds are very strong covalent type of bondings, the films show a tendency for tackiness, resulting in irreversible agglomeration of the pellets. The mechanism of anti-sticking agents is obviously based on their strong capability to reduce hydrogen bonds existing in the wet film coatings (also to break water bridges) and to form simultaneously an increased number of competitive hydrophobic bondings in the coating system.

Traditionally, talc and magnesium stearate have been used as a glidants to reduce the sticking of cores during the coating process. Petereit et al. (1995) and Wesseling et al. (1999) were of the opinion that GMS is a promising alternative to talc in coating suspensions of acrylic and cellulosic polymer films and more effective and less toxic. The present results are in accordance with the earlier results obtained with GSM. High amounts of anti-sticking (solid) additives may block the nozzle.

In the present study this was observed especially with SiCO2 and TiO2 at the concentration of 0.3%.

The drug release profiles of chitosan film-coated pellets with anti-sticking additives in buffer 7.4 are illustrated in Fig. 3. Drug release from uncoated and coated pellets without additives was about 100% of the drug at approximately 30 min. Incorporation of additives possibly enhanced the hydrophobic nature of the film coat which reduces penetration of the dissolution medium and may prolong slightly drug release. The apparent reversal dissolution of the 0.1 and 0.3% magnesium stearate results may be due to the unhomogeneous dispersion of the solid (magnesium stearate) in the coating liquid.

The greater efficiency of the addition of magnesium stearate to prolong drug release compared with the other anti-sticking agents could be attributed to the ionic interaction between protonoted amino groups on chitosan and carbonyl groups of stearates in magnesium stearate molecule. This electrostatic charge interaction with further amide formation and its effect as a barrier to prolong drug release have been demonstrated previously (Ritthidej et al., 2000).

3.4. Determination of film tackiness using minimum fluidization velocity

A novel method based on determination of the experimental minimum fluidization velocity (w_mf) in a fluidized bed was used to evaluate the influence of anti-sticking agents on the tackiness of aqueous chitosan films. The pressure difference over the fluidized bed as a function of velocity represented the effect

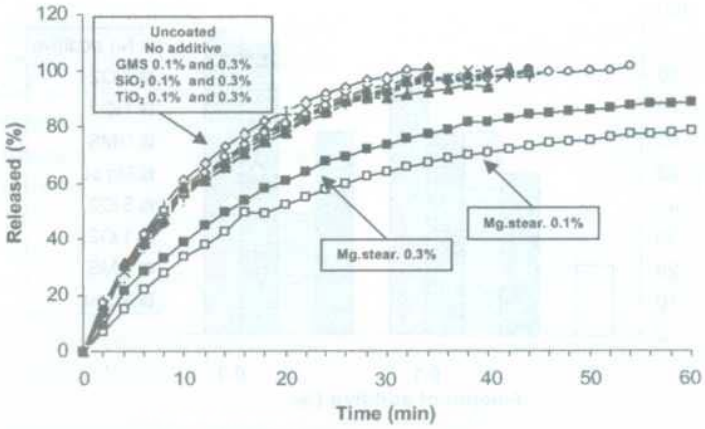

Fig. 3. Effect of anti-sticking agents on dissolution of chitosan film-coated pellets in phosphate buffer (pH 7.4) solution ($n = 6$). *Key*: Uncoated pellets (◇), film-coated pellets without antisticking agent (◆) and film-coated pellets with magnesium stearate (□, ■), titanium dioxide (○, ●), colloidal silicon dioxide (△, ▲) and GMS (+, ×) (0.1 and 0.3%).

of anti-sticking agents on the fluidization behavior of the coated pellets studied (Figs. 4 and 5). The shape of the pressure curve changed with the amount and type of anti-sticking agent used thus allowing to distinguish the anti-sticking efficiency of the adjuvants tested.

As seen in Fig. 4 and Table 5, the lowest values for experimental u_{mf} were obtained with uncoated

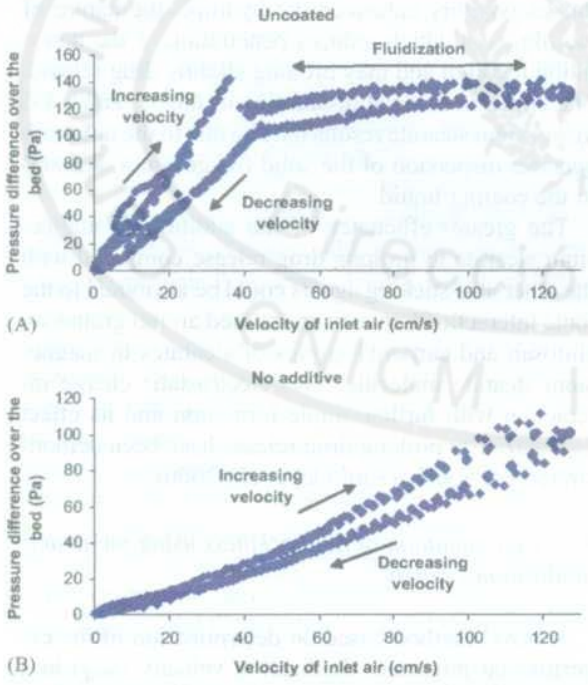

Fig. 4. Pressure difference over the bed profiles of (A) uncoated pellets (= reference sample representing non-sticking behaviour) and of (B) HMW-chitosan film-coated pellets without any anti-sticking agent.

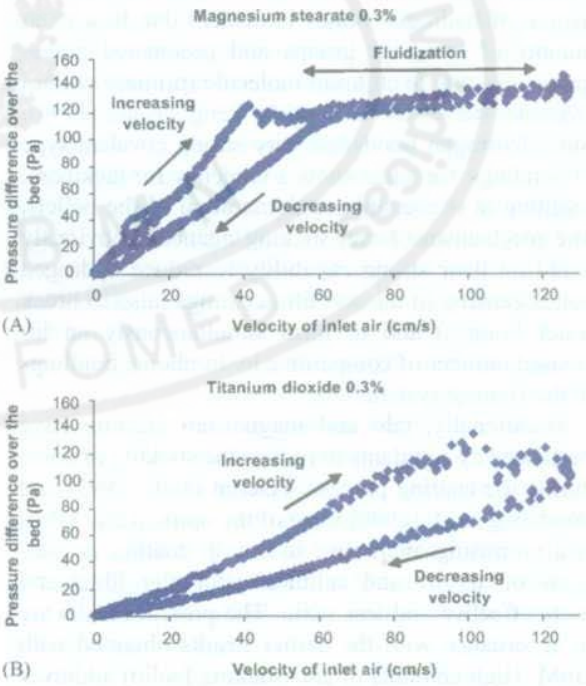

Fig. 5. Pressure difference over the bed profiles of HMW-chitosan film-coated pellets containing (A) magnesium stearate 0.3% (w/w) and (B) titanium dioxide 0.3% (w/w) as an anti-sticking agent.

Table 5
Values for minimum fluidization velocity (i/$_m$f)

Formulation	Increasing velocity u_mf (cm/s)	Decreasing velocity u_mf (cm/s)	Difference
Uncoated pellets	35	59	24
Film-coated pellets			
No anti-sticking agent	>130	>130	-
Colloidal silicon dioxide 0.1%	71	122	51
Colloidal silicon dioxide 0.3%	60	127	67
Titanium dioxide 0.1%	74	126	52
Titanium dioxide 0.3%	91	>130	-
Magnesium stearate 0.1%	63	120	57
Magnesium stearate 0.3%	41	71	30
GMS 0.1%	69	112	43
GMS 0.3%	44	94	50

reference pellets. With lower values of w_mf the fluidization capacity of the pellets increased and enhanced fluidization behavior and the non-sticking behaviour. This phenomenon was observed as the amount of anti-sticking agent was increased from 0.1 (w/w) to 0.3% (w/w) with exception of titanium dioxide. Film-coated pellets containing magnesium stearate as an anti-sticking agent were very easily fluidized (showing very low values of minimum fluidization velocity). The present film-coated pellets were more readily fluidized compared with those containing, e.g. titanium dioxide (Fig. 5). Since the film-coated pellets that contained no anti-sticking agent did not fluidize in the present testing system, values for ¡/$_m$f could not be detected. In Table 5, the lowest and highest values for w_mf difference between increasing and decreasing velocity shows better fluidization (i.e. non-sticking tendency) and poorer fluidization (sticking tendency) of pellets, respectively.

Chitosan film-coated pellets without anti-sticking additives could not be fluidized and were thus classified as the worst flowing sample. Film-coated pellets containing magnesium stearate and GMS as anti-sticking agents (0.3% (w/w)) were easily fluidized and were classified as the best flowing and the least tacking sample. Both these additives are anti-sticking agents of choice for aqueous chitosan film coatings. The present method has interesting possibilities as a method for quantifying film tack.

Acknowledgements

The Centre for International Mobility for Foreign Students (CIMO) is gratefully acknowledged for financial support of the present study and Maria Joao Cravo Martins (University of Coimbra, Portugal) for assistance in the contact angle measurements.

References

Chitester, D.C., Komosky, R.M., Fan, L.-S., Danko, J.P., 1984. Characteristics of fluidization at high pressure. Chem. Eng. Sci. 39, 253-261.

Davidson, J.F., Clift, R., Harrison, D., 1985. Fluidization, second ed. Academic Press, Orlando, FL.

Dodane, V., Vilivalam, V.D., 1998. Pharmaceutical applications of chitosan. Pharm. Sci. Technol. Today 1, 246-253.

He, P., Davis, S.S., Ilium, L., 1998. In vitro evaluation of the mucoadhesive properties of chitosan microspheres. Int. J. Pharm. 166, 75-88.

Ilium, L., 1998. Chitosan and its uses as a pharmaceutical excipient. Pharm. Res. 15, 1326-1331.

Kienzle-Sterzer, C., Rodriguez-Sanchez, D., Rha, C., 1982. Dilute solution behaviour of a cationic polyelectrolyte. J. Appl. Polym. Sci. 27, 4467-4470.

Koizumi, T., Ritthidej, G.C., Phaechamud, T., 2001. Mechanistic modeling of drug release from chitosan coated tablets. J. Control. Rel. 70, 277-284.

Kunii, D., Levenspiel, O., 1991. Fluidization Engineering, second ed. Butterworth-Heinamann, Stoneham, MA.

Lippens, B.C., Mulder, J., 1993. Prediction of the minimum fluidization velocity. Powder Technol. 75, 67-78.

Noda, K., Uchida, T., Makino, T., Kamo, H., 1986. Minimum fluidization velocity of binary mixture of particles with large size ratio. Powder Technol. 46, 149-154.

Paul, M., Sharma, C.P., 2000. Chitosan, a drug carrier for the 21st century: a review. S.T.P. Pharma Sci 10, 5-22.

Patel, D., Smith, A.W., Grist, N., Barnett, P., Smart, J.D., 1999. An in vitro mucosal model predictive of bioadhesive agents onto the oral cavity. J. Control. Rel. 61, 175-183.

Peng, T., Yao, K.D., Yuan, C., Goosen, M.FA.., 1994. Structural changes of pH-sensitive chitosan/polyether hydrogels in different pH solution. J. Polym. Sci. A: Polym. Chem. 32, 591-596.

Petereit, H.U., Assmus, M., Lohmann, K., 1995. Glyceril monostearate as a glidant in aqueous film-coating formulations. Eur. J. Pharm. Biopharm. 41, 219-228.

Rao, T.R., Bheemarasetti, J.V.R., 2001. Minimum fluidization velocities of mixtures of biomass and sands. Energy 26, 633- 644.

Rasanen, E., Antikainen, O., Yliruusi, J., 2003. A new method to predict flowability using a microscale fluid bed. AAPS Pharm. Sci. Tech., 4(4) Article 53 (http://www.aapspharmscitech.org).

Ritthidej, G.C., Phaechamud, T., Koizumi, T., 2000. Additives in moist-heat-treated chitosan acetate films: a method to extend the release of propranolol hydrochloride-coated tablets. S.T.P. Pharm. Sci. 10, 112-119.

Saxena, S.C., Vogel, G.J., 1977. The measurement of incipient fluidization velocities in a bed of coarse dolomite at temperature and pressure. Trans. IChemE. 55, 184-189.

Singla, A.K., Chawla, M., 2001. Chitosan: some pharmaceutical and biological aspects-an update. J. Pharm. Pharmacol. 53, 1047-1067.

Upadrashtra, S.M., Katikaneni, PR., Nuessle, N.O., 1992. Chitosan as a tablet binder. Drug Dev. Ind. Pharm. 18, 1701-1708.

Wells, J.I., Aulton, M.E., 1998. Preformulation. In: M.E. Aulton (Ed.), Pharmaceutics, the Science of Dosage Form Design. Churchill Livingstone, New York, pp. 223-253.

Wen, C.U., Yu, Y.H., 1966. A generalized method for predicting the minimum fluidization velocity. AIChE J. 12, 610- 612.

Wesseling, M., Kuppler, F., Bodmeier, R., 1999. Tackiness of acrylic and cellulosic polymer films used in the coating of solid dosage forms. Eur. J. Pharm. Biopharm. 47, 73-78.